FINAL REPORT

ARPA Order Number 675

University of Rochester, Contractor

INTERACTION BETWEEN INTENSE OPTICAL RADIATION AND MATTER

Contract DA-31-124-ARO-D-401

Program Element Code No. 6.25.03.01R

Date of Contract : 6 August, 1965

Amount of Contract : $196,956

Contract Expiration Date: 28 February, 1969

Project Scientist (Responsible Investigator) : Michael Hercher

Office telephone : 716-275-2327

Home telephone : 716-436-4981

SPONSORED BY

Advanced Research Projects Agency

Project DEFENDER

ARPA Order No. 675

December, 1970

"INTERACTION BETWEEN INTENSE OPTICAL RADIATION AND MATTER"

FINAL REPORT

I. Scope of Work Performed

The initial intent of research performed under this grant was to study the interaction of intense laser radiation with various optical media, in order to gain an understanding of the physical processes involved. We then intended to put this knowledge to work in order to avoid the type of permanent damage to optical components which was -- and still is -- being widely experienced when working with lasers at multi-megawatt power levels.

Although we were primarily interested in the interaction between laser radiation and nominally transparent optical media (such as crystals and glasses), we decided first to study the interaction of focused laser beams with various gases. The rationale behind this decision was essentially that a gas was a much simpler, cleaner medium, and would provide a basic insight into the more general interaction problem. If we couldn't discover the mechanism responsible for laser radiation-induced breakdown in gases, we would have little hope of solving the problem for solid media. As a result of an extensive experimental and

theoretical study of radiation-induced breakdown in inert gases, we found that the breakdown process was essentially due to inverse Bremsstrahlung, in which free electrons were accelerated by the intense optical field. This produced a chain-reaction in which previously accelerated electrons produced a copious supply of free electrons by means of impact ionization of the gas molecules. The reaction is essentially triggered by the initial production of a relatively small number of free electrons. It was our well-supported conclusion that these initial electrons were provided by multi-photon ionization of impurities having a low ionization potential. These impurities need only be present in a few parts per million in order to be effective in initiating the chain reaction leading to breakdown. Moreover, the threshold radiation density necessary to produce a chain reaction of inverse Bremsstrahlung is generally well in excess of that required to provide the initial free electrons via multi-photon photoionization. As a result, the breakdown process is essentially a linear one (it would be non-linear if multiphoton effects played a more dominant role). The results of these studies of laser-induced gas breakdown have been described in earlier reports, and have been

published in the open literature (see publications list). Subsequent work published by other workers has confirmed our conclusions.

As a result of our findings with gas breakdown, we were very pessimistic about being able to avoid similar effects in solids. Damage in transparent media is basically unavoidable when the radiation density is high enough to initiate the inverse Bremsstrahlung chain reaction. This threshold occurs in the vicinity of 1,000 to 10,000 megawatts/cm^2. The mechanism is essentially the same as in a gas, but the hot plasma produced inside a solid produces thermal stresses which lead to gross permanent damage. Of course, damage will occur at lower radiation density levels if the material contains any sizable impurities which are capable of absorbing the laser radiation (for example, platinum particles of the type often found in glass). Damage arising in this manner can be avoided by more careful preparation of the materials. After gathering enough data to confirm our opinions on laser-induced damage to solids, we stopped work in this area. Work by others doing research in this area has yielded similar results, with similar conclusions. Some workers have observed laser radiation-induced bulk

photo-conductivity in transparent media just below the damage threshold (we had observed a similar production of free electrons just below the breakdown threshold in gases).

The second major area in which we did research supported by this grant, was saturable absorption. A simple two-level atomic system, exhibiting absorption at a given frequency, will become increasingly transparent at photon irradiances (i.e. photons/cm^2sec) in excess of $(\sigma\tau)^{-1}$, where σ is the absorption cross-section of a single atom and τ is the lifetime of the excited state. The situation is more complicated when the energy-level structure of the atom is more complex, and when excited-state transitions have to be taken into account. Organic dyes are particularly interesting saturable absorbers because of their very large cross-sections. These dyes have been extensively used for both Q-switching and mode-locking in solid laser systems.

After a relatively superficial study of a number of saturable absorbers, we decided to make an extensive study of a small number of organic dyes (with basically differing characteristics) which exhibit saturable absorption at the wavelength of a ruby laser. Some of the results of

this study have been published, and the entire study is described in detail in Appendix I. As a result of this study we are now able to set criteria for various applications of saturable absorbers, and we feel we have an extensive understanding of the particular dyes which we have studied. In addition, we have found that the saturation characteristics of a dye can provide considerable insight into the energy-level structure of the dye -- particularly with regard to excited states and intersystem crossing times.

II. Publications Resulting from the Work Supported by this Grant

1. M. Hercher, M. Young and C. Wu, "Some Characteristics of Laser-Induced Air Sparks," J. Appl. Phys. 37, 4938 (1966).

2. M. Young and M. Hercher, "Dynamics of Laser-Induced Breakdown in Gases," J. Appl. Phys. 38, 4393 (1967).

3. E. Panizza and P.J. Regensburger, "Optical Probe Attenuation in CS_2 Induced by a Ruby Laser," Phys. Letters 24A, 321 (1967).

4. M. Hercher, D.L. Stockman and W. Chu, "An Experimental Study of Saturable Absorbers for Ruby Lasers," J. Quantum Electronics, QE-4, 954 (1968).

(A more comprehensive paper on saturable absorption in organic dyes is in preparation.)

APPENDIX 1

A STUDY OF SATURABLE ABSORBERS FOR RUBY LASERS

William P. Chu

Submitted in partial fulfillment
of the requirements
for the degree Doctor of Philosophy
in the Department of Physics and Astronomy
1970

Supervised by Prof. Michael Hercher

The Institute of Optics

ABSTRACT

This thesis describes a study of the nonlinear absorption properties of a number of the organic dye molecules which have been widely used in conjunction with ruby lasers. The dominant characteristic of this nonlinear behavior is a reduction in the optical transmission of a dye sample when irradiated with intense laser light. The three dye molecules studied are cryptocyanine, metal-free phthalocyanine, and chloroaluminum phthalocyanins, which were dissolved in a variety of solvents.

In chapters II and III, the primary photophysical processes of polyatomic molecules are discussed. Several excited-state lifetime of the three molecules have been determined experimentally. It was found that the nonradiative internal conversion lifetime for the transition from the first excited singlet to the ground state for metal-free phthalocyanine is 7×10^{-9} sec.

In chapter IV, the saturation of molecular absorption for these three molecules is analyzed on the basis of a rate equation approach to a simple three-level model plus excited-state absorptions. Experimental results on the saturation of absorption and fluorescence are comparable to analytical results for the range of Q-switched pulse

durations being used. Excited singlet-state absorptions are found to be the dominant cause of the residual losses exhibited by phthalocyanine molecules. The excited singlet-singlet absorption cross-section was found to be $\sim 10^{-17}$ cm^2. The observed saturation maximum in the nonlinear absorption of chloroaluminum phthalocyanine at high laser intensity is explained in terms of a model involving three absorptive transitions in the singlet manifold. A value of $\sim 10^{-11}$ sec for internal conversion from the second excited singlet to the first singlet state is deduced from the experimental data.

The general characteristics of dye Q-switched laser pulse evolution are discussed in chapters V and VI. We describe experiments which were performed to study the nature of the spectral hole-burning responsible for frequency-locking between different lasers. Several possible mechanisms for the phenomenon are discussed.

TABLE OF CONTENTS

CHAPTER I

INTRODUCTION

Since the first successful operation of passively Q-switched lasers using strongly absorbing organic dye molecules as saturable absorbers, [1,2] general interests have been to investigate the nonlinear absorption properties of these organic molecules with high intensity laser radiation. In particular, saturation of molecular transitions which is the basic mechanism for the switching process in a passively Q-switched laser has been intensely studied both experimentally and theoretically. Organic polyatomic molecules are known to have complex energy-level structures which can be separated into the singlet and the triplet manifolds, and these excited levels which are coupled to the photo-excitation will have different relaxation processes.[3] A detailed study of the saturation mechanism of these molecules will require knowledge of the nature of the excited levels involved and their respective relaxation rates. Under high intensity excitation, in addition to the absorption processes which originate in the ground state of the molecules, excited-state absorption will also become significant if the

transition is allowed and if the steady-state concentration of the excited level is significant.[4]

Early experiments on the saturation of molecular transitions for organic dye molecules were done by Armstrong,[5] in which the transmission of several phthalocyanine molecules dissolved in some inert solvents was measured as a function of incident power from a Q-switched ruby laser. The experimental results were then compared with a steady-state mechanism for a two-level system, even though some of his results indicated that the triplet states had been appreciably populated. Gires and Combaud[6] similarly studied a variety of phthalocyanine molecules, where they concluded that the triplet states of the phthalocyanine were negligibly populated, thus a steady-state two-level system for the molecules would be adequate to describe the saturation of absorption. Later investigation by Kosonocky[7,8] showed that after the passage of a high intensity laser pulse, almost all of the molecules can be in the triplet state. The question arises as to how important a role does the triplet state play in determining the saturation of absorption. Since the intersystem crossing time and the triplet-state lifetime are not precisely known, experimental results on saturation of absorption are generally compared to models which assume the two relaxations to be either short,[9] or long[10] with regard to the incident laser pulse duration.

Under a fast-relaxation steady-state condition, the saturation of absorption for any two or three level models was shown to depend on the input power level.[11] Shelden[12] has considered the case for a two-level system in which the excited-state lifetime is long enough to invalidate the steady-state assumption. Calculation on saturation of absorption indicated significant departure from the steady-state results. Hercher, et. al.[13] have considered systems with a long-lived triplet state and fast inter-system crossing: the saturation of absorption in this case was shown to depend on the integrated energy input. Experimental results have not been obtained which would verify these predictions.

Measurements on the saturation of absorption for organic molecules indicated that the molecules do not become completely transparent even at a very high intensity level;[10] there are residual losses present. Gires[10] first proposed this as due to excited-state absorption. Hercher,[11] and Huff,[14] have considered different aspects of the excited-state absorption on saturation of molecular absorptions. The experimental observations of Gibbs[4] indicated that significant excited-state absorption does take place in chloroaluminum phthalocyanine molecules when excited with a Q-switched ruby larer pulse. Furthermore, an increase in the transmission of the molecules up to some maximum value with a subsequent decrease at a

still higher intensity level was observed. However, it is not clear whether this is due to excited-singlet or triplet-state absorption.

Another problem associated with the saturable absorbers which has been of considerable interest, concerns the question of the homogeniety of the broadening mechanism of the electronic transitions in these molecules. Since the output spectral bandwidth of dye Q-switched laser is extremely narrow,[1] some frequency selective mechanism by the dye molecules may be involved. Sooy[15] has pointed out that natural selection of mode by the absorber in the laser cavity would be possible due to the large number of loop transits in the cavity required for the buildup of the Q-switched pulse. Soffer and McFarland,[16] in their experiments with frequency-locking of two lasers, indicated significant spectral hole-burning does exist in the phthalocyanine molecules. The term "spectral hole-burning" implied a reduction in absorption in the vicinity of a specific frequency. However, measurements on the bleaching spectrum of the phthalocyanine molecules indicated no permanent (i.e. of greater duration than 20 nsec or so) holes exist in the spectral transition.[8] This problem is still unresolved at this stage.

The purpose of this thesis is to study the three most commonly used saturable absorbers for Q-switching

ruby laser; cryptocyanine, metal-free phthalocyanine, and chloroaluminum phthalocyanine. Their saturation characteristics will be investigated by first determining several of their excited-state lifetimes. Then experimental results on saturation of absorption will be compared with theoretical results. Experiments will be performed to investigate the nature of residual absorption and the problem of spectral hole-burning. In Chapter II, the primary photophysical processes of organic polyatomic molecules which are important in the saturation of molecular absorptive transitions will be discussed briefly. Chapter III is concerned with the general spectroscopy of these three molecules. Various excited-state lifetimes will be determined. In Chapter IV, different mechanisms leading to the saturation of molecular absorption will be discussed, and the experimental results compared with the theoretical expressions. Additional measurements will be performed to investigate the excited-state absorption processes, which will serve to determine the nature of the residual losses. Chapter V and VI are concerned with the output characteristics of passively Q-switched laser. Experiments on the frequency-locking of two lasers will be performed to investigate the nature of the spectral hole-burning exhibited by the dye molecules. Several possible mechanisms leading to frequency-locking of two lasers will be discussed.

REFERENCES

1. B. H. Soffer, J. Appl. Phys. 35, 2551 (1964).
2. P. Kafalas, J. I. Masters, and E. M. E. Murray, J. Appl. Phys. 35, 2349 (1964).
3. J. G. Calvert, and J. N. Pitts, "Photochemistry". New York: Wiley, 1966, chapter 3.
4. W. E. K. Gibbs, Appl. Phys. Letters 11, 113 (1967).
5. J. A. Armstrong, J. Appl. Phys. 36, 471 (1965).
6. F. Gires, and F. Combaud, J. Phys. 26, 325 (1965).
7. W. F. Kosonocky, S. E. Harrison, and R. Stander, J. Chem. Phys. 43, 831 (1965).
8. W. F. Kosonocky, and S. E. Harrison, J. Appl. Phys. 37, 4789 (1966).
9. C. R. Giuliano and L. D. Hess, IEEE J. Quantum Electronics, QE-3, 358 (1967).
10. F. Gires, IEEE J. Quantum Electronics, QE-2, 624 (1966).
11. M. Hercher, Appl. Opt. 6, 947 (1967).
12. A. C. Selden, Brit. J. Appl. Phys. 18, 743 (1967).
13. M. Hercher, D. Stockman, and W. Chu, IEEE J. Quantum Electronics, QE-4, 966 (1968).
14. L. Huff, and L. G. DeShazer, J. Opt. Soc. Am. 59, 505A (1969).
15. W. R. Sooy, Appl. Phys. Letters 7, 36 (1965).
16. B. H. Soffer, and B. B. McFarland, Appl.Phys. Letters 8, 166 (1966).

CHAPTER II

GENERAL PROPERTIES OF THE MOLECULES

II-1 Introduction

In this chapter we consider briefly some aspects of the spectroscopy and related relaxations of the molecules which are most commonly used as saturable absorbers for Q-switching ruby lasers. These will be of direct interest to us in studying the dynamics of these molecules when used as Q-switching devices inside ruby laser cavities, in particular, for the study of the saturation of absorption under strong laser radiation.

II-2 The Interaction of Light with Polyatomic Molecules

Due to the manifolds of vibrational and rotational levels associated with each electronic state of a polyatomic molecule, its interaction with an electromagnetic field is significantly different from that of a simple atomic system. In particular, radiationless relaxations will be greatly enhanced due to overlapping of vibrational and rotational levels. Triplet states, under the zeroth

Figure II-1. Potential energy diagram for a diatomic molecule, S_o, S_1, and T_1 denote ground singlet, first excited singlet, and first triplet respectively.

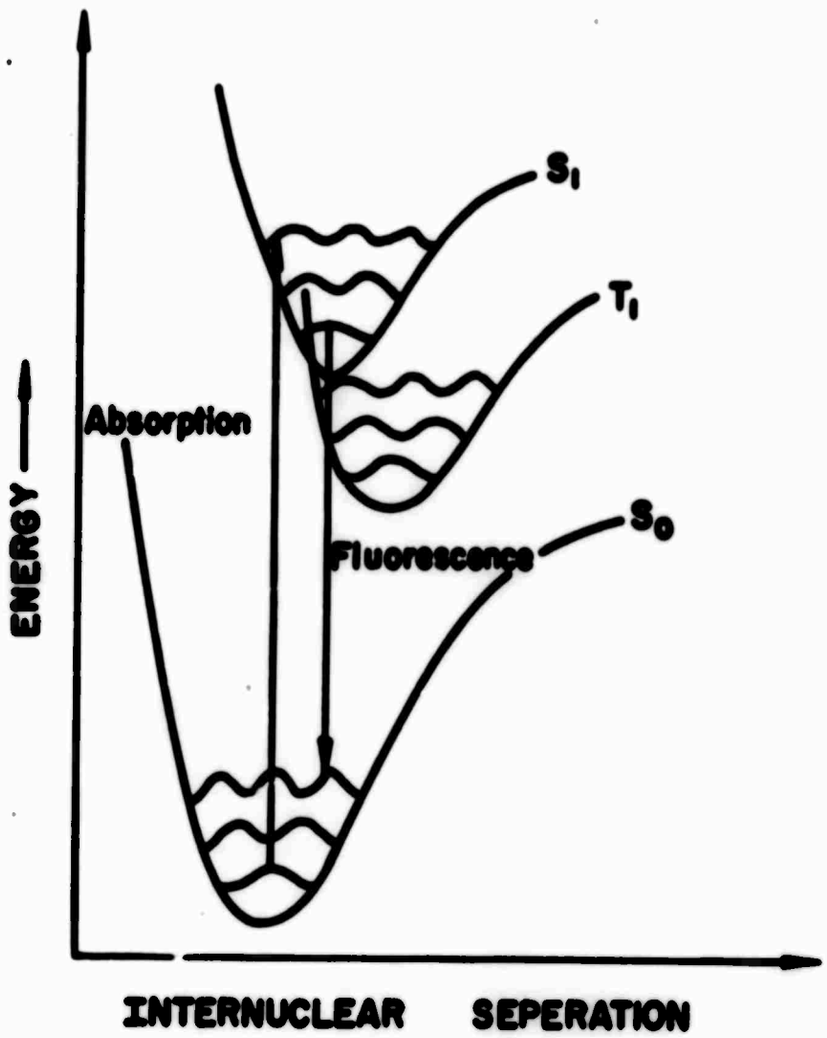
S_1
T_1
Absorption
S_0
Fluorescence
ENERGY
INTERNUCLEAR SEPERATION

order restriction of spin selection rules, cannot be optically excited from the ground singlet; however, with small inter-molecular perturbation, weak coupling still exists. The coupling between the triplet and the excited singlet is stronger than with the ground singlet due to stronger vibronic overlapping, thus making this coupling one of the major channels of decay for the excited singlet state.

As a simple illustration, a diagram for the potential energy curves of a diatomic molecule is shown in figure II-1. Within each potential well several vibrational levels are drawn; the corresponding wavefunctions are also shown. It should be noted that for a polyatomic molecule, potential energy surfaces have to be constructed with the associated vibrational levels. Photon absorption processes generally obey the Franck-Condon principle, which states that the time required for the absorption of a quantum of light and the resultant transition of an electron to an excited state is so short (10^{-15} sec) compared to the period of vibration of the molecule (10^{-13} sec) that during the act of absorption and excitation the nuclei do not appreciably alter their relative position or their kinetic energies. Thus the vertical straight lines represent transitions to the various vibrational levels of the excited electronic state.

Relaxation of the excitation normally follows several different channels of decay. Resonant fluorescence is rarely observed for polyatomic molecules even in vapor phase, as the molecules vibrationally equilibrate quickly, usually dropping to the zeroth vibrational level[1]. Fluorescence will originate from the zeroth vibrational level to the various vibrational levels in the ground state with a lifetime which is determined by the dipole strength of the electronic transition. Radiationless relaxation from the excited state to the ground state depends strongly on the overlapping of the two different vibronic manifolds, and also on environmental effects; such as solvent quenching.

Intersystem crossing to the triplet state has been known to play a vital role in depopulating the excited singlet. At present, the nature of the radiationless intersystem crossing is still not well understood. Transfer via the vibronic overlapping is believed to be the dominating mechanism, but solvent perturbation and spin-orbital coupling due to paramagnetic constituted atoms are also important[2].

Radiative relaxation of the triplet state is known to be relatively long due to small coupling between the triplet and the ground singlet, which gives rise to afterglow or phosphorescence. In a liquid state no phosphorescence can normally be observed, generally due to solvent

or impurity quenching. Oxygen has been known to be a particularly effective quencher of organic triplets in solution. Second order processes, most notably excited-state concentration quenching, will be important if the concentration of the excited molecules is high. The overall rate of decay of the triplet can be written as,

$$-\frac{d(N_2)}{dt} = k_1(N_2) + k_2(N_2)^2 + k_3(M)(N_2) \qquad \text{(II-1)}$$

where (N_2) is the concentration of the triplet, (M) is the concentration of the quenching molecules or the impurities, k_1, k_2, and k_3 are the radiative decay, second order decay, and the bimolecular quenching rates respectively.

Absorptive transitions to higher excited states are also possible if the transitions are allowed. Relaxations of the higher excited states will be extremely fast, of order 10^{-11} to 10^{-12} sec, due to strong overlapping of the different vibronic manifolds[1]. The triplet-triplet absorption spectrum can be measured with the technique of flash photolysis if the lifetime of the first triplet is sufficiently long; however, little work has been done on the first excited singlet's absorption due to the fact that its lifetime is of the order of 10^{-8} sec or less for strongly allowed transition.

Figure II-2. Jablonski energy-level diagram, showing the singlet and triplet manifolds, with the associated vibronic sub-structure.

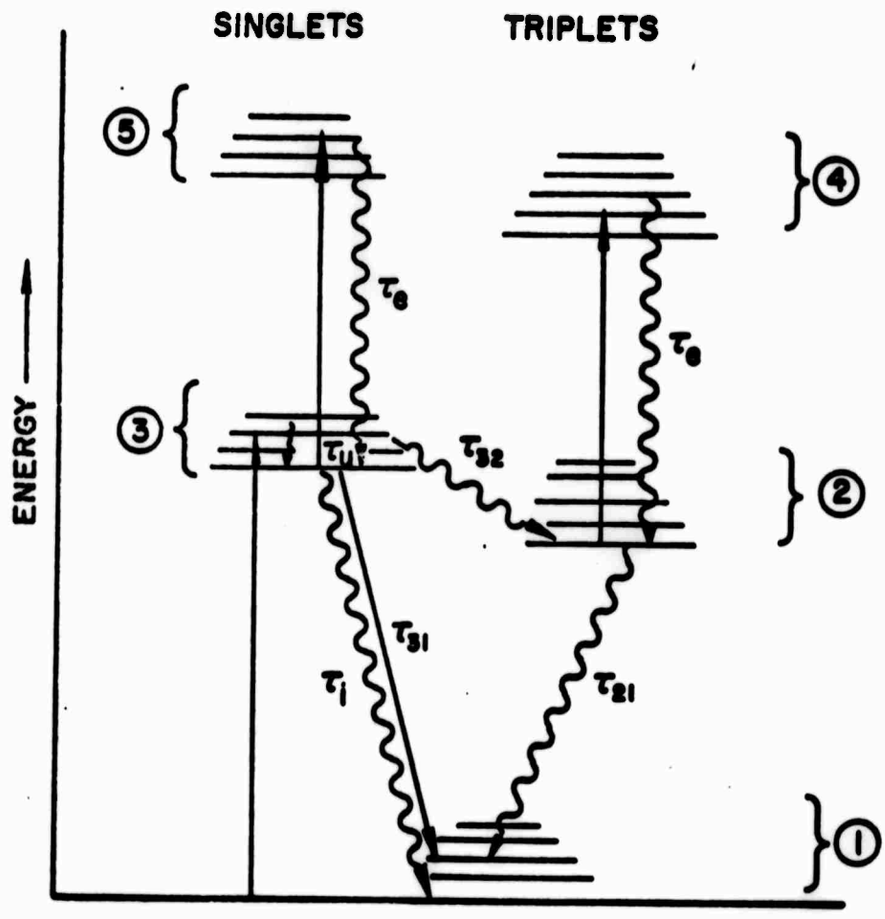
SINGLETS
TRIPLETS
ENERGY
5
4
3
2
1
τ_e
τ_e
τ_{32}
τ_{31}
τ_i
τ_{21}

II-3 Modified Jablonski Diagram and Related Parameters

In figure II-2, we have used a modified Jablonski diagram to describe the energy-level structure of a typical polyatomic molecule, showing the singlets and the triplets with their associated vibrational manifolds. Various first order relaxations are labelled at τ_i. We neglect rate processes of second order in dye concentration because in all cases a dilute solution of the molecules was used.

The following is a brief discussion of each of the parameters which is important in treating the interaction of light with a typical polyatomic molecule.

(1) σ - (absorption cross-section): In terms of the Einstein B coefficient the probability of an induced transition from the i^{th} level to the j^{th} level in a unit volume per unit time is

$$P_{ij} = u(\nu_{ij})\ B_{ij}\ N_i \qquad \text{(II-2)}$$

Here $u(\nu_{ij})$ is the energy density of the incident electromagnetic radiation at frequency ν_{ij}, N_i is the number of molecules in the i^{th} level, and the coefficient B_{ij} is

$$B_{ij} = \frac{2\pi|\mu_{ij}|^2}{3\hbar^2 g_i c} \qquad \text{(II-3)}$$

Here g_i is the degeneracy of the initial state, $|\mu_{ij}|^2$ is the total dipole moment matrix element squared, which is summed over all degenerate final and initial substates. If we assume that the exciting radiation is in the form of a quasi-collimated beam having a photon irradiance $I(\nu_{ij})$ photons/cm^{2}sec. at the frequency ν_{ij}, we can write the probability of the induced transitions per sec as

$$P_{ij} = I(\nu_{ij})\ \sigma_{ij}\ N_i \qquad \text{(II-4)}$$

Where $\sigma_{ij} = B_{ij}h\nu_{ij}/c$ is the absorption cross-section of the molecule at frequency ν_{ij}. This quantity is a characteristic of the moelcules involved and is independent of the incident radiation.

A determination of the absorption cross-section for a particular transition can easily be made. According to Beer's law

$$\frac{I_\nu}{I_{o\nu}} = e^{-N_o\sigma_\nu x} \qquad \text{(II-5)}$$

The transmission of the small signal incident intensity I_o is determined by N_o, the concentration of the molecules, σ_ν, the absorption cross-section at frequency ν, and x, the thickness of the cell being used.

(2) τ_{31} - (spontaneous radiative lifetime): This is just the inverse of the Einstein A coefficient and is given by

$$A_{31} = \frac{1}{\tau_{31}} = \frac{64\,\pi^4 \nu^3 |\mu_{13}|^2}{3h\,c^3\,g_3} \qquad \text{(II-6)}$$

For polyatomic molecules, if the excited state is homogeneously broadened, τ_{31} can be approximated from the integrated absorption curve by the modified Fuchbauer-Ladenburg formula[3]

$$\frac{1}{\tau_{31}} = 2.88 \times 10^{-9} \eta^2 \langle \tilde{\nu}_f^{-3} \rangle_{Ave.}^{-1} \frac{g_1}{g_3} \int \varepsilon d\ell n\tilde{\nu} \qquad \text{(II-7)}$$

where $\langle \nu_f^{-3} \rangle_{Ave}^{-1} = \int I(\nu)d\nu / \int \nu^{-3} I(\nu)d\nu$, $I(\nu)$ is the fluorescence intensity profile, ε is the extinction coefficient, g_i's are the degeneracy parameters associated with each i^{th} level, and η is the index of refraction.

(3) τ_3 - (overall lifetime of the excited state): Since second order kinetics are not important in a dilute solution, we consider only the several first order relaxations from the first singlet. τ_3 will be given by

$$\frac{1}{\tau_3} = \frac{1}{\tau_{32}} + \frac{1}{\tau_{31}} + \frac{1}{\tau_i} \qquad \text{(II-8)}$$

Experimentally, τ_3 can be determined if the radiative lifetime τ_{31} and the quantum yield of fluorescence $\phi_{fl.}$ is known, then τ_3 will be given by

$$\tau_3 = \phi_{fl.} \tau_{31} \qquad \text{(II-9)}$$

τ_3 can be measured directly by exciting the molecules with short duration light pulses and observing the fluorescence with a high speed detecting system. Using a mode-locked laser as an exciting light source with output pulses of duration in the 10^{-11} sec region, decay times of the order of 10^{-9} sec can be measured with a high speed photomultiplier. Duguay and Hansen[4] recently were able to measure lifetimes in the region of 10^{-11} sec with an ultrafast light gate.

(4) τ_{32} - (Intersystem crossing time): No direct spectroscopic method can be used to determine the intersystem crossing to the triplets. Techniques by which the populations of the triplet are being measured have been used to estimate the intersystem crossing rates. For strongly phosphorescing molecules, measurements of the quantum yield of phosphorescence will give an order of magnitude for the intersystem crossing rates[5]. For molecules exhibiting strong triplet-triplet absorptions, the time development of the triplet state populations under

excitation of a short duration pulse to the first singlets can be used to deduce the values of τ_{32}[6]. However, if the values of τ_3, τ_{31}, and τ_i are known, τ_{32} can be determined from equation (II-8). In some of the organic molecules, non-radiative relaxations back to the ground states are not significant, and τ_{32} can be determined by the simple expression

$$\tau_{32} = \frac{\tau_3 \tau_{31}}{\tau_{31} - \tau_3} \qquad \text{(II-10)}$$

(5) τ_{21} - (Overall lifetime of the triplet): From (II-1) we see that the triplet will relax with the three different mechanisms. Neglecting second order decay, we assign τ_{21} as an overall lifetime. Details concerning the triplet decay and its determination have been discussed before. However, it should be emphasized that triplet decays are generally long compared to other excited-state relaxations, and are usually dominated by non-radiative processes.

(6) $\phi_{fl.}$ - (Quantum yield of fluorescence): This quantity is defined as

$$\phi_{fl.} = \frac{\text{Number of fluorescent photons}}{\text{Number of absorbed photons}}$$

The relation between the radiative lifetime and the quantum yield of fluorescence is given by (II-9). Ordinary fluorescence measurements can be used to determine ϕ_{fl}. by integrating the total fluorescence output as compared with the amount of light absorbed by the sample.

(7) Non-radiative relaxations: These include relaxation processes from the first excited singlet to the ground singlet τ_i, intersystem crossing τ_{32}, vibronic relaxation within an electronic state τ_v, and higher excited electronic state relaxation processes to the adjacent lower excited state τ_e. The theory of non-radiative transitions is still incomplete due to the complexity of the problem. Environmental perturbation, especially the interaction with the phonon field of the solvent molecules, have been treated theoretically by Gouterman[7]. Perturbations due to various vibronic manifold overlappings have been treated by Siebrand,[8,9,10,11] and Robinson[2,12]. Comparing theoretical predictions with experimental data, Siebrand was able to obtain sufficiently good agreements for the case of aromatic hydrocarbons[9,10]. As for other large organic molecules, experimental data are still lacking for a detailed theoretical analysis. Experimental determinations of the various non-radiative relaxation processes are generally difficult since direct detection method can seldom be used. For the case of internal

conversion rates $(\tau_i)^{-1}$ from the first excited singlet states, one has to deduce their values by determining the rates for the various competing channels of decay: intersystem crossing and radiative decay. Vibrational relaxation rates $(\tau_v)^{-1}$ are believed to be very fast for relatively large molecules, due to the fact that fluorescence is generally observed to be originated from the thermally broadened lowest vibronic levels of the excited singlets. Using the ultrafast light gate technique, Duguay and Hansen[4] have been able to measure this relaxation rate, which is $\sim 10^{12}$ sec^{-1} for polymethine dye molecules. Internal conversion rates among the higher excited states $(\tau_e)^{-1}$ will be greatly enhanced for large molecules due to the strong overlappings among the different vibronic manifolds each associated with the closely spaced excited electronic states. Intersystem crossings from higher excited states to states with different multiplicity have been found to be insignificant compared to internal conversion[13], indicating that spin-selection rules are still preserved at higher excited levels.

II-4 Homogeneously versus Inhomogeneously Broadened System

In contrast to atomic system, polyatomic molecules exhibit diffused absorption bands due to the overlapping of the manifolds of broadened vibrational levels. The

broadening mechanisms for each individual vibronic level can generally be seperated into two categories. Firstly, the thermal broadening caused by random fluctuations of the nuclear coordinates in the molecules; and secondly, the collisional broadening caused by environmental perturbations. Low temperature measurements on the absorption and emission spectra can sometimes reveal the fine structure of the vibrational levels[14]. Similarly, some molecules show diffused absorption and emission bands in the presence as well as absence of collisions[15]. One infers that thermal broadening is the dominating mechanism for the broadening of the vibronic levels. Environmental perturbations, in particular collisions between solvent and molecules in liquid solutions, provide the means for the transfer of the excited vibrational energy to the surroundings.

For a system of absorbing centers, either in the gas phase or in the liquid phase with some inert solvent, if the absorption and emission profiles of each individual absorbing center are identical, the system is said to be homogeneously broadened. If, on the contrary, the absorption and emission profiles of some of the absorbing centers are different, it is inhomogeneously broadened. A system of molecules in the gas phase is a typical example of an inhomogeneously broadened system (i.e. Doppler broadening), while that in a dilute solution is

generally homogeneously broadened. However, if the system of molecules comprises different isomers, the absorption profile will be inhomogeneously broadened. Cyanine dye molecules have been shown to consist of equilibrium mixtures of two or more isomers at room temperature; the system exhibits strongly overlapping absorption bands which can be resolved only at very low temperature[16].

A particularly interesting property associated with inhomogeneously broadened system is that an intense monochromatic light of frequency ν_o can burn a spectral hole in the absorption curves, similar to the hole-burning in gas laser system[17]. Spectral hole-burning denotes reduction of absorption occurs only in the vicinity of frequency ν_o. For homogeneously broadened molecular system, spectral hole-burning can occur only on a transient basis due to the finite vibrational relaxation time of the excited states of the molecules[18]. This property will be discussed further in Chapter VI.

REFERENCES

1. J. G. Calvert and J. N. Pitts, "Photochemistry", New York: Wiley, 1966, Chapter 4.
2. G. W. Robinson and R. P. Frosh, J. Chem. Phys. 38, 1187 (1963).
3. S. J. Strickler and R. A. Berg, J. Chem. Phys. 37, 814 (1962).
4. M. A. Duquay and J. W. Hansen, to be published.
5. J. G. Calvert and J. N. Pitts, "Photochemistry", New York: Wiley, 1966, 668.
6. D. Stockman, private communication.
7. M. Gouterman, J. Chem. Phys. 36, 2845 (1962).
8. W. Siebrand, J. Chem. Phys. 44, 4055 (1966).
9. W. Siebrand, J. Chem. Phys. 46, 440 (1967).
10. W. Siebrand, J. Chem. Phys. 47, 2411 (1967).
11. W. Siebrand and D. F. William, J. Chem. Phys. 49, 1860 (1968).
12. C. W. Robinson, J. Chem. Phys. 47, 1967 (1967).
13. V. D. Kotsubanov, et.al., Opt. and Spectry. 25, 251 (1968).
14. E. V. Shpol'skii, Usp. Fiz. Nauk., 71, 216 (1960).
15. D. Eastwood, et.al., J. Mol. Spectry. 20, 381 (1966).
16. W. West, S. Pearce and F. Grum, J. Phys. Chem. 71, 1316 (1967).

17. W. V. Smith and P. P. Sorokin, "The Laser", New York: McGraw-Hill, 1966, 48.

18. M. Hercher, D. Stockman and W. Chu, IEEE, J. Quantum Electronics, QE-4, 954 (1968).

CHAPTER III

GENERAL SPECTROSCOPY OF THE THREE MOLECULES: CRYPTOCYANINE, METAL-FREE PHTHALOCYANINE, AND CHLOROALUMINUM PHTHALOCYANINE

III-1 Introduction

In this chapter, we shall discuss the general spectroscopy of cryptocyanine (1,1' diethyl-4,4'-monomethin-equinocyanine iodide), metal-free phthalocyanine, and chloroaluminum phthalocyanine (hereafter referred to as CC, H_2PC, and CAPC respectively), in considerable detail. Experimental determinations of the various parameters associated with these three molecules are also given.

III-2 Molecular Structures and Energy Levels

The molecular structures of these three molecules are shown in figure III-1. Earliest calculations of the energy levels of these molecules had been done by Kuhn[1] assuming a free-electron model for the π-electrons, circulating in the ring system of the phthalocyanine molecules or in the long chain system of the cyanine molecules.

Figure III-1. Molecular structure for (a) H_2PC, (b) CAPC, and (c) CC.

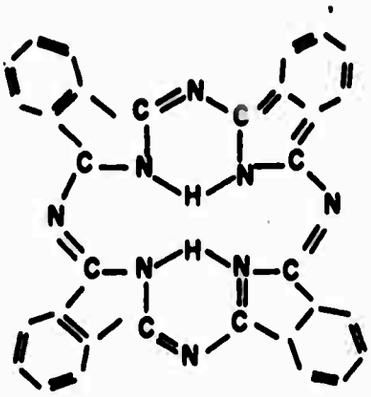

(a)

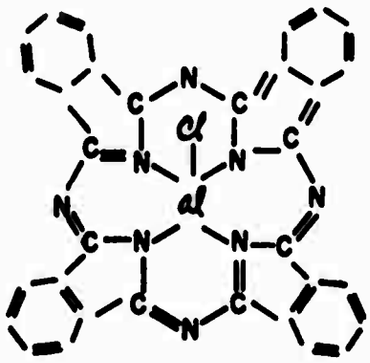

(b)

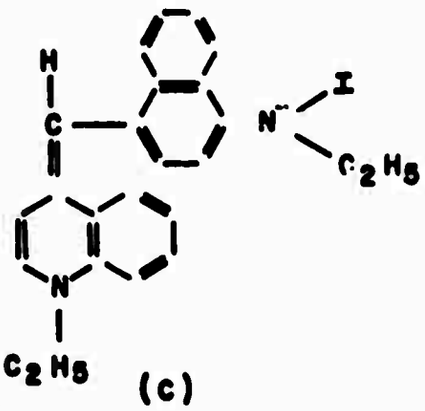

(c)

Figure III-2. Absorption and fluorescence spectra of (a) H_2PC in 1-chloronaphthalene, (b) CAPC in pyridine, and (c) CC in methanol. Solid lines are for absorption, broken lines are for emission. The vertical scales are relative.

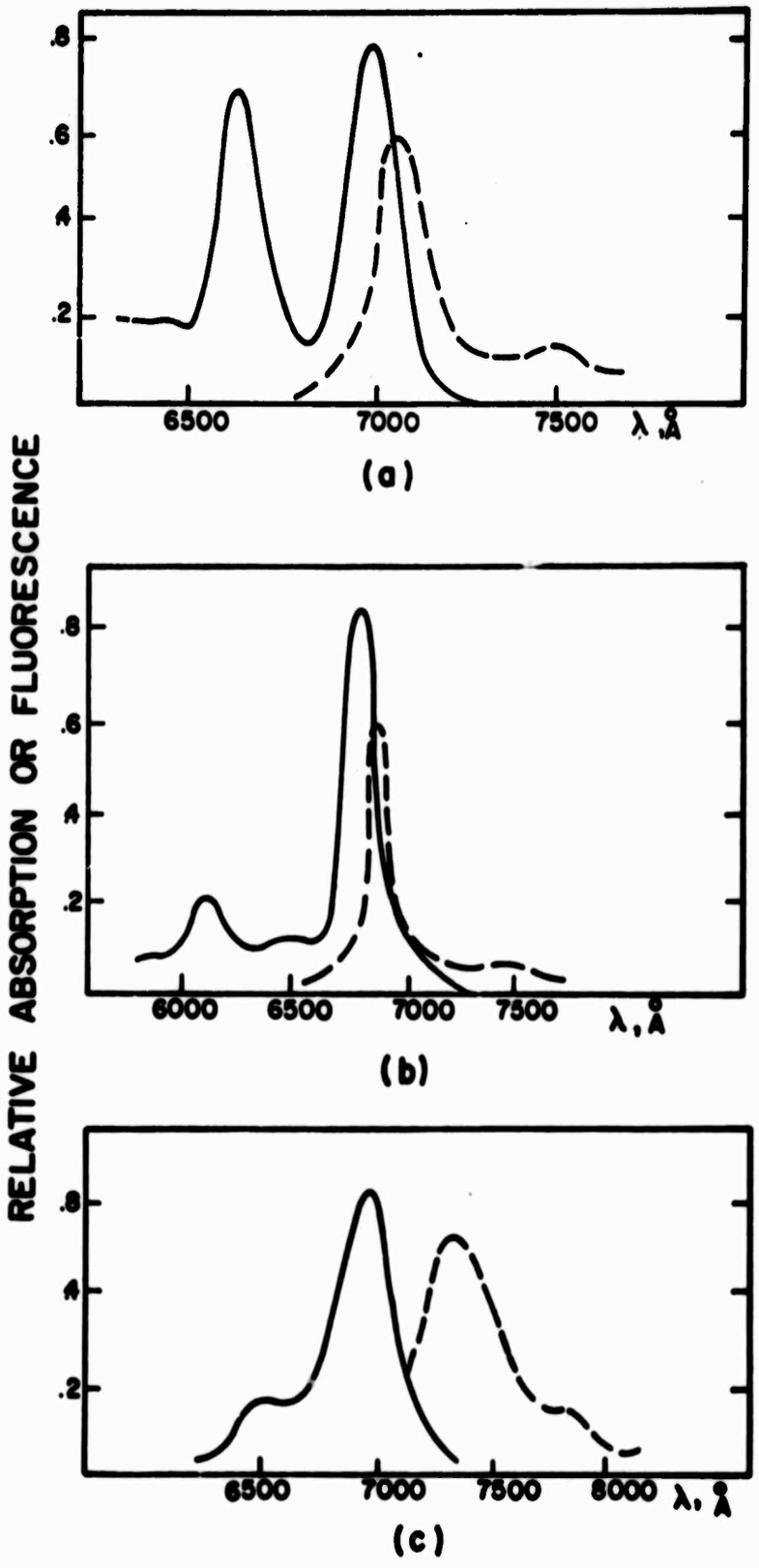
RELATIVE ABSORPTION OR FLUORESCENCE
.8
.6
.4
.2
6500
7000
7500
λ, Å
(a)
6000
6500
7000
7500
λ, Å
(b)
8000
(c)

BLANK PAGE

Qualitative agreements with the absorption spectrum of these molecules can be obtained from this simple theory. Recently Chen[2] did a detailed molecular orbitals calculation of the phthalocyanine, showing good agreement for the oscillator strength and the locations of the transitions.

III-3 Absorption and Fluorescence. Determination of Quantum Yield of Fluorescence for H_2PC

The first electronic absorption and fluorescence spectra of these molecules are shown in figure III-2. Mirror images of the absorption profile are generally observed for the fluorescence spectrum, indicating that the ground and the first excited state Franck-Condon curves are similar. The splitting in the metal-free phthalocyanine absorption curves is due to the lifting of the degeneracy by the lower symmetry of the molecular structure (two-fold symmetry for the metal-free versus four-fold symmetry for the metal phthalocyanine[2]). The Stokes shifts of the fluorescence peaks are approximately 50 Å for both phthalocyanine, whereas cryptocyanine exhibits a large Stokes shift of 200 Å. Solvent effects on the locations of the absorption peak have been measured for CAPC. For the four solvents used, viz. 1-chloronaphthalene, quinoline, pyridine, and ethyl alcohol, the absorption peaks occur at 6940 Å, 6870 Å, 6800 Å, and 6750 Å

Figure III-3. Experimental setup for fluorescence measurements.

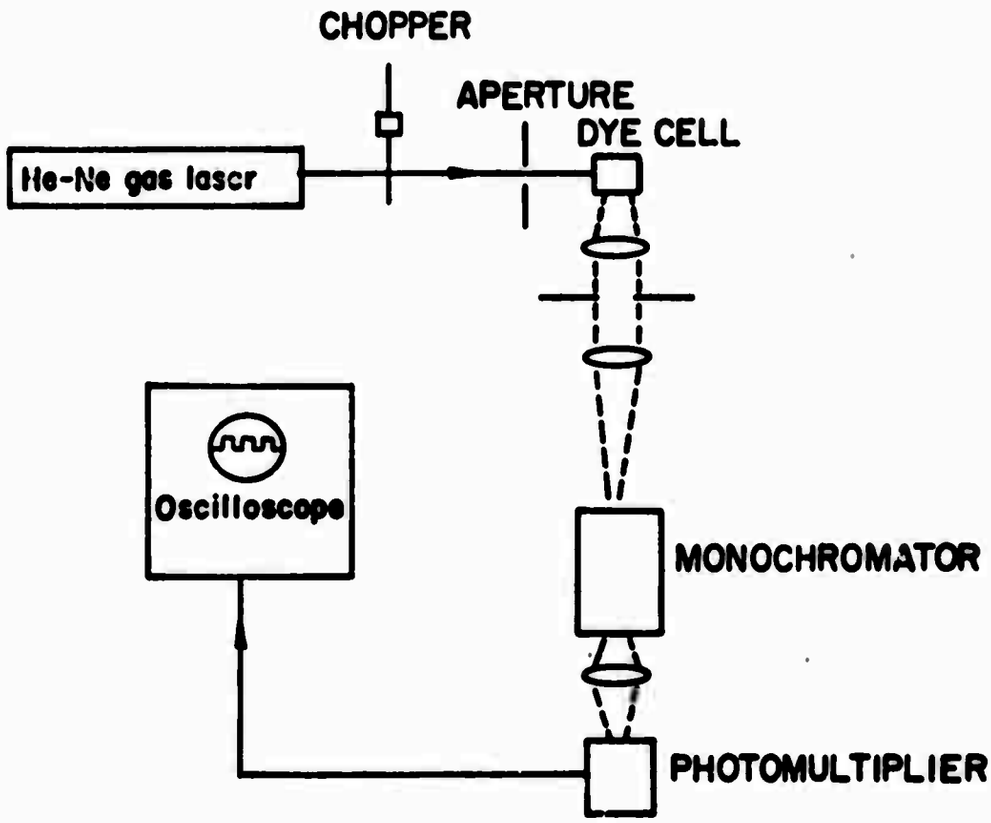
CHOPPER
APERTURE
DYE CELL
He-Ne gas laser
Oscilloscope
MONOCHROMATOR
PHOTOMULTIPLIER

respectively.

The absorption profile of the phthalocyanine molecules has been shown to be homogeneously boradened[3]. Uniform reduction of absorption across the absorption curve occurs during the passage of a high power Q-switched ruby laser pulse. Cryptocyanine behaves differently when pumped by a Q-switched ruby laser: significant reduction in absorption occurs only in the immediate vicinity of the ruby laser line (of order 10 Å) as observed by Sooy[4]. The mechanism responsible for the inhomogeniety of the absorption curves for cryptocyanine is still not clear, and will be discussed further in the next chapter in relation to the saturation of the molecules.

Measurement of the quantum yield of fluorescence for H_2PC in 1-chloronaphthalene was done using CAPC in pyridine as a standard. A schematic of the instrument is shown in figure III-3. An EML model LS-32 He-Ne gas laser was used to excite the molecules at 6328 Å. The solutions were contained in standard 1.0-cm-square cells. The dye concentrations of the solutions were kept at sufficiently low levels to insure that the optical densities of the solutions were no more than 0.05 so that Beer's law was obeyed and true solutions obtained. Fluorescence light was gathered through a B & L 33-86-25 grating monochromator and detected by an IT & T F4034 photomultiplier with an S-20 surface.

The ratio of quantum yield of fluorescence of H_2PC to CAPC was found to be approximately 0.6 after integrating the two emission curves. Taking the value of $\phi_{fl.}$ for CAPC to be 0.7,[5] we have $\phi_{fl.} \simeq 0.4$ for H_2PC.

The value of $\phi_{fl.}$ for crypotocyanine in methanol was estimated to be approximately 0.01, whereas in viscous glycerol, $\phi_{fl.}$ was measured to be a factor of 10 larger.[4] The solvent dependence of $\phi_{fl.}$ suggests either strong non-radiative decay or photochemical isomerization[6] through the excited singlet state of the cryptocyanine molecules.

III-4 Determination of the Lifetimes for the First Excited Singlet

The radiative lifetime for CC in methanol, H_2Pc in 1-chloronaphthalene, and CAPC in pyridine calculated from the absorption curves using equation (II-7) were found to be 5×10^{-9}, 7.6×10^{-9}, and 14.7×10^{-9} sec respectively.

Measurements on the fluorescence lifetimes τ_3 for the three dyes were done using a mode-locked ruby laser output as exciting source. The experimental setup is similar to that shown in figure III-3. A water cooled, 3 inches long ruby rod with anti-reflection coatings at both ends was pumped with a linear flash lamp in an elliptical cavity. The optical axis of the crystal was ~60° to the rod axis. The laser cavity lengths were

Figure III-4. Photographs for mode-locked laser output and fluorescence decay. (a) Scope photograph showing mode-locked ruby laser output. (b) Fabry-Perot interferogram showing mode-locked spectrum. (c) Scope photograph showing fluorescence decay for CAPC in pyridine excited with mode-locked laser output.

(a)

(b)

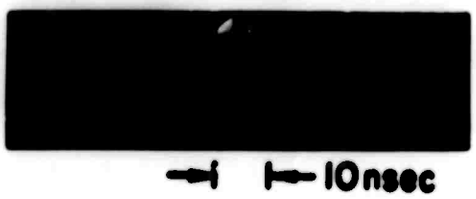

(c)

varied from 1.2 to 1.5 m with a 55% reflectivity dielectric mirror at the front end, and a 99% reflective dielectric mirror at the back end. The separation from the end mirror to the ruby rod was kept longer than 50 cm to ensure good locking of the modes[7]. Cryptocyanine dissolved in a mixture of methanol and ethyl alcohol was found to give stable mode-locked outputs. A typical oscilloscope trace of the mode-locked laser output is shown in figure III-4, together with the photograph for the output spectrum taken with a 9 mm quartz Fabry-Perot etalon. The relatively small number of modes being locked together suggests that the parallel end faces of the ruby rod act as a resonant reflector in discriminating against off resonant modes. The individual pulse-width estimated from the Fabry-Perot spectrum is of the order $\tau \sim 1/\Delta\nu \sim 10^{-9}$sec. It is to be noted that the ringing behavior associated with each pulse was due to the residual impedence mismatching in the detecting system. The total energy output in an envelope of pulses was 0.1 joule, giving an average of 10 MW peak power per pulse in the train.

The dye solutions were contained in a standard 1.0-cm-square cell. Fluorescence outputs were detected with an IT & T plano-photodiode and displayed on a Tektronix 519 travelling wave oscilloscope. RG-10 filters were used to eliminate scattered laser light. The overall risetime of the detecting system was less than two

nsec. Figure III-4 (c) shows a typical fluorescence output for CAPC in pyridine, the lifetime was measured to be $(10.0 \pm 0.6) \times 10^{-9}$ sec. Cryptocyanine in methanol showed a fluorescence lifetime less than the detector response time, i.e. $<2 \times 10^{-9}$ sec. H_2PC in 1-chloronaphthalene showed a lifetime comparable to the detector response time; the exact magnitude could not be determined due to the ringing in the detecting system.

The measured value of τ_3 for CAPC agreed well with the measurement done by Mack,[8] and also agreed with the value deduced from equation (II-9). Cryptocyanine in methanol exhibits a lifetime of 2.2×10^{-11} sec as measured by Dugnay and Hansen with the ultrafast light gate technique[9]. Using the value of 2.2×10^{-11} sec for τ_3, one obtains from (II-9) a value for $\phi_{f1.} = 0.005$, agreeing with the estimate of Sooy[4]. The lifetime of H_2PC is estimated from (II-9) to be $\sim 3 \times 10^{-9}$ sec; this value will be compared with later results on the saturation of the H_2PC molecules.

III-5 Determination of the Intersystem Crossing Times τ_{32} and the Triplet Relaxation Times τ_{21}

Triplet-state lifetimes of H_2PC and CAPC in air-equilibrated solutions have been shown to be relatively long; an order of 5×10^{-7} to 10^{-6} sec has been obtained

by Kosonocky and Harrison,[8] and Stockman[5], using the laser flash photolysis technique. For degassed solutions, the lifetime increases to $\geq 10^{-4}$ sec, indicating the quenching action of dissolved oxygen molecules on the population of the triplet states. Intersystem crossing rates in these molecules deduced from (II-8), assuming slow non-radiative relaxation processes, are 33.4×10^{-9}, and 5×10^{-9} sec for CAPC and H_2PC respectively. The value $\tau_{32} = 33.4 \times 10^{-9}$ sec for CAPC agrees with the recent measurement by Stockman[5]. The apparently fast crossing rate for H_2PC is questionable since the two molecules (CAPC and H_2PC) have similar molecular structures. Two measurements were performed to estimate the value of τ_{32} for the two phthalocyanine molecules. The results have great bearing on deciding the mechanism responsible for the saturation of these molecules by high intensity light pulses, viz, energy saturation or power saturation.

The technique used to measure τ_{32} is based on the assumption of a three-level scheme for the moelcules. The rate equations describing the population changes of n_1, n_2, and n_3, which are the normalized populations of the ground, triplet and first excited singlet state respectively, can be written as

$$dn_1/dt = -I\sigma_{13}n_1 + n_3/\tau_{31} \qquad \text{(III-1)}$$

$$dn_2/dt = n_3/\tau_{32} \qquad \text{(III-2)}$$

$$dn_3/dt = I\sigma_{13}n_1 - n_3/\tau_3 \qquad \text{(III-3)}$$

here we have let $\tau_{21} \to \infty$, which is true for phthalocyanine molecules under the time scale of interest ($<10^{-7}$ sec). Stimulated emission terms are neglected due to the fast relaxation from the excited vibronic level to the zeroth vibronic level. The solutions to these coupled differential equations can be solved exactly assuming a step input irradiance, giving,

$$n_1(t) = (\lambda_1 - \lambda_2)^{-1}[(\lambda_1 + 1/\tau_3)e^{\lambda_1 t} - (\lambda_2 + 1/\tau_3)e^{\lambda_2 t}] \qquad \text{(III-4)}$$

$$n_3(t) = -[I\sigma_{13}/(\lambda_1 - \lambda_2)]\ (e^{\lambda_1 t} - e^{\lambda_2 t}) \qquad \text{(III-5)}$$

$$n_2(t) = 1 - n_1(t) - n_2(t) \qquad \text{(III-6)}$$

$$\lambda_1 = (1/2)[-(I\sigma_{13} + 1/\tau_3) - \sqrt{(I\sigma_{13}+1/\tau_3)^2 - 4I\sigma_{13}/\tau_{32}}] \qquad \text{(III-7)}$$

$$\lambda_2 = (1/2)[-(I\sigma_{13} + 1/\tau_3) + \sqrt{(I\sigma_{13} + 1/\tau_3)^2 - 4I\sigma_{13}/\tau_{32}}]$$

Figure III-5. Transient development of n_1, n_2, and n_3 for a high intensity input pulse. It is assumed that the exciting radiation field is a rectangular pulse of duration 30 nsec. The curves labeled n_2 and n_3 show the buildup and decline of the triplet and the first excited singlet respectively, with a time constant $\tau_{32}^{-1} = 3 \times 10^7$ sec^{-1} during the presence of the exciting pulse. The broken line shows the transient development of the ground state n_1. The figure is intended to be illustrative only.

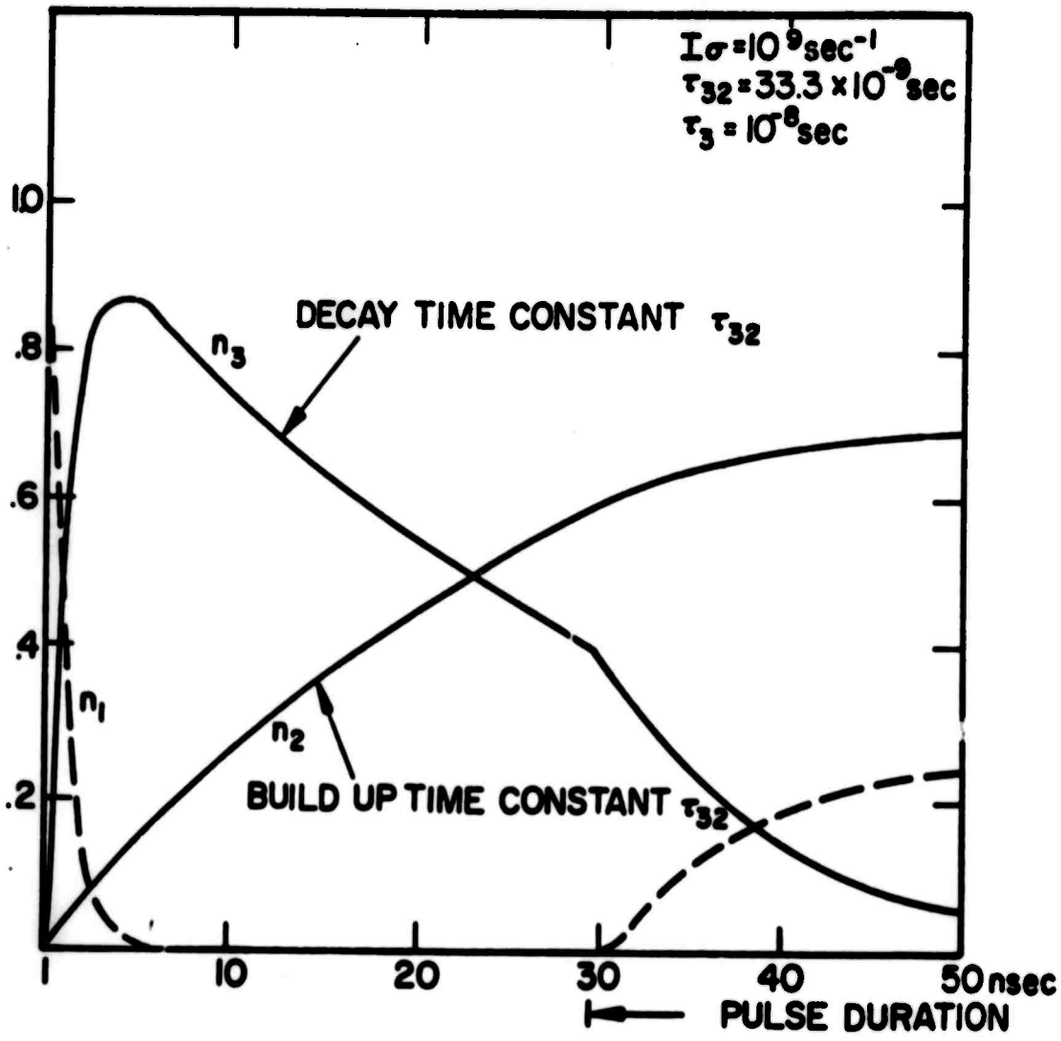
$I\sigma = 10^9 sec^{-1}$
$\tau_{32} = 33.3 \times 10^{-9} sec$
$\tau_3 = 10^{-8} sec$
1.0
.8
.6
.4
.2
n_3
DECAY TIME CONSTANT τ_{32}
n_1
n_2
BUILD UP TIME CONSTANT τ_{32}
1
10
20
30
40
50 nsec
PULSE DURATION

For $I > 1/(\tau_3\sigma_{13})$, we have $\lambda_1 \sim -I\sigma_{13}$, $\lambda_2 \sim -1/\tau_{32}$, and the solutions simplify to

$$n_3(t) = e^{-I\sigma_{13}t} - e^{-(1/\tau_{32})t} \qquad \text{(III-8)}$$

$$n_2(t) = 1 - e^{-(1/\tau_{32})t} \qquad \text{(III-9)}$$

The first exponential for n_3 described the rapid buildup of the n_3 state population, while the second exponential described the crossing rate into the triplet state. For a rectangular input pulse, the relative time development of the three levels are shown in figure III-5. One infers from this figure that exciting the molecules with high intensity light pulses, the value of τ_{32} and τ_{21} can be deduced by measuring the decay rate of n_3 and the buildup for n_2 during the transient region.

Two measurements were carried out to investigate the time development of n_3 and n_2 separately under excitation by a high power Q-switched pulse. Fluorescences output from these molecules give a direct measure of the population of n_3. Phthalocyanine molecules exhibit strong triplet-triplet absorption near 4850 Å with a peak extinction coefficient of the order of 4×10^4 lit-ers/mole-cm.[5,10] The strong triplet-triplet absorptions were used to monitor the buildup of the triplet state.

The experimental setup for the fluorescence output

Figure III-6. Output from Q-switched ruby laser and fluorescence output from H_2PC. (a) Q-switched ruby laser output pulse. (b) Fluorescence output for H_2PC in 1-chloronaphthalene exciting with pulse as shown in (a). (Both drawings are traced from scope photographs).

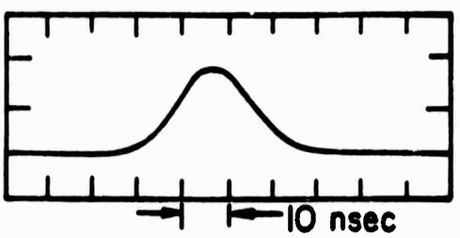

(a)

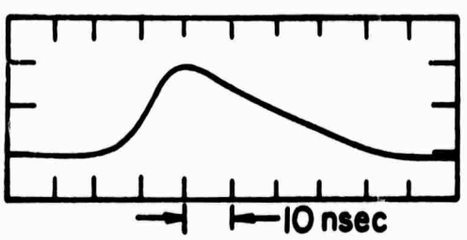

(b)

Figure III-7. Experimental setup for triplet-triplet absorption measurements.

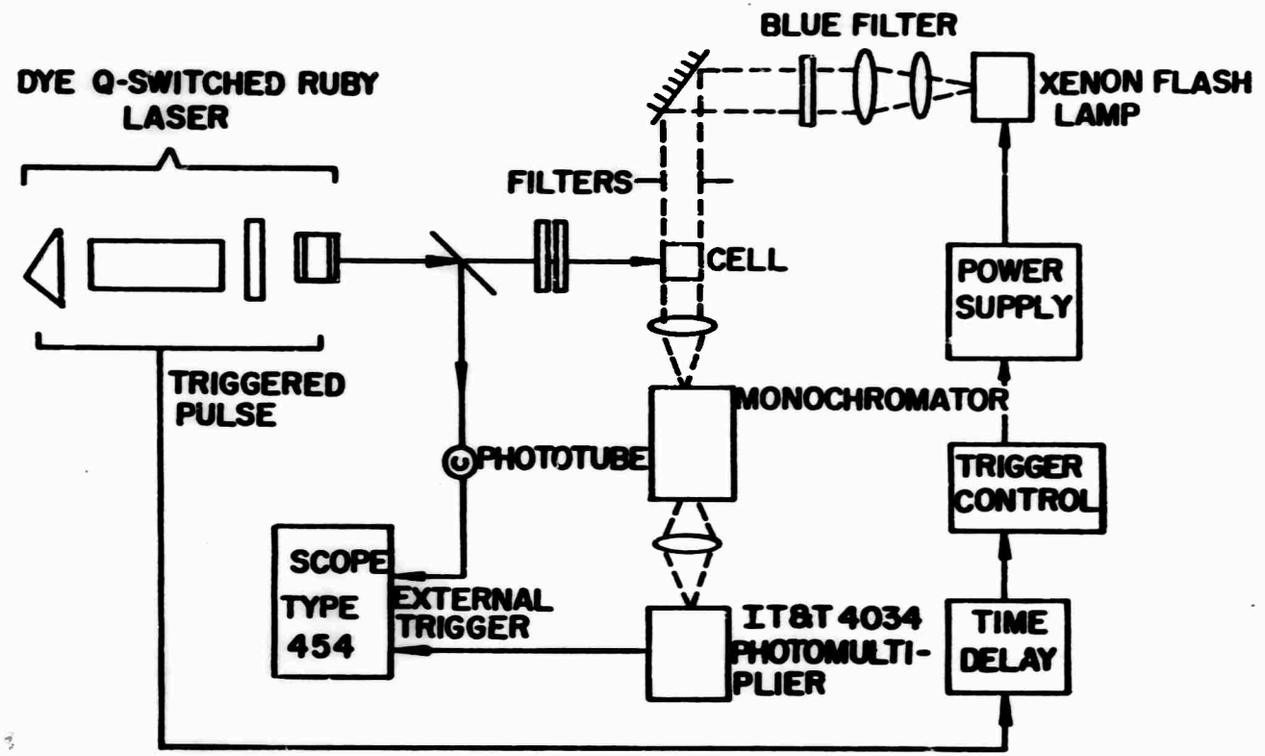
BLUE FILTER
DYE Q-SWITCHED RUBY LASER
XENON FLASH LAMP
FILTERS
CELL
POWER SUPPLY
TRIGGERED PULSE
MONOCHROMATOR
PHOTOTUBE
TRIGGER CONTROL
SCOPE TYPE 454
EXTERNAL TRIGGER
IT&T 4034 PHOTOMULTI-PLIER
TIME DELAY

measurements is similar to those shown in figure III-3. The Q-switched ruby laser used was the same as described before except that a resonant reflector[11] and a Brewster angle roof prism were used as front and back reflectors. The laser was Q-switched using a cryptocyanine saturable filter; the peak power was approximately 20 MW with a spectral bandwidth of no greater than 200 MHZ. The Q-switched pulse duration was varied from 10 to 30 nsec. Solutions were contained in a standard 1.0-cm cell with dye concentrations kept below 10^{-5} molar. Fluorescence outputs were detected at right angles to the laser beam with an IT & T planophotodiode. Outputs were displayed on a Tektronix 454 scope with a 3 nsec risetime. RG-10 filters were used to eliminate scattered laser light. Figure III-6 shows a typical fluorescence output for H_2PC in 1-chloronaphthalene, showing a long decay in the saturation region. Similar results were obtained for CAPC in pyridine with a slightly longer decay time. The intersystem crossing times deduced from these data were $(25 \pm 3) \times 10^{-9}$ and $(28 \pm 3) \times 10^{-9}$ sec. for H_2PC in 1-chloronaphthalene and CAPC in pyridine respectively.

The experimental setup for the triplet-triplet absorption measurements is shown in figure III-7. A xenon flash lamp powered by a Trion laser power supply was used as the probe light for the absorptions from the triplet states. Blue and green filters were used to cut off red

Figure III-8. Scope photographs showing transient development of the triplet-triplet absorption. (a) Xenon flash lamp output. Horizontal scale: 10 μsec/div. (b) Ruby laser output. Horizontal scale: 100 nsec/div. (c) Transient development of the triplet-triplet absorption for H_2PC in 1-chloronaphthalene. Horizontal scale: 50 nsec/div.

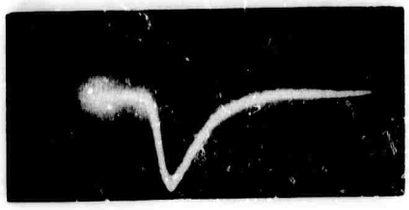

(a)

(b)

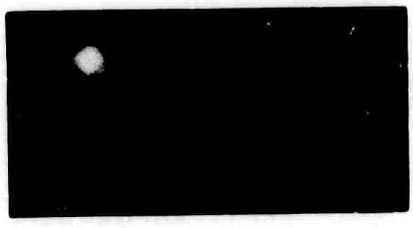

(c)

and UV emissions from the xenon flash lamp. The Q-switched ruby laser was the one described before with the output beam intersecting the probe light at a right angle inside the 1.0 cm solutions cell. The transmitted probe light was detected by the IT & T F4034 photomultiplier, through a B & L monochromator with a bandpass of 20 Å, set at 4850 Å. The flash lamp output duration was 20 μsec, and and electronic time-delay triggering system was used to synchronize the Q-switched output with the flash lamp output. The signals were displayed on the Tektronix 454 scope which was triggered by the Q-switeche pulses. Dye concentrations of $\sim 10^{5}$ molar were used to give a maximum signal-to-noise ratio in the photomultiplier output.

Figure III-8 shows the time development of the triplet-triplet absorption for CAPC in pyridine. Values of τ_{32} deduced from these data agree with the results obtained from the fluorescence output measurements for both H_2PC and CAPC. The long decay of the triplet-triplet absorptions ($\sim 5 \times 10^{-7}$ sec), agree with the measurement of τ_{21} by Hercher et al.[6] using different equipment.

Cryptocyanine in methanol are different from the phthalocyanine molecules in that most of the ground state population returns within 3×10^{-9} sec after being irradiated with a high intensity Q-switched ruby laser pulse[4]. This suggests that cryptocyanine in methanol either have fast decay rates for τ_{21} and τ_{32} (less than

Dye	τ_{31} * sec	τ_3 sec	τ_{32} sec	τ_{21} sec	$\phi_{fl.}$	Solvent
CAPC	15×10^{-9}	10^{-8} †	2.8×10^{-8} †	5×10^{-7} †	~0.7 ††	pyridine
H_2PC	8×10^{-9}	3×10^{-9} †	2.5×10^{-8} †	5×10^{-7} †	~0.4 †	1-chloro-naphthalene
CC	5×10^{-9}	2×10^{-11} **	$3 \times 10^{-9} <$ †	$3 \times 10^{-9} <$ †	0.05 ***	methanol

Table I - Lifetimes for the three molecules

* Calculated from equations (II-7)

† Measurements performed in this chapter

†† Reference 5

** Reference 9

*** Reference 4

3×10^{-9} sec), or slow decay rates (greater than the Q-switched pulse duration, >> 30 nsec). Evolution of the fluorescence for the cryptocyanine in methanol when excited with a Q-switched ruby laser pulse show that the fluorescence follows the Q-switched pulse to within the detecting system resolution time. This result rules out the possibility of a long-lived triplet state associated with cryptocyanine in methanol.

III-6 Summary

Table I contains all the known parameters associated with the three dyes being investigated; these values will be used in the next chapter to study the saturation mechanisms of these three molecules. The accuracy in the determination of τ_{32} for the phthalocyanine molecules is only of order of magnitude due to the following two assumptions; (1) a rectangular incident pulse is used instead of an actual near-Gaussian Q-switched pulse, and (2), stimulated emission is not taken into account. By inspection of equation (III-7), as the intensity I is greater than $\sigma_{13}\tau_3$, the population n_3 and n_2 will be relatively insensitive to small variation in I; thus no major error will be introduced by the first assumption. The second assumption concerns the stimulated emission from the excited state. Since the excited level is one of the

excited subvibronic levels which decays rapidly to the zeroth vibronic level, stimulated emission should not be significant.

Using equation (II-8), taking τ_3, τ_{32}, τ_{31} respectively as 3×10^{-9}, 25×10^{-9}, and 7.6×10^{-9} sec for H_2PC in 1-chloronaphthalene, one deduces a non-radiative lifetime of 7×10^{-9} sec. The fact that non-radiative decay does play a role in H_2PC is not surprising when one considers the results obtained by Eastwood,[12] in which $\phi_{fl.}$ was found to be ten times greater than at 300° C (liquid), and one hundred times greater than at 350° C (vapor).

REFERENCES

1. H. Kuhn, J. Chem. Phys. 17, 1198 (1949).
2. I. Chen, J. Mol. Spectry. 23, 131 (1967).
3. W. F. Kosonocky and S. E. Harrison, J. Appl. Phys. 37, 4789 (1966).
4. W. R. Sooy, and M. L. Spaeth, J. Chem. Phys. 48, 2315 (1968).
5. D. Stockman; private communication.
6. M. Hercher, D. Stockman, and W. Chu, IEEE J. Quantum Electronics, QE-4, 966 (1968).
7. H. W. Mocker and R. J. Collins, Appl. Phys. Letters 7, 270 (1965).
8. M. Mack, J. Appl. Phys. 39, 2483 (1968).
9. M. A. Dugney and J. W. Hansen, to be published.
10. J. Villar and L. Lindquist, Compt. Rend. Acad. Sci. (Paris), B264 1807 (1967).
11. M. Hercher, Appl. Phys. Letters 7, 39 (1965).
12. D. Eastwood, et al., J. Mol. Spectry. 20, 381 (1966).

CHAPTER IV

SATURATION CHARACTERISTICS OF DYE MOLECULES

IV-1 Introduction

In this chapter we study the saturation of molecular absorption under high intensity light pulses. Three different mechanisms leading to the saturation of absorption will be investigated theoretically. Experimental results obtained from the three dye molecules; CC, H_2PC, and CAPC will be compared with the theoretical expressions. Experimental measurements of the excited-state absorption will be analyzed to determine the cause of residual losses.

IV-2 Theoretical Treatment of the Interaction

Consider the molecules being irradiated with a monochromatic light pulse of duration from 10 to 30 nsec. The response of these molecules can be described by a set of differential equations giving the rates of change of each level involved in the interaction. Using the modified Jablonski diagram for the energy scheme of all the molecules as in figure II-2, we have

$$dn_1/dt = -I(t)\sigma_{13'}(n_1 - n_{3'}) + n_2/\tau_{21} + n_3/\tau_{31} + n_5/\tau_{51}$$

$$dn_2/dt = n_3/\tau_{32} - n_2/\tau_{21} - I(t)\sigma_{24}n_2 + n_4/\tau_{42}$$

$$dn_{3'}/dt = I(t)\sigma_{13'}(n_1 - n_{3'}) - n_{3'}/\tau_v$$

(IV-1)

$$dn_3/dt = n_{3'}/\tau_v - n_3/\tau_3 - I(t)\sigma_{35}n_3 + n_5/\tau_{53}$$

$$dn_4/dt = I(t)\sigma_{24}n_2 - n_4/\tau_4$$

$$dn_5/dt = I(t)\sigma_{35}n_3 - n_5/\tau_5$$

where n_i are the normalized populations of each i^{th} level. We have assumed that the dye sample is optically thin, and that the time variation in intensity is negligible during the transit time for light through the dye sample. This is equivalent to the approximation that each molecule experiences the same intensity at a given instant of time. This assumption is approximately true for a dilute system.

The use of rate equations for the description of the interaction of light with molecules is valid only under specific conditions. Tang[1] has shown that the semi-classical approach with a density matrix formalism for a two-level system reduces to simple rate equations if $T_1 >> T_2$, where T_1 is the relaxation time for the excited level, and T_2 is the transverse relaxation for the excited

level[2], which is inversely proportional to the halfwidth of the homogeneous absorption profile. In liquids, dye molecules experience high collision rates with the solvent molecules at room temperature, giving $T_2 \sim (\text{collision rate})^{-1} \sim 10^{-12}$ sec. The excited state lifetime for large organic molecules is of the order of 10^{-9} sec, thus giving a ratio of $T_2/T_1 \sim 10^{-3}$. Thus the application of rate equations to a two-level model is justified in this case, generalizing to a system of multi-levels is also reasonable valid.

Due to the vibronic overlapping for higher excited states, the relaxations τ_4 and τ_5 are of the same order as τ_v, which is extremely fast. The above equations can therefore be simplified to give only three equations describing the three levels which are of major importance in the interaction,

$$dn_1/dt = -I(t)\sigma_{13}n_1 + n_3/\tau_{31} + n_2/\tau_{21}$$

$$dn_3/dt = I(t)\sigma_{13}n_1 - n_3/\tau_3 \qquad \text{(IV-2)}$$

$$dn_2/dt = n_3/\tau_{32} - n_2/\tau_{21}$$

Generally, three different types of saturation regime can be applied to all molecules with different rate constants. The classification of the three regimes is

BLANK PAGE

(1) steady state saturation; excited molecules having relaxation times faster than the duration of a normal Q-switch pulse fall into this category. (2) Energy saturation; excited molecules with a fast decay to a long-lived metastable state (the triplet state in our case) which will accommodate all the excited electrons into that level with a complete depletion of ground state population. (3) Transient saturation; excited molecules with relaxation times comparable to the duration of the Q-switch pulse.

(1) Steady state saturation

If all the relaxation times are short compared to the temporal structure of the incident light pulse, then at each instant of time the system will be very nearly in a steady-state. Thus, for an optically thin sample, the population densities can be expressed as functions of the instantaneous photon irradiance:

$$n_1 = 1/(1 + I/I_s)$$

$$n_2 = I\sigma_{13}\tau_3/(1 + I/I_s) \qquad \text{(IV-3)}$$

$$n_3 = I\sigma_{13}\tau_3(\tau_{21}/\tau_{32})/(1 + I/I_s)$$

Figure IV-1. Steady-state saturation. Curves showing the steady-state transmission of an optically thick saturable absorber as a function of irradiance (normalized to the saturation irradiance I_s). Excited-state absorption is included as $I_s b = 0.143$.

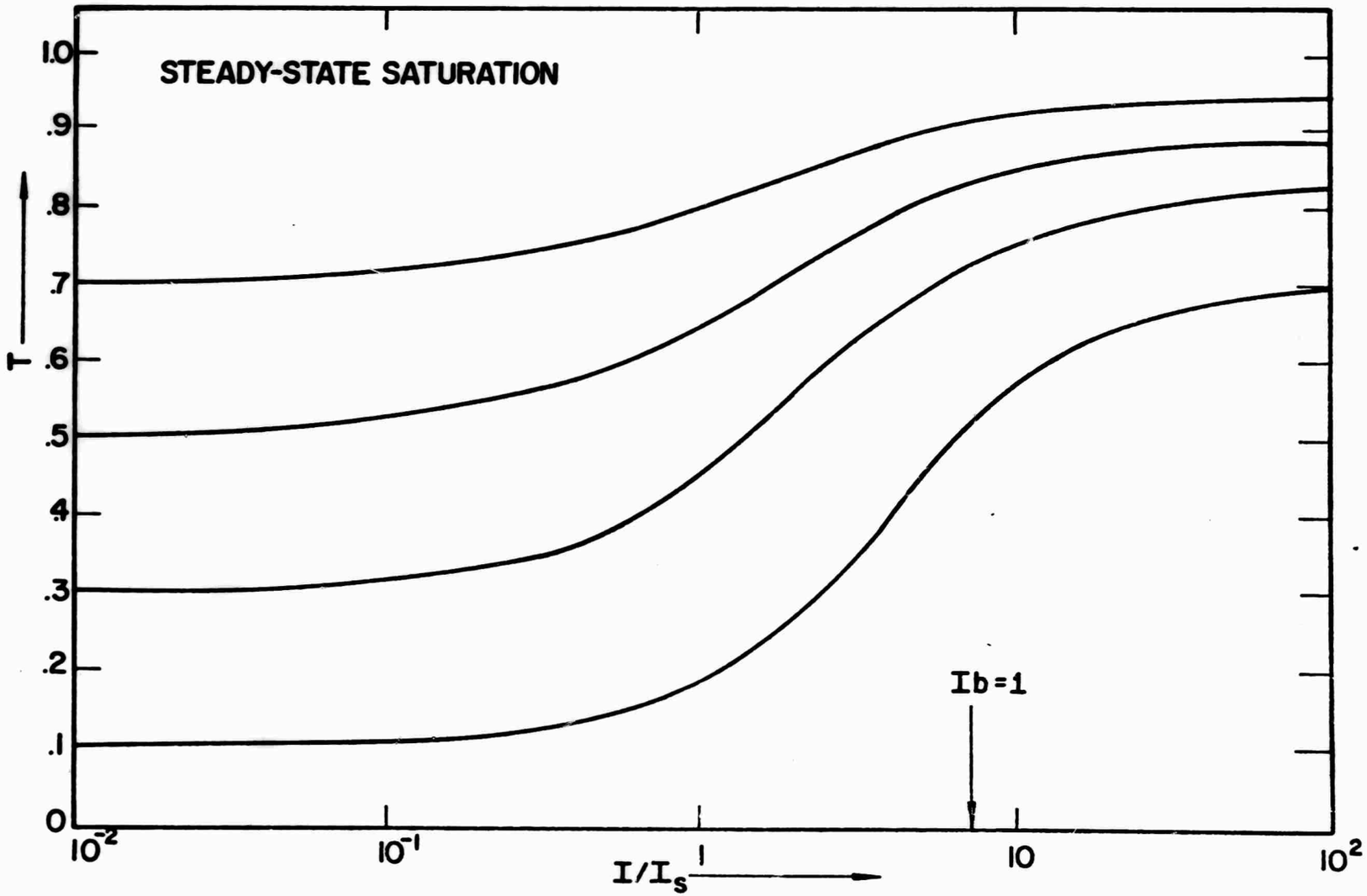
STEADY-STATE SATURATION
1.0
.9
.8
.7
.6
.5
.4
.3
.2
.1
0
T
Ib=1
10^{-2}
10^{-1}
1
10
10^{2}
I/I_s

Where $I_s = [\sigma_{13}\tau_3(1 + \tau_{21}/\tau_{32})]^{-1}$ is the saturation irradiance; it is the photon irradiance for which the steady state absorption coefficient is reduced by a factor of two over the small-signal absorption coefficient[3].

The transmission characteristics of an optically thick sample can be derived starting with

$$dI/dx = - I\alpha_o(n_1 + \gamma n_2 + \beta n_3) \qquad \text{(IV-4)}$$

where $\gamma = \sigma_{24}/\sigma_{13}$, and $\beta = \sigma_{35}/\sigma_{13}$. The excited singlet and the triplet absorptions are taken into account by assuming that the higher excited levels are not appreciably populated. Substituting the steady-state values of n_i and integrating, we obtain finally

$$T_o = [(1 + bIT)/(1 + bI)]^{1/(I_s b)-1} \qquad \text{(IV-5)}$$

Where $T_o = e^{-\alpha_o x}$, $T = I_{transmitted}/I_{incident}$, and $b = \sigma_{13}\tau_3\beta[1 + (\gamma/\beta)(\tau_{21}/\tau_{32})]$. Figure IV-1 shows the steady-state transmission characteristics. It is to be noted that the excited-state absorption contribution to the residual loss gives a large signal transmission of $T_{I \to large} = T_o^{I_s b}$.

(2) Energy saturation

The metastable state involved in this case is the long-lived triplet level. With all other relaxations fast compared with the Q-switched pulse duration, we have for the three-level system $1/\tau_{21} \to 0$, and (IV-2) becomes:

$$\begin{aligned} dn_1/dt &= -I\sigma_{13}n_1 + 1/\tau_{31} \\ dn_2/dt &= n_3/\tau_{32} \\ dn_3/dt &= I\sigma_{13}n_1 - n_3/\tau_{31} \end{aligned} \qquad \text{(IV-6)}$$

For a fast τ_3, n_3 will also be small, one can write $n_1 + n_2 \sim 1$. Solving (IV-6) for this case, we have $n_3 \sim I\sigma_{13}\tau_3 n_1$. Substituting into (IV-6), we have

$$\begin{aligned} dn_1/dt &= -I\sigma_{13}(1 - \tau_3/\tau_{31})n_1 \\ &= I\sigma_{13}(1 - \phi_{fl.})n_1 \end{aligned} \qquad \text{(IV-7)}$$

Integrating, for $E = \int_0^t dtI(t)$, we have $n_1 = e^{-E/E_s}$, where $E_s = [\sigma_{13}(1 - \phi_{fl.})]^{-1}$, and $\phi_{fl.} = \tau_3/\tau_{32}$. Similarly we have $n_2 \sim 1 - n_1$. So that the change of the ground state population depends on the integrated energy input (or number of photons/cm^2)

The transmission characteristics of an optically

thick sample can be derived by separating the contributions into three parts: (a) Ground state absorption: The number of photons absorbed is proportional to the number of molecules excited into the triplet,

$$dE/dx = - N_o[n_1(O) - n_1(E)]/(1 - \phi_{fl.}) = - N_o(1 - e^{-E/E_s})/(1 - \phi_{fl.}) \qquad \text{(IV-8)}$$

(b) Triplet state absorption: We have

$$dI/dx = - I\sigma_{13}\gamma n_2 N_o \qquad \text{(IV-9)}$$

The time dependence of n_2 is neglected, i.e., we assume n_2 to be a slowly varying function of time, which is true for τ_{21} long and τ_{32} short. Integrating equation (IV-9), we have

$$dE/dx = -\sigma_{13}\gamma N_o E(1 - e^{-E/E_s}) \qquad \text{(IV-10)}$$

(c) Singlet excited state absorption

Due to the short lifetime of n_3 state, it will not be appreciably populated even for high incident intensity. The n_3 state in this treatment acts as an intermediate level from which excited molecules are continuously transferred to the triplet state and has little contribution

to the excited state absorption even when we allow for a large absorption cross-section.

Combining the various contributions, we have

$$dE/dx = N_o(1 - e^{-E/E_s})/(1 - \phi_{fl.}) - \gamma\sigma_{13}N_oE(1 - e^{-E/E_s})$$

or

$$-N_o\, dx = dE/[(1 - e^{-E/E_s})(E_s + E)]$$

with $T_o = e^{-N_o\sigma_{13}x}$, we have

$$\ln T_o = \int_{E_{in}/E_s}^{E_{out}/E_s} dy/(1 - e^{-y})(1 + \gamma y) \qquad \text{(IV-11)}$$

The above expression cannot be integrated analytically and numerical solutions are required. However, extreme behaviors can be obtained for small and large value of E.

(i) $E/E_s \ll 1$, then $\gamma E \ll 1$

$$\ln T_o = \int_{y_{in}}^{y_{out}} dy/(1 - e^{-y})$$

Figure IV-2. Energy saturation. Curves showing energy transmission T_E as a function of the integrated incident energy E (normalized to the saturation energy E_s). Excited-state absorption cross-section is one-fifth that of the saturable transition, $\gamma = 0.2$.

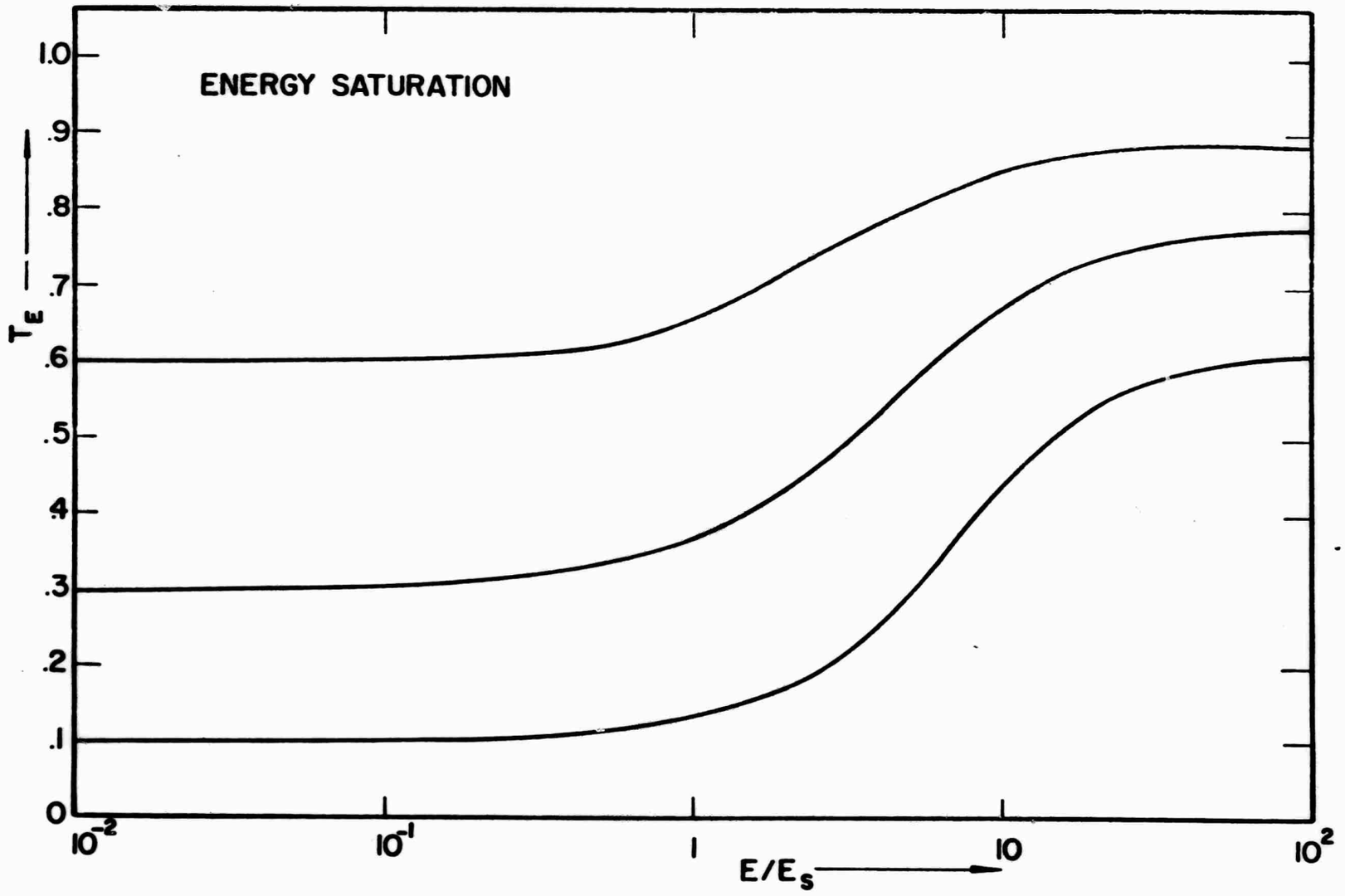
ENERGY SATURATION
T_E
1.0
.9
.8
.7
.6
.5
.4
.3
.2
.1
0
10^{-2}
10^{-1}
1
10
10^2
E/E_s

$$T_o = \frac{1 - e^{TE/E_s}}{1 - e^{E/E_s}} \qquad \text{(IV-12)}$$

Which is the same as in the case of no excited-state absorption.

(ii) $E/E_s >> 1$, we have $1 - e^{-\gamma} \sim 1$, then

$$\ln T_o = \int_{y_{in}}^{y_{out}} \frac{dy}{1 + \gamma y} \qquad \text{(IV-13)}$$

$$T_o = \frac{1 + TE/E_s}{1 + \gamma E/E_s}$$

Where, as $E \to \infty$, $T \to T_o^{\gamma}$. Numerical solutions for equation (IV-12) are shown in figure IV-2 for the case of $\gamma = 0.2$.

(3) Transient saturation

In this case, the molecules relax in a time of the same order as the duration of the Q-switch pulse. Exact solution for the three rate equations for constant I are

$$n_1 = \frac{(\lambda_1 + 1/\tau_3)(\lambda_1 + 1/\tau_{21})}{\lambda_1(\lambda_1 - \lambda_2)} e^{+\lambda_1 t} - \frac{(\lambda_2 + 1/\tau_3)(\lambda_2 + 1/\tau_{21})}{\lambda_2(\lambda_1 - \lambda_2)} e^{+\lambda_2 t} + \frac{(\tau_{21}\tau_3)^{-1}}{\lambda_1 \lambda_2}$$

$$n_3 = \frac{I\sigma(\lambda_1+1/\tau_{21})}{\lambda_1(\lambda_1-\lambda_2)} e^{+\lambda_1 t} - \frac{I\sigma(\lambda_2+1/\tau_{21})}{\lambda_2(\lambda_1-\lambda_2)} e^{\lambda_2 t} + \frac{I\sigma}{\tau_{21}\lambda_1\lambda_2}$$

where $\lambda_1 = -\frac{1}{2}\{(I\sigma + 1/\tau_3 + 1/\tau_{21})$

$$+ \sqrt{[(I\sigma + 1/\tau_3 - 1/\tau_{21})^2 - 4I\sigma/\tau_{32}]}\}$$

$$\lambda_2 = -\frac{1}{2}\{(I\sigma + 1/\tau_3 + 1/\tau_{21})$$

$$- \sqrt{[(I\sigma + 1/\tau_3 - 1/\tau_{21})^2 - 4I\sigma/\tau_{32}]}$$

and

$$\lambda_1\lambda_2 = [1 + I\sigma\tau_3(1 + \frac{\tau_{21}}{\tau_{32}})/(\tau_{21}\tau_3) \qquad \text{(IV-14)}$$

In treating the transmission properties of a sample of molecules for time varying I(t), computer solutions were needed to describe the interaction.

IV-3 Experimental Apparatus

A single mode Q-switched ruby laser was used to measure the transmissions of the dye molecules. The ruby rod was 3 inches long with anti-reflectivity coatings at both ends, pumped with a linear flash lamp in an elliptical cavity. Both the flash lamp and the ruby rod were

Figure IV-3. Experimental setup for transmission measurement.

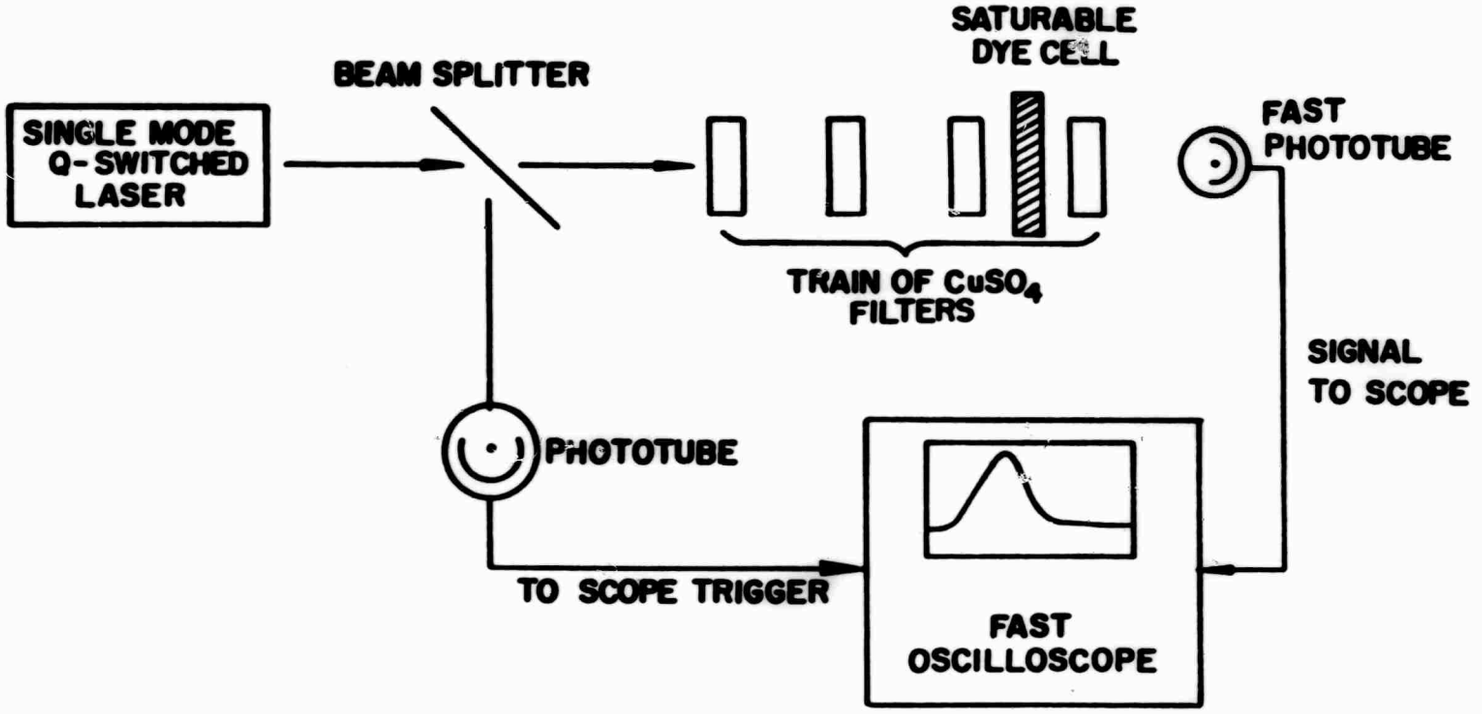
SATURABLE
DYE CELL
BEAM SPLITTER
SINGLE MODE
Q-SWITCHED
LASER
FAST
PHOTOTUBE
TRAIN OF $CuSO_4$
FILTERS
SIGNAL
TO SCOPE
PHOTOTUBE
TO SCOPE TRIGGER
FAST
OSCILLOSCOPE

water cooled to 20°C. A 65% reflectivity resonant reflector was used as output mirror, while a Brewster angle roof prism was used at the back end instead of 99% reflectivity dielectric mirror to avoid the frequent damage caused by the high flux density in the cavity. The laser was Q-switched by either CAPC in pyridine or cryptocyanine in methanol depending on the power level required. Insertion of an aperture of diameter from 1 mm to 3 mm gave stable output pulses, reproducible tc 10% with pulse duration in the range 10 to 30 nsec. Power outputs were between 10 and 20 MW/cm^2 depending on the size of the aperture used. For high power measurements, the pulse outputs were focused down to a small cross-sectional area with a maximum obtainable irradiance of 200 MW/cm^2.

The setup for the transmission measurements is shown in figure IV-3. The outputs from the Q-switched laser were used to irradiate the dye sample cell after being attenuated by the calibrated filters made from solutions of $CuSO_4$. The transmitted outputs were detected with an IT & T plano-photodiode, and displayed on a Tektronix 519 scope with an overall rise time less than 2 nsec. Part of the output from the laser was detected by an RCA 925 photodiode, whose output was used to externally trigger the scope, and which served as a time reference in the detecting system. Transmission data were obtained by comparing the transmitted outputs for the cell

Figure IV-4. Satruation of absorption for CC. Experimental data of peak intensity transmission T versus incident peak intensity I for CC in methanol. Theoretical curves from equation (IV-5) with I_s = 2.2 MW/cm^2, and $I_s b$ = 0.143 are drawn for comparison.

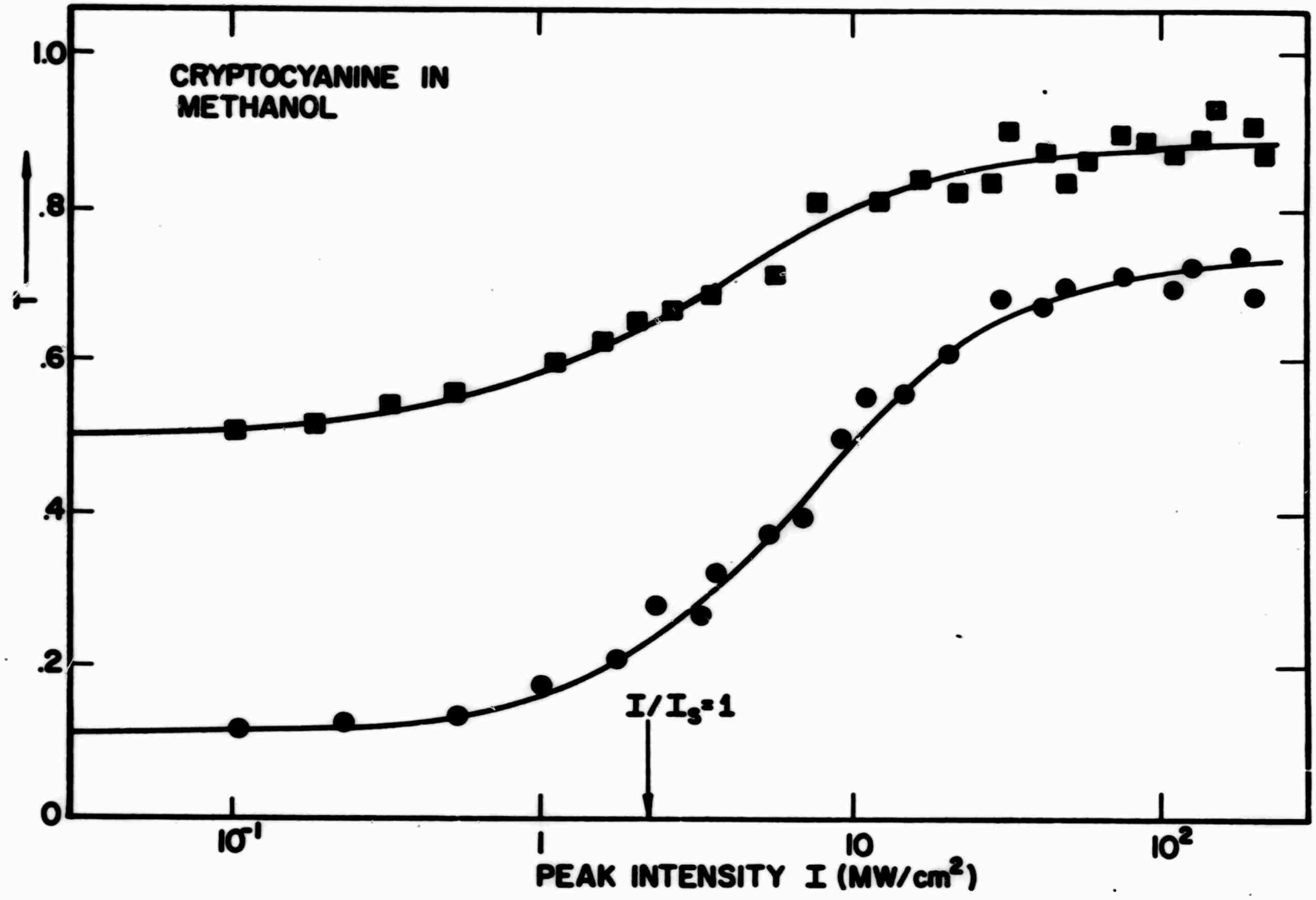
CRYPTOCYANINE IN
METHANOL
T
1.0
.8
.6
.4
.2
0
I/I_s=1
10^-1
1
10
10^2
PEAK INTENSITY I (MW/cm^2)

containing the dye molecules to the same cell containing the solvent alone. Different incident levels could be obtained by adjustment of the number of filters in the train. The dye solution weas contained in a commercial Kodak Q-switch cell with AR-coated windows, and thickness 1.6 mm. Dye solution was prepared by dissolving the dyes in powder form into different solvents. Specially purified solvents were not used.

IV-4 Saturation of the Cryptocyanine Molecules

(1) Saturation of absorption

Cryptocyanine, with its short relaxation times as discussed in the last chapter, falls within the steady-state saturation category. Experimental results for peak intensity transmission versus peak intensity for cryptocyanine in methanol is shown in figure IV-4, together with the theoretical curves from equation (IV-5) for $I_s b = 1/7$ and $I_s = 2.2$ MW/cm^2, giving $\tau_3 \sigma_{13}(1 + \tau_{21}/\tau_{32}) = 1.3 \times 10^{-25}$ cm^2-sec.

(2) Saturation of fluorescence

Measurements on the peak fluorescence outputs versus peak input intensity were also done for cryptocyanine in methanol with the same Q-switched laser output. The fluorescence outputs were observed at right angles to the

Figure IV-5. Saturation of fluorescence for CC. Experimental data on CC in methanol showing peak fluorescence intensity versus incident peak intensity. The vertical scale is relative. Theoretical curve for the steady-state value of n_3 (equation IV-3) is drawn for comparison. The best fitted curve is with $I_s = 2.6$ MW/cm^2.

laser beam through a B & L monochromator with 20 Å bandpass by an IT & T F-4034 photomultiplier. The monochromator was set at 7300 Å which is at the peak of the fluorescence curve for cryptocyanine. Solutions were contained in a 2 mm diameter, 2 cm length glass tube with concentrations kept below 10^{-5} molar to avoid large variations of pulse intensity across the cell length due to residual losses.

Figure IV-5 shows the results of such a measurement, which is compared with the theoretical curve from equation (IV-3) describing the steady state behavior of n_3 population. Since only relative fluoresence outputs were measured, an arbitrary scaling is used for the magnitude of fluorescence output. One deduces from these data that $\tau_3\sigma_{13}(1 + \tau_{21}/\tau_{32}) = 1.1 \times 10^{-25}$ cm^2-sec., which nicely confirms the figure deduced from transmission measurements.

(3) Evaluation of the various parameters

The results on the saturation of absorption and fluorescence for cryptocyanine agree to within an error of 20%. Due to the large scattering of data points, this is satisfactory. The results obtained for I_s agree in general with similar measurements done by Giuliano and Hess[4], and Cire[5], to within a factor of 2.

Taking the value of $\sigma = 5 \times 10^{-16}$ cm^2 deduced from the absorption curve, assuming that cryptocyanine is

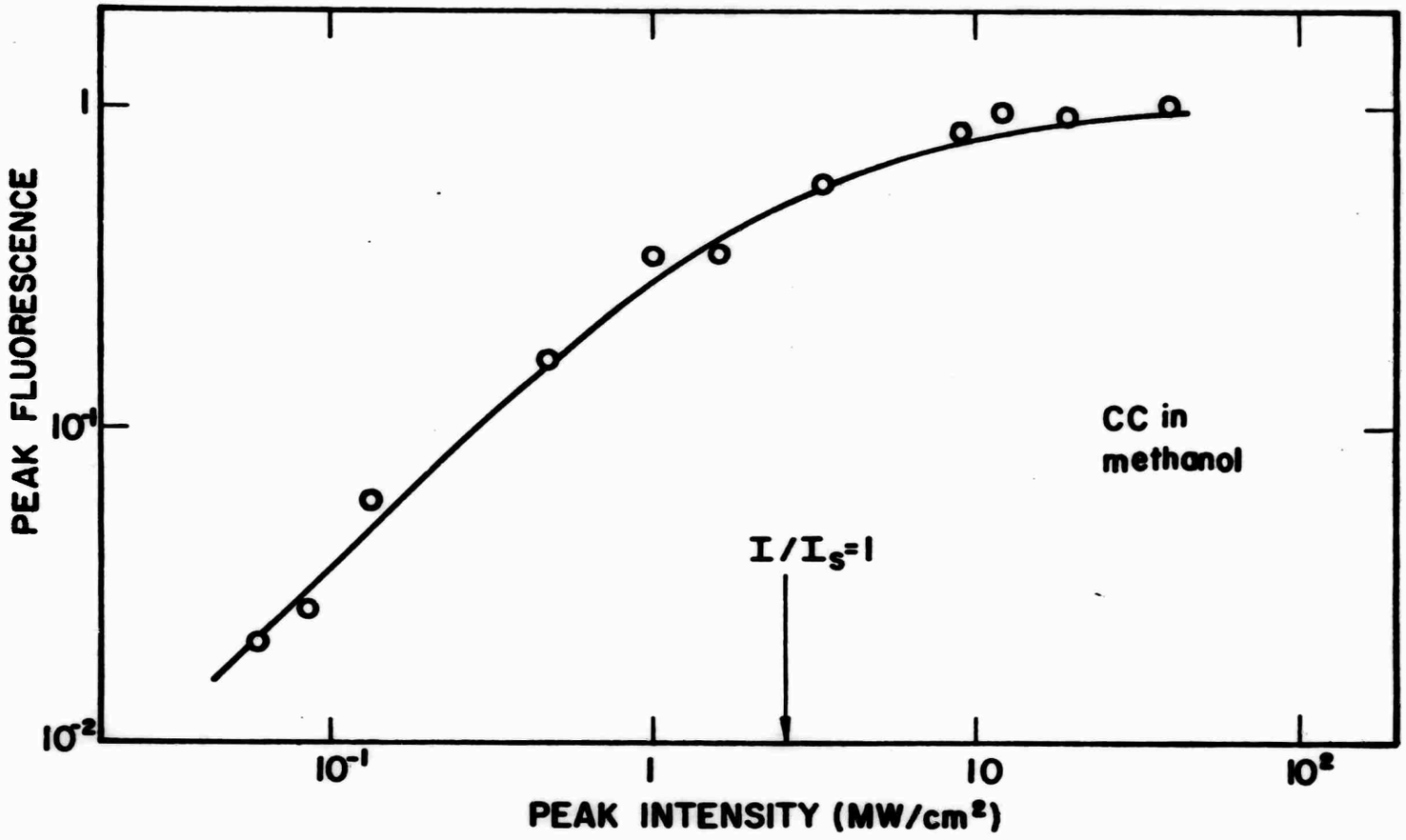
PEAK FLUORESCENCE
1
10^{-1}
10^{-2}
10^{-1}
1
10
10^{2}
PEAK INTENSITY (MW/cm^2)
CC in
methanol
$I/I_s=1$

homogeneously broadened, and $\tau_3 = 2.2 \times 10^{-11}$ sec, we have $1 + \tau_{21}/\tau_{32} \cong 1$, implying $\tau_{32} > \tau_{21}$. We thus see that the saturation of cryptocyanine can also be described by a simple two-level model, as the contribution to the saturation from the triplet state is relatively small. Excited state absorption deduced from the above analysis gives $\beta = 0.14$, an excited singlet-singlet absorption cross-section of $\sim 7 \times 10^{-17}$ cm^2 at 6943 Å.

The experimental results on the saturation of cryptocyanine molecules agree with a steady-state model. The triplet state of cryptocyanine is found to have little effect on the saturation of absorption and residual losses, and is apparently only slightly populated.

The absorption band of cryptocyanine is inhomogeneously broadened. The width of the spectral hole being burnt into the absorption band by a Q-switched ruby laser output was found to be $\lesssim 20$ Å by Sooy and Spaeth[6], indicating that only a small fraction of the molecules absorbs light at 6943 Å. Since room temperature solutions of the cyanine dyes have been shown[7] to consist of equilibrium mixtures of two or more isomers with strongly overlapping absorption bands that can be resolved only at very low temperature, spectral hole-burning may occur by saturating one or a few of the isomers in the solutions. Detailed information concerning the isomer states of cryptocyanine are still unknown at present. However, a

Figure IV-6. Saturation of absorption for H_2PC with different laser pulse width. Experimental data on H_2PC in 1-chloronaphthalene showing peak intensity transmission T versus incident peak intensity I for pulse width, 10, 20 and 30 nsec. Theoretical curve from equation (IV-5) with $I_s b = 0.13$, $I_s = 0.12$ MW/cm^2 is drawn for comparison.

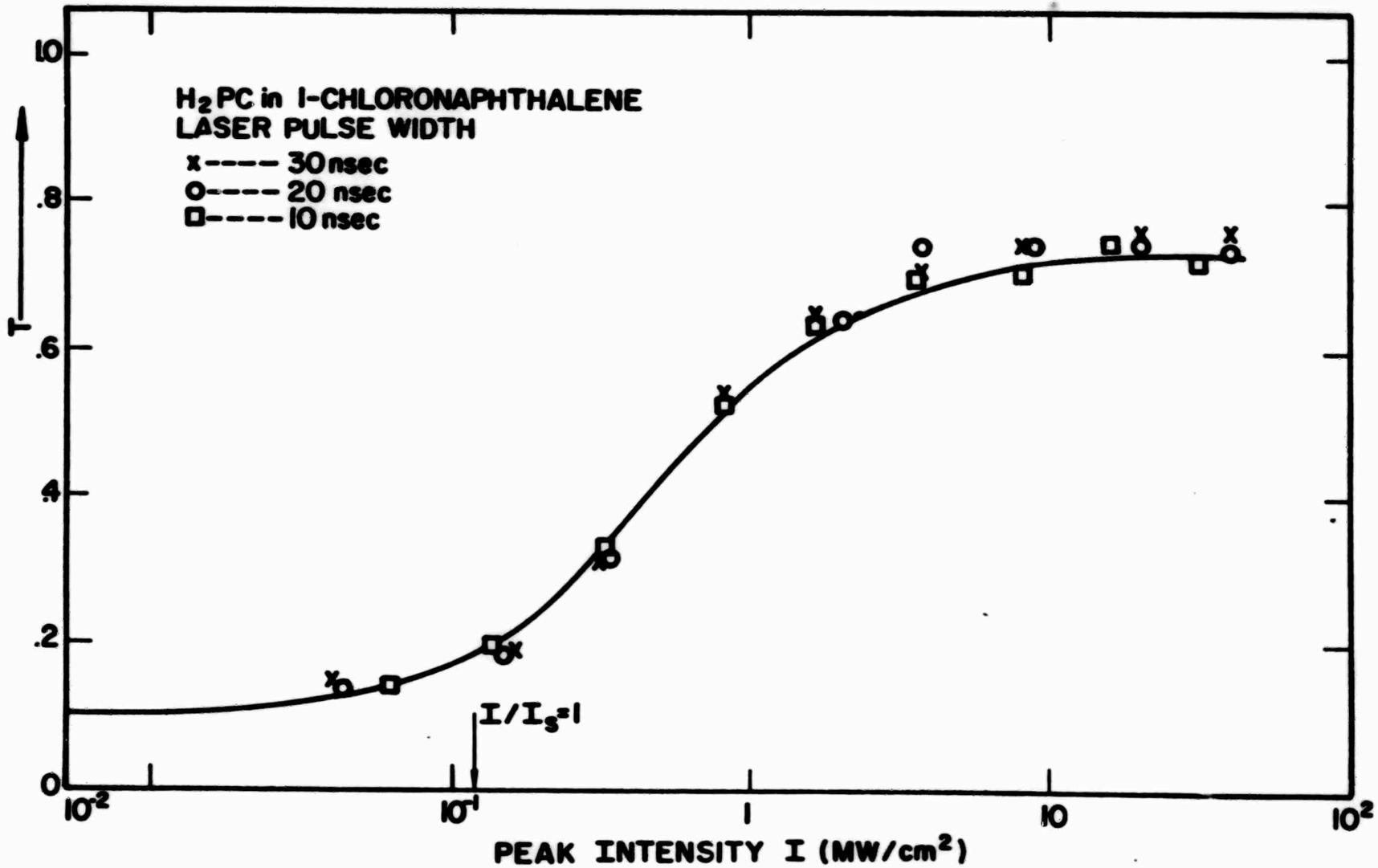
H2PC in 1-CHLORONAPHTHALENE
LASER PULSE WIDTH
x---- 30 nsec
o---- 20 nsec
□---- 10 nsec
T
1.0
.8
.6
.4
.2
0
I/Is=1
10-2
10-1
1
10
102
PEAK INTENSITY I (MW/cm2)

steady-state model does give a good description for the saturation of cryptocyanine with Q-switched ruby laser pulses.

IV-5 Saturation of H_2PC

(1) Saturation of absorption

H_2PC with its long triplet lifetime can be classified into either the energy-saturation or transient-saturation category. An experiment was carried out to investigate saturation of the molecular absorption under different duration of the laser pulses. A Q-switched cell of H_2PC in 1-chloronaphthalene with small signal transmission of 0.1 at 6943 Å was irradiated with Q-switched ruby laser pulses of duration (FWHM) 10, 20 and 30 nsec. The results are shown in figure IV-6. Since peak intensity transmission of the molecules show a similar characteristic dependence on the input intensity irrespective of the input pulse duration, one can conclude immediately that H_2PC is not energy saturated. A theoretical curve from equation (IV-5) for steady state saturation with $I_s b = 0.13$ is drawn for comparison. It is interesting to note that even though H_2PC has a very long triplet-state lifetime, one can still describe the saturation under steady state basis.

To see why steady state approximation can be applied

Figure IV-7. Saturation of absorption for H_2PC. Experimental data on H_2PC in 1-chloronaphthalene showing peak intensity transmission T versus incident peak intensity I for three samples with different initial transmissions. The laser pulse duration was 10 nsec. Theoretical curves from equation (IV-5) with $\beta = 0.13$, $I_s = (\sigma\tau_3)^{-1} = 0.12$ MW/cm^2 are drawn for comparison.

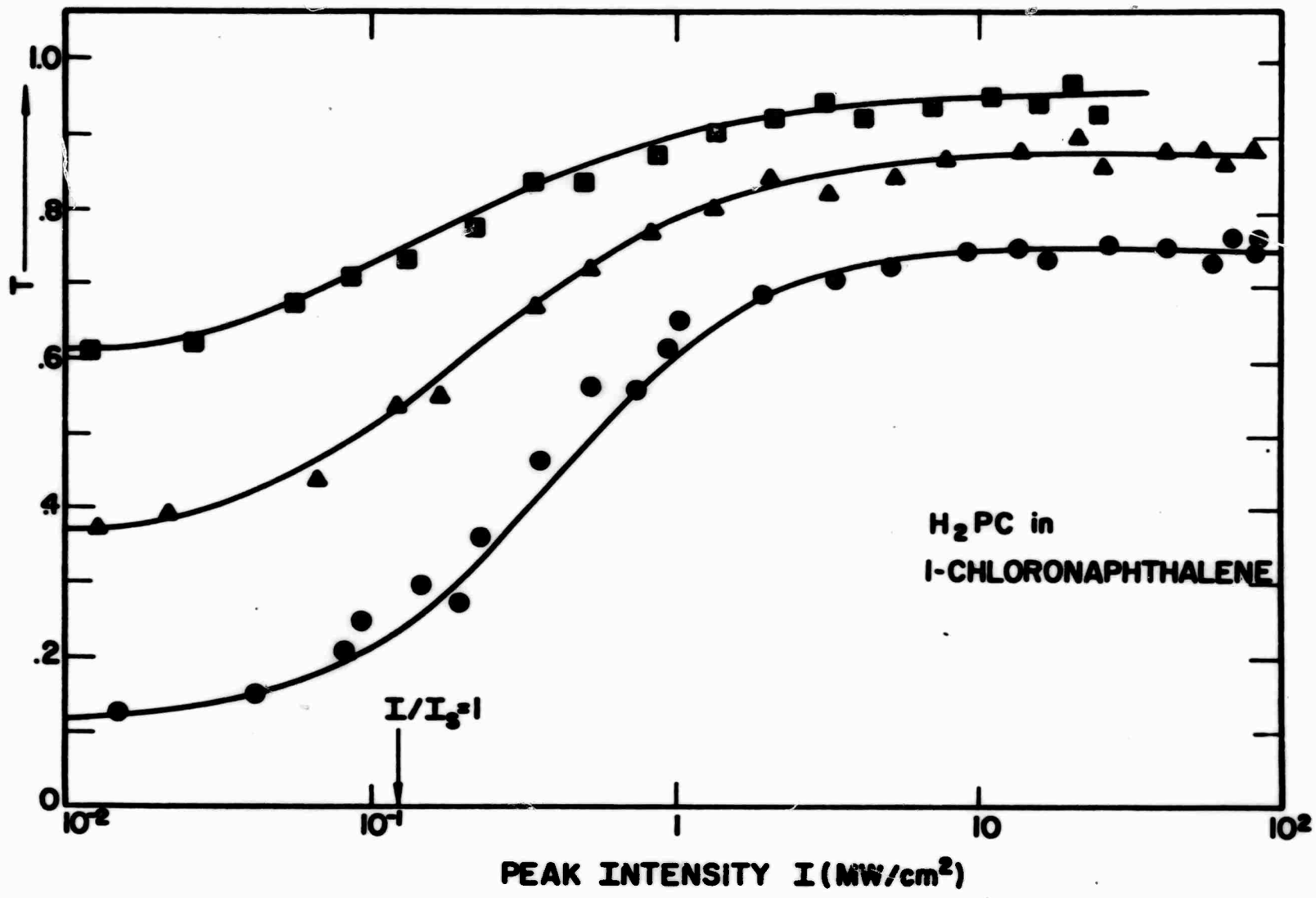
1.0
.8
.6
.4
.2
0
T
10^{-2}
10^{-1}
1
10
10^{2}
$I/I_s=1$
H_2PC in
1-CHLORONAPHTHALENE
PEAK INTENSITY I(MW/cm²)

to H_2PC molecules, we refer to equation (III-7) describing the time developments of each level under a constant irradiance I. Two characteristic time constants, $\lambda_2^{-1}, \lambda_2^{-1}$ are associated with each level, and for $\tau_{32} > \tau_3$, we have $\lambda_1 \sim -(I\sigma + 1/\tau_3)$, $\lambda_2 \sim -1/\tau_{32}(1 + 1/I\sigma\tau_3)^{-1}$. Taking the case for H_2PC with $\tau_3 \sim 3 \times 10^{-9}$ sec, $\tau_{32} \sim 25 \times 10^{-9}$ sec, then, $1/\lambda_1 \leq 3 \times 10^{-9}$ sec, $1/\lambda_2 \leq 25 \times 10^{-9}$ sec will also hold. For an incident pulse duration from 10 to 20 nsec, populations n_1 and n_3 will reach quasi-steady-state values in time $1/\lambda_1 < 3 \times 10^{-9}$ sec, which is short compared to the input pulse duration. The relatively long time constant λ_2 describes the rate at which population of n_3 is converted into the triplet level n_2, and will have negligible effect on the saturation of the ground state absorption. The quasi-steady-state populations n_1 and n_3, assuming τ_{32} to be long, will have identical expressions as steady-state case, equation (IV-3), except that the saturation irradiance will now be given by $I_s = (\sigma\tau_3)^{-1}$.

Experimental results for peak intensity transmission versus peak intensity for H_2PC in 1-chloronaphthalene with three different small-signal transmissions are shown in figure IV-7, together with the theoretical curves from equation (IV-5) with $\beta = 0.13$ for comparison. One obtains $I_s = 1(\sigma\tau_3) = 0.12$ MW/cm^2 $= 4.2 \times 10^{23}$ photons/cm^2-sec.

Figure IV-8. Saturation of fluorescence for H_2PC. Experimental data on H_2PC in 1-chloronaphthalene showing peak fluorescence intensity versus incident peak intensity. The vertical scale is relative. Theoretical curve for the steady-state value of n_3 (equation (IV-3) is drawn for comparison. The best fitted curve is with $I_s = 0.15$ MW/cm^2.

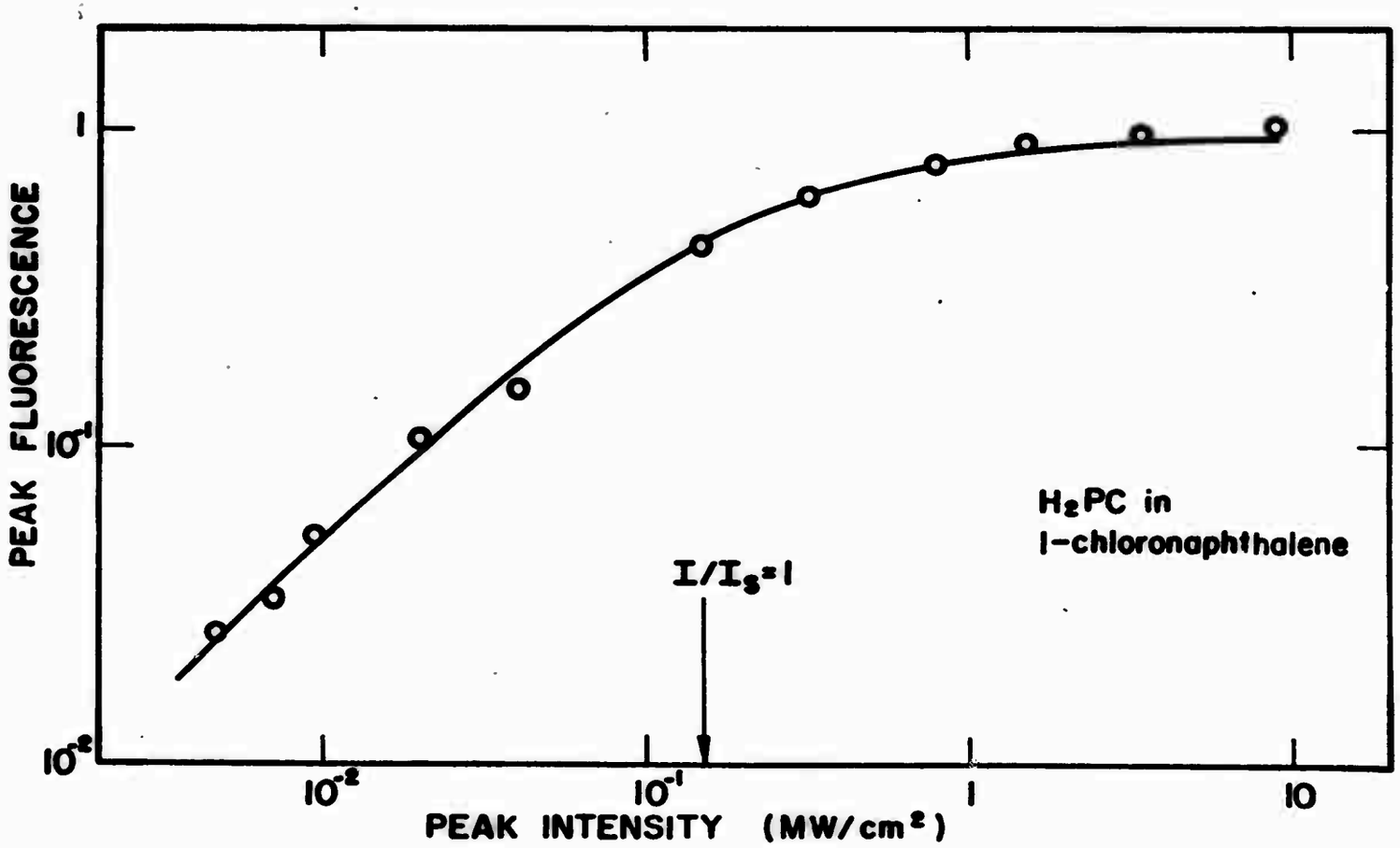
PEAK FLUORESCENCE
1
10^{-1}
10^{-2}
10^{-2}
10^{-1}
1
10
PEAK INTENSITY (MW/cm²)
$I/I_s=1$
H_2PC in
1-chloronaphthalene

(2) Saturation of fluorescence

Measurements on the peak fluorescence output versus peak input intensity were done for H_2PC in 1-chloronaphthalene. The fluorescence was observed at 7100 Å which is near the peak of the fluorescence band. Figure IV-8 shows the experimental results together with a theoretical curve from equation (IV-3). One deduces from these data that $I_s = 0.15$ MW/cm^2 $= 5.1 \times 10^{23}$ photons/cm^2-sec.

(3) Evaluation of the various parameters

The values of saturation irradiance I_s deduced from the above absorption and fluorescence measurements agree to within an error of 20%. Taking $\tau_3 = 3 \times 10^{-9}$ sec, $I_s = 4.5 \times 10^{23}$ photons/cm^2-sec, we have $\sigma = 7.3 \times 10^{-16}$ cm^2. The ground state absorption cross-section for H_2PC has been measured and different values obtained; Kuhn[8] estimated 4.3×10^{-16} cm^2, Gire[5] used a value of 2×10^{-16} cm^2, Kosonocky[9] measured the absorption cross-section to be 5×10^{-16} cm^2. The larger value is more accurate, as pointed out by Harrison[10], due to undissolved colloidal particles suspended in the solution.

Based on a model with two absorptive transitions, the residual loss of $\beta = 0.13$ for H_2PC will give an excited state absorption cross-section at 6943 Å of $0.13 \times \sigma_{ground} \sim 9 \times 10^{-17}$ cm^2. The triplet-triplet absorption cross-section at 6943 Å for H_2PC was measured by

Figure IV-9. Analog computer results on pulse shaping for H_2PC. The excited-state lifetimes of H_2PC are taken from Table I. The sample is assumed to have $T_o = 0.1$, $\beta = 0.13$. A relative delay of the peak of the transmitted pulse at ~0.5 MW/cm^2 is clearly observable.

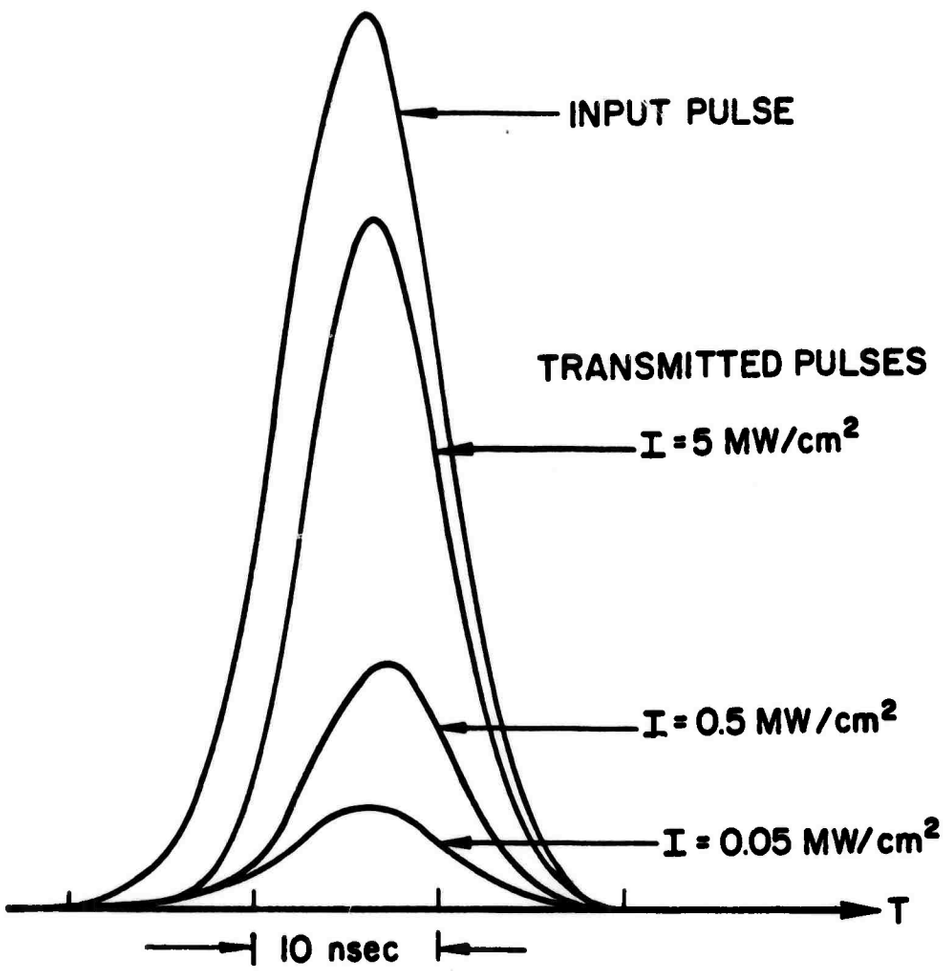
INPUT PULSE
TRANSMITTED PULSES
I = 5 MW/cm²
I = 0.5 MW/cm²
I = 0.05 MW/cm²
T
10 nsec

Figure IV-10. Experimental results on pulse shaping for H_2PC. Data obtained from the experimental setup shown in Fig. IV-3. In each case pulse shapes obtained with and without the saturable filter are shown superimposed to facilitate comparison. Peak intensity (a) 10 MW/cm^2, (b) 0.8 MW/cm^2, (c) 0.2 MW/cm^2. Horizontal scale: 10 nsec/div.

(a) $I = 10\ MW/cm^2$

(b) $I = 0.8\ MW/cm^2$

(c) $I = 0.2\ MW/cm^2$

Stockman[11], to be $\sim 7.7 \times 10^{-18}$ cm^2, which is of an order of magnitude too small to account for the residual losses observed. We attribute the residual losses to be due to higher singlet-singlet absorption, and will discuss this point further in section 7.

Equation (IV-2) for a three-level system was simulated on an analog computer with an incident pulse of Gaussian profile $I(t) = e^{-t^2/a^2}$. Values of different life times were taken from Table I for H_2PC. In treating the transmission of the dye molecules, the dye cell is assumed to be optically thin, such that each molecule in the beam experiences the same pumping rate at a given instant of time. The instantaneous transmission is defined as $T(t) = e^{-\alpha(t)\chi_o}$, where χ_o is the cell length, and $\alpha(t) = \alpha_o[n_1(t) + \beta n_3(t) + \gamma n_2(t)]$ is the instantaneous absorption coefficient. Figure IV-9 shows the pulse shaping results obtained with $T_o = 0.1$, $\beta = 0.13$. A relative delay of the peak of the transmitted pulse at $\sim$0.5 MW/cm^2 is clearly observable. Experimental results confirming this pulse shaping behavior are shown in figure IV-10 for H_2PC in 1-chloronaphthalene with $T_o = 0.15$. The distortion of the transmitted pulse arises from initial absorption of the leading edge in saturating the molecular transitions, and is common to all molecules with excited-state lifetimes comparable to the incident pulse duration. Computer results on the

Figure IV-11. Saturation of absorption for CAPC for different laser pulse width. Experimental data showing peak intensity transmission versus incident peak intensity for laser pulses of durations 10, and 25 nsec. Solid lines are analog computer results obtained with the corresponding pulse width, with lifetimes appropriate to CAPC, and $\beta = 0.22$. Broken line is the steady-state transmission result with $\beta = 0.22$, and $\tau_3 = 10^{-8}$ sec.

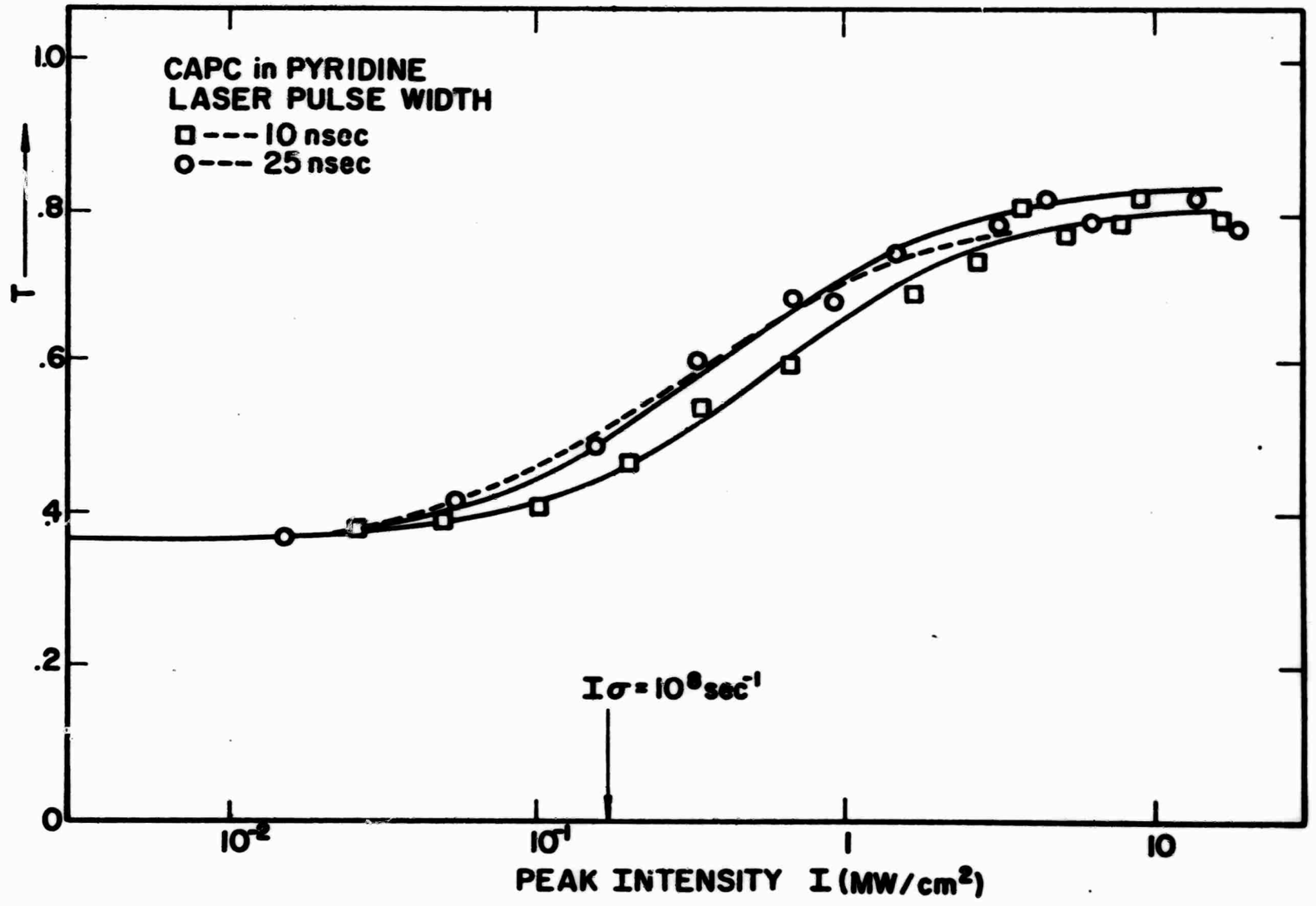
CAPC in PYRIDINE
LASER PULSE WIDTH
□ --- 10 nsec
○ --- 25 nsec
T
1.0
.8
.6
.4
.2
0
Iσ = 10⁸ sec⁻¹
10⁻²
10⁻¹
1
10
PEAK INTENSITY I (MW/cm²)

BLANK PAGE

peak intensity transmission characteristics for the range of typical Q-switched pulse durations confirm the approximation of steady-state saturation.

IV-6 Saturation of CAPC

(1) Saturation of absorption

CAPC with an excited singlet-state lifetime of 10 nsec should be classified into the transient saturation category. Measurements on the peak intensity transmission versus peak intensity for laser pulses of duration 10 and 25 nsec are shown in figure IV-11. Analog computer results, with lifetimes appropriate to CAPC, and a higher singlet absorption cross-section ratio of $\beta = 0.22$ for peak intensity transmission are drawn for comparison. The fact that shorter pulse duration requires a higher intensity-level for initially saturating the absorption is confirmed by the computer results. To see how the steady state approximation will deviate from the transient case, a broken line showing the quasi-steady state transmission for $I\sigma = 10^8 sec^{-1}$, $\tau_3 = 10^{-8}$ sec is drawn on the same figure. One sees that as the pulse duration increases, the peak intensity transmission curve approaches that of the quasi-steady-state case. This behavior is consistent with the analytical results obtained by Selden[13] for a two-level absorptive system. The slight

Figure IV-12. Saturation of absorption for CAPC. Experimental data showing peak intensity transmission versus incident peak intensity for CAPC in pyridine for laser pulse width of 10 nsec. Analog computer results with $\beta = 0.22$ are also shown for comparison.

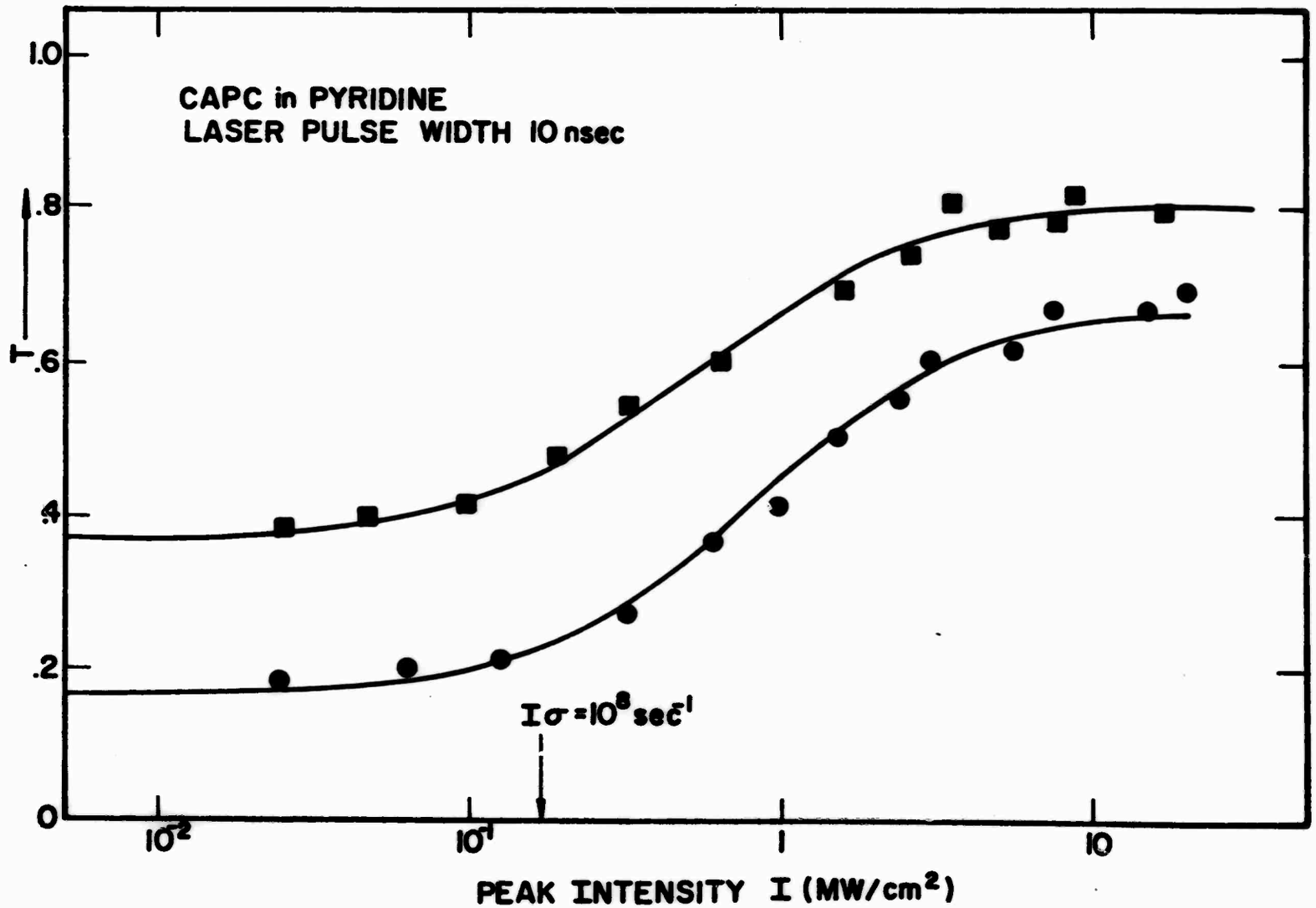
CAPC in PYRIDINE
LASER PULSE WIDTH 10 nsec
1.0
.8
.6
.4
.2
0
T
$I\sigma = 10^8 sec^{-1}$
10^{-2}
10^{-1}
1
10
PEAK INTENSITY I (MW/cm^2)

Figure IV-13. Saturation of fluorescence for CAPC. Experimental data showing fluorescence peak intensity versus incident peak intensity for CAPC in pyridine. Analog computer results for the peak value of $n_3(t)$ are also shown for comparison.

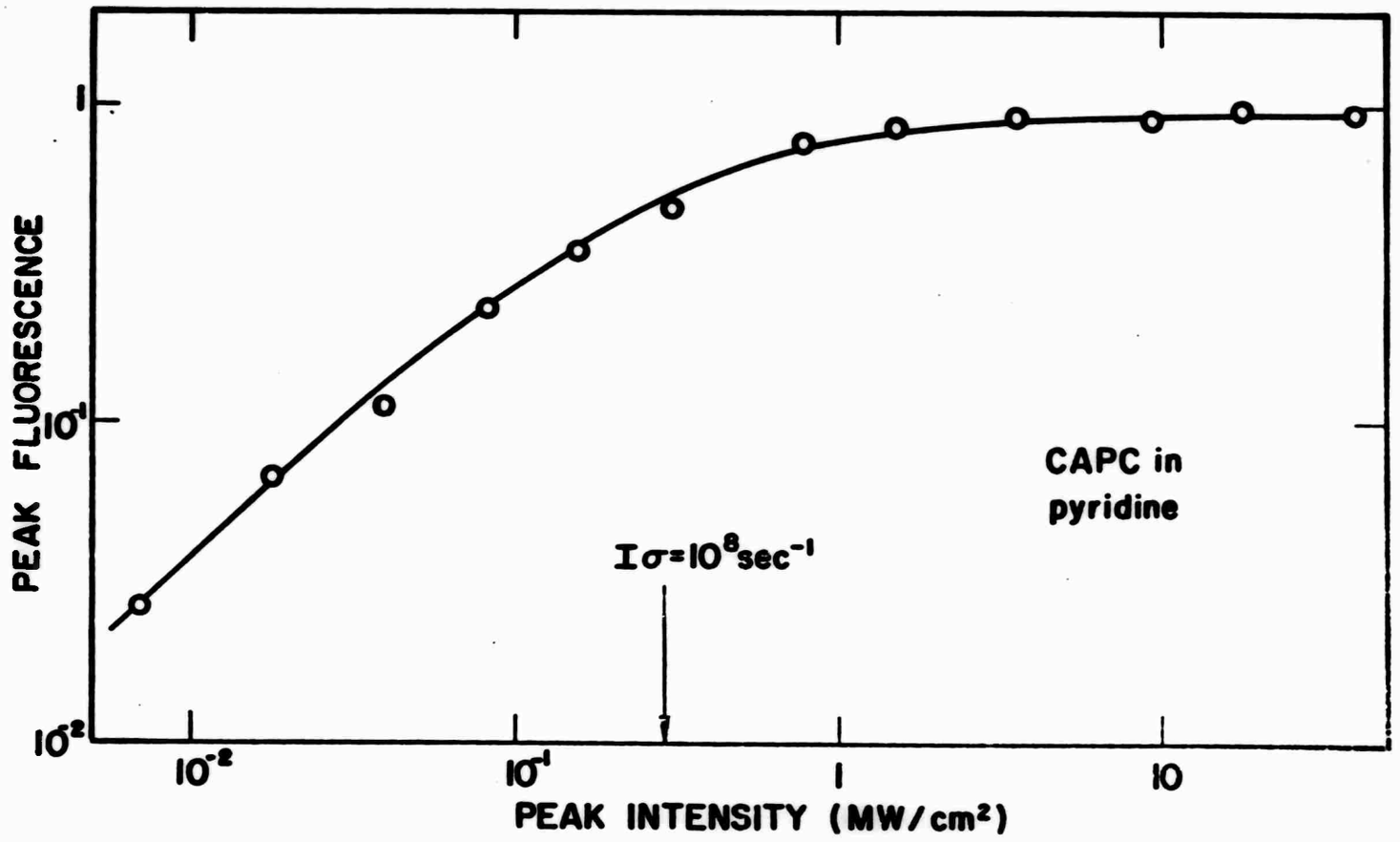
PEAK FLUORESCENCE
1
10^{-1}
10^{-2}
10^{-2}
10^{-1}
1
10
PEAK INTENSITY (MW/cm²)
CAPC in
pyridine
$I\sigma=10^{8}sec^{-1}$

decrease in residual loss for longer pulse duration arises from the depopulation of the excited singlet state into the triplet level. For the case in which the pulse duration is much shorter than the excited singlet-state lifetime, the saturation of absorption may be described by energy saturation. The peak intensity level required in this case for initially saturating the absorption will be, according to equation IV-11, $I \sim 1/\Delta t\sigma$, where Δt will be approximately the pulse width. Figure IV-12 shows transmission curves for CAPC in pyridine with two different initial transmissions, using laser pulses of 10 nsec duration. Analog computer results with $\beta = 0.22$ are drawn for comparison. One deduces from this figure that $I\sigma = 10^8 sec^{-1}$ for $I = 0.17$ MW/cm^2, giving $\sigma \cong 1.7 \times 10^{-16}$ cm^2.

(2) Saturation of fluorescence

Measurements on the peak fluorescence output versus peak intensity at 7100 Å are shown in figure IV-13. The laser pulse duration in this case was 25 nsec. Analog computer results for the peak value of n_3 with a pulse duration of 25 nsec are shown for comparison. One obtains $I\sigma = 10^8 sec^{-1}$ for $I = 0.2$ MW/cm^2, giving $\sigma = 1.5 \times 10^{-16} cm^2$.

(3) Evaluation of the various parameters

The ground state absorption cross-sections at 6943 Å deduced from the above two measurements agree to within an error of 20%. Conventional measurement of absorption cross-section at 6943 Å with a known concentration of molecules gives $\sigma \sim 1.5 \times 10^{-16}$ cm^2, in good agreement with the saturation measurements. The excited singlet state absorption cross-section at 6943 Å obtained from the transmission curves is found to be $0.22 \times \sigma_{ground} \sim 3.3 \times 10^{-17}$ cm^2. Triplet-triplet absorption has been neglected due to the small absorption cross-section at 6943 Å.[11]

The locations of the peak of the absorption band for CAPC in different solvents vary considerably, consequently the absorption cross-section at 6943 Å will vary from solvent to solvent. Experimental findings indicate that for CAPC in 1-chloronaphthalene and quinoline, where the cross-section at 6943 Å are significantly larger than 1.5×10^{-16} cm^2, the intensity levels for initially saturating the absorption, and the residual losses are consequently smaller. For CAPC in ethyl alcohol, with $\sigma < 1.5 \times 10^{-16}$ cm^2 an increase of residual loss and intensity level for saturation are observed.

Transient pulse distortion for CAPC was also observed, with results similar to those shown in figure IV-10. This pulse distortion behavior is also confirmed by

computer results.

IV-7 Contribution from Higher Excited-state Absorptions to the Saturation of Organic Molecules

(1) Residual losses

For all three of the molecules being considered, residual losses of order 0.2 (i.e. peak transmission ~0.8) were observed at high intensity level, showing that the absorbers are not completely transparent. In particular, an increase in the transmission of CAPC in 1-chloronaphthalene to some maximum value with a subsequent decrease at still higher intensity levels has been observed[14]. Several possibilities which lead to residual loss at high intensity will be considered here.

(a) Scattering: Scattering at 6943 Å of the laser pulse was found to be an order of 10^{-5} smaller than that necessary to account for the residual losses observed. Stimulated scattering, either Brillouin scattering or Raman scattering, will show different spectral components in the scattered light. Measurements on forward and backward scattering by the dye solutions show no detectable different spectral components besides the laser line, indicating that stimulated scattering cannot be the cause for residual losses.

(b) Triplet-triplet absorption: For the phthalocyanine molecules, triplet-triplet absorption cross-sections have been measured by Stockman[11], and Villar and Lindquist[12], with an upper limit of 7×10^{-18} cm^2. Assuming that the triplet state is completely populated at an intensity level of 20 MW/cm^2, triplet absorption can only contribute to a residual loss of order ~ 0.02. The fact that intersystem crossing is not complete during the laser pulse for either CAPC or H_2PC is a further indication that residual losses cannot be explained by triplet-triplet absorption.

(c) Excited singlet absorption: Energy level structures for phthalocyanine molecules calculated by Chen[15], show symmetry-allowed transitions from the first excited singlet state into higher levels with energy gaps close to the ruby laser photon energy. Evidence for populating the higher level is the fact that blue fluorescence from CAPC in 1-chloronaphthalene has been observed under excitation by a Q-switched ruby laser pulse[14]. Higher triplet cross-over into the higher singlet manifold can be ruled out as spin-selection rules hold true even at higher excited levels[16].

We thus conclude that excited singlet absorptions are the most probable cause for residual losses of phthalocyanine molecules. In the case of cryptocyanine molecules with lifetimes of all excited states shorter

Figure IV-14. Blue emission spectra of the phthalocyanine excited with Q-switched laser output. Experimental data showing blue emission of (a) CAPC in pyridine, and (b) H_2PC in 1-chloronaphthalene, excited with Q-switched laser output. Blue absorption bands for the two dyes are also shown. Vertical scale is relative.

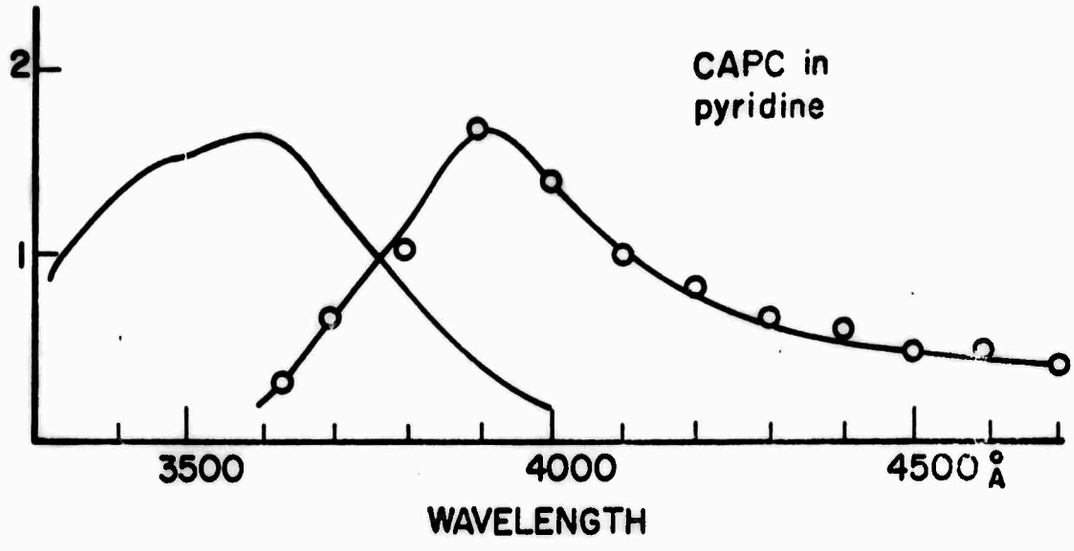
2
1
CAPC in
pyridine
3500
4000
4500 Å
WAVELENGTH

(a)

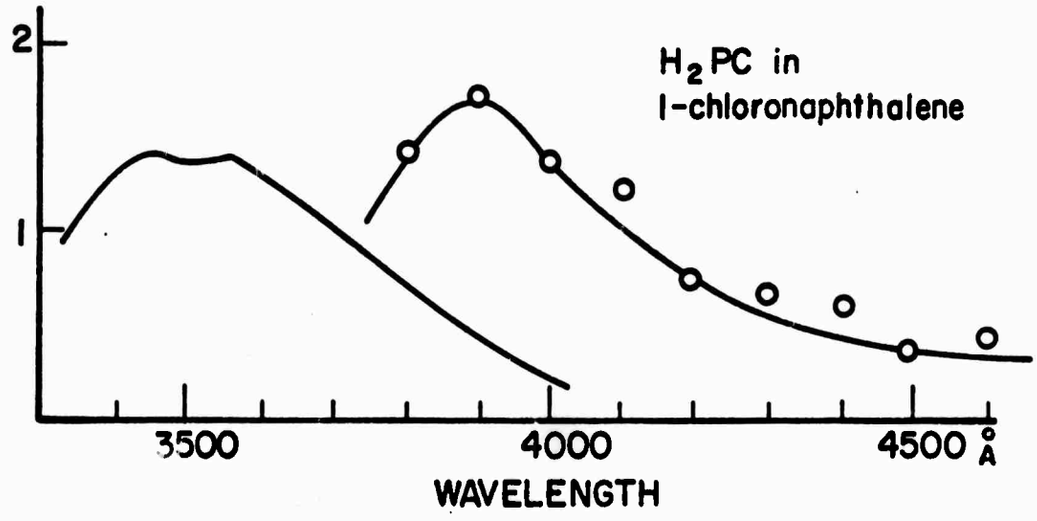
2
1
H2PC in
1-chloronaphthalene
3500
4000
4500 Å
WAVELENGTH

(b)

BLANK PAGE

than the Q-switched pulse duration, triplet-triplet and excited singlet-singlet absorptions cannot be distinguished.

(2) Emission spectra from the higher excited singlet levels

Measurements on the blue fluorescence from the phthalocyanine molecules excited by Q-switched ruby laser pulses were done with an experimental setup similar to the previous fluorescence measurement setup. An RCA 7850 high gain photomultiplier tube with S-11 cathode surface was used to detect the relatively weak blue fluorescence output. Both solvents used, pyridine and 1-chloronaphthalene, show detectable blue fluorescence by themselves, which amount to $\leq$ 5% of the signal observed at peak intensity level of 80 MW/cm^2, and which was subtracted from the final results. Figure IV-14 shows the blue fluorescence spectrum for CAPC in pyridine and H_2PC in 1-chloronaphthalene, excited with Q-switched ruby pulses of duration 20 nsec, peak intensity 20 MW/cm^2. The results for CAPC agree with similar results obtained by Gibb[14]. The blue absorption bands for both molecules are also shown for comparison. One sees that the blue emission bands are approximately the mirror images of the blue absorption profile, indicating that the blue emission originated from those states which have different parity from the ground state. On the contrary, the second excited singlet state which has the same parity as the ground state will

Figure IV-15. Model of the dye molecules with three absorptive transitions in the singlet manifold to explain higher excited-state absorption behavior.

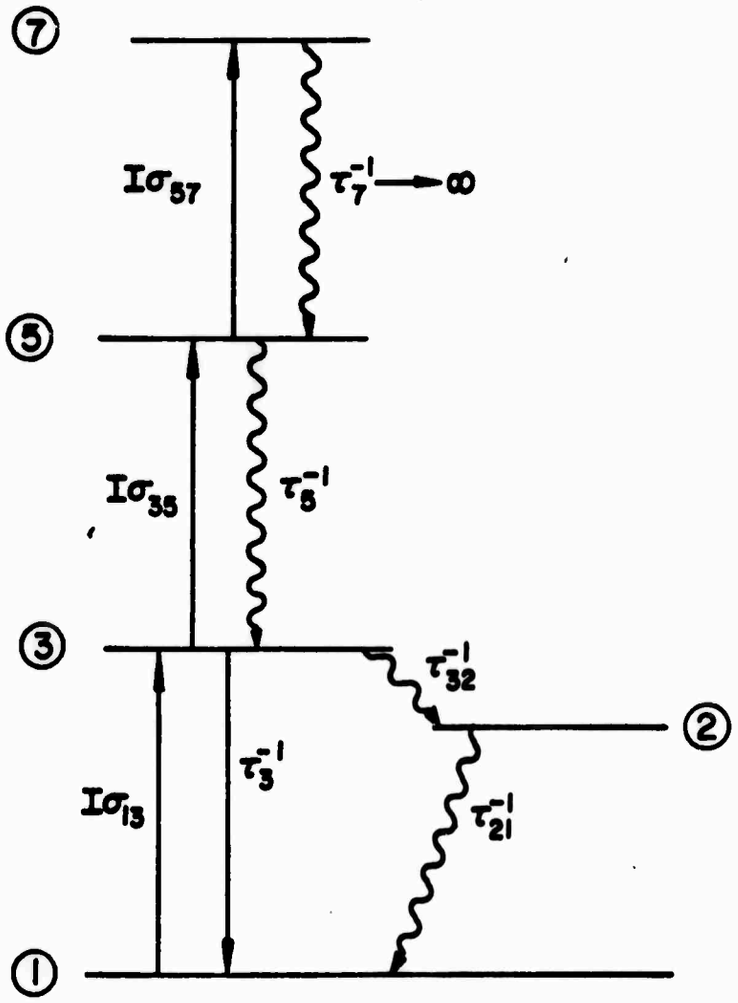
⑦
$I\sigma_{57}$
$\tau_7^{-1} \rightarrow \infty$
⑤
$I\sigma_{35}$
τ_5^{-1}
③
τ_{32}^{-1}
②
τ_3^{-1}
$I\sigma_{13}$
τ_{21}^{-1}
①

be forbidden to fluoresce. Chen's[15] calculations on the energy-level structure for phthalocyanine molecules showed that levels with both parities are present with energy gaps respect to the ground state of approximately twice the ruby laser photon energy. Thus the blue emission from the phthalocyanine excited with ruby laser output must be due to transfer of excitation from the second excited singlet to the fluoresing level via vibronic coupling. The rate of transfer should be very fast and has been confirmed by the experimental observation that the blue emission followed the Q-switched pulse to within the detector response time. Peak blue fluorescence output, excited with 20 MW/cm^2 laser pulse, was an order of 10^{-5} smaller in magnitude compared to red fluorescence at 7100 Å excited with the same intensity pulse.

(3) Model for three absorptive transitions in the singlet manifold

In order to investigate the behavior of the higher singlet levels under high intensity excitation, we consider a model of three absorptive transitions in the singlet manifold, $n_1 \rightarrow n_3$, $n_3 \rightarrow n_5$, $n_5 \rightarrow n_7$, as shown in figure IV-15. Relaxations (non-radiative) for each level will be assumed to be predominated by relaxation to the next lower singlet level. Intersystem crossing from the first excited singlet to the triplet is long compared to

the pulse duration, so that the triplet state can be neglected in our treatment. Moreover, the laser pulse duration is long compared to the first excited singlet-state lifetime. The above assumptions are approximately true for both phthalocyanine molecules. We then have the following set of equations,

$$\begin{aligned} dn_1/dt &= -I\sigma_{13}n_1 + n_3/\tau_3 = 0 \\ dn_3/dt &= I\sigma_{13}n_1 - n_3/\tau_3 - I\sigma_{35}n_5 + n_5/\tau_5 = 0 \\ dn_5/dt &= I\sigma'_{35}n_3 - n_5/\tau_5 = 0 \end{aligned} \qquad \text{(IV-15)}$$

Here we set $\tau_7 \to 0$; solving the above equations with the condition that $n_1 + n_3 + n_5 = 1$, we have

$$\begin{aligned} n_1 &= 1/(\alpha\beta I'^2 + I' + 1) \\ n_3 &= I'/(\alpha\beta I'^2 + I' + 1) \\ n_5 &= \alpha\beta I'^2/(\alpha\beta I'^2 + I' + 1) \end{aligned} \qquad \text{(IV-16)}$$

Where $I' = I\sigma_{13}\tau_3$, $\alpha = \tau_5/\tau_3$, $\beta = \sigma_{35}/\sigma_{13}$. The transmission characteristic of an optically thick sample can now be derived from

Figure IV-16. Transmission characteristic for CAPC at high intensity level. Experimental data showing peak intensity transmission versus incident peak intensity up to 100 MW/cm^2 for CAPC in pyridine. Theoretical curve from equation IV-18 with $\beta = 0.22$, $\alpha = 2.5 \times 10^{-3}$ and $\epsilon = 1$, is shown for comparison.

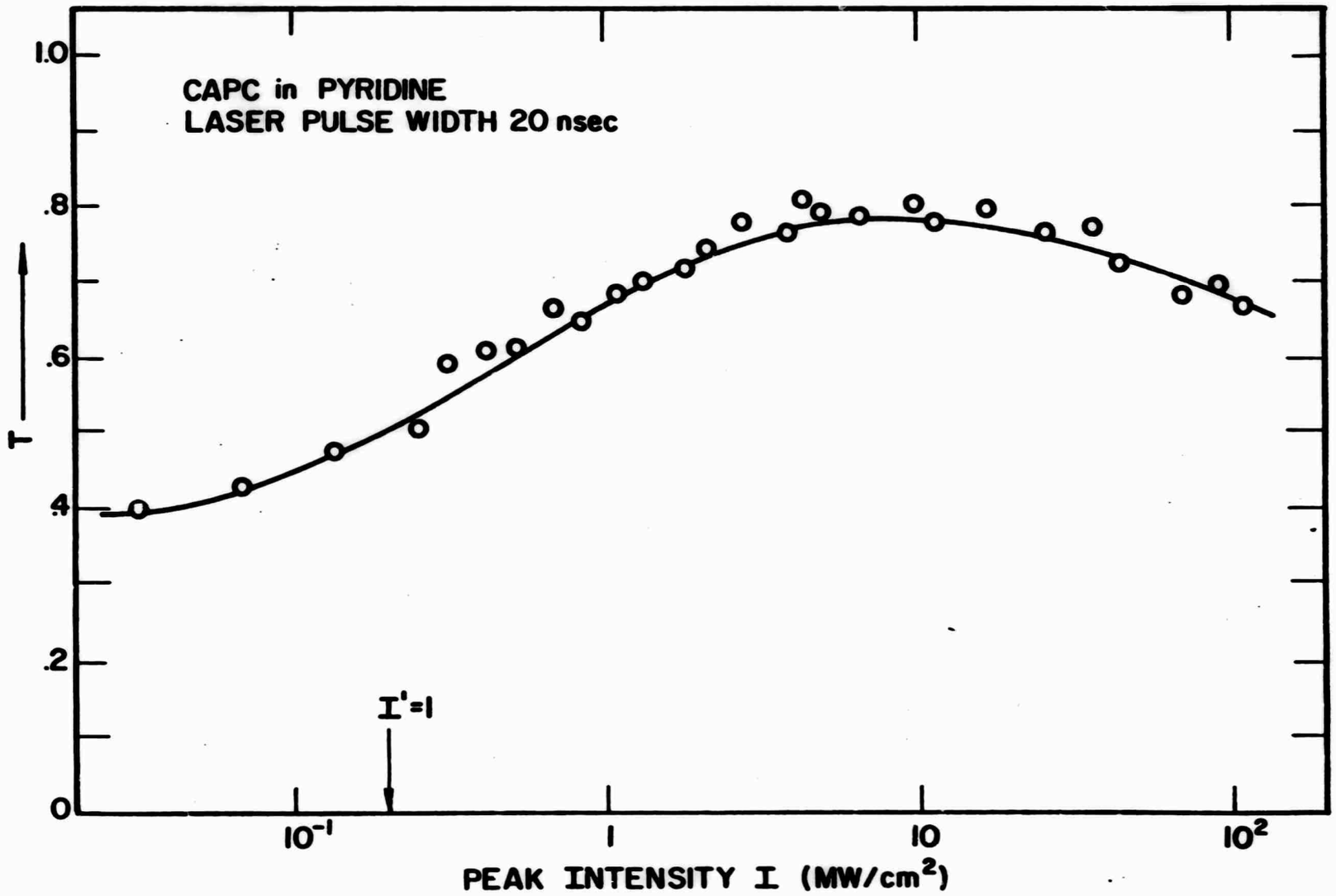
CAPC in PYRIDINE
LASER PULSE WIDTH 20 nsec
1.0
.8
.6
.4
.2
0
T
I'=1
10^{-1}
1
10
10^2
PEAK INTENSITY I (MW/cm^2)

$$dI/dx = N_o I\sigma_{13}(n_1 + \beta n_3 + \varepsilon n_5) \qquad \text{(IV-17)}$$

Where $\varepsilon = \sigma_{57}/\sigma_{13}$. After integrating with proper boundary conditions, we obtain,

$$\ln \frac{T_o}{T} = (1/2\varepsilon - 1/2) \ln \left| \frac{1 + \beta I'T + \alpha\beta\varepsilon(I'T)^2}{1 + \beta I' + \varepsilon\beta\varepsilon I'^2} \right|$$

$$+ \frac{1 - \beta(1/2\varepsilon - 1/2)}{(\beta^2 - 4\varepsilon\beta\alpha)^{1/2}} \ln \left\{ \frac{2\alpha\beta\varepsilon I'T + \beta - (\beta^2 - 4\alpha\beta\varepsilon)^{1/2}}{2\alpha\beta\varepsilon I'T + \beta - (\beta^2 - 4\varepsilon\beta\alpha)^{1/2}} \right.$$

$$\left. \left\{ \frac{2\alpha\beta\varepsilon I' + \beta + (\beta^2 - 4\alpha\beta\varepsilon)^{1/2}}{2\alpha\beta\varepsilon I' + \beta - (\beta^2 - 4\alpha\beta\varepsilon)^{1/2}} \right\} \right.$$

(IV-18)

There are only three independent parameters in the transmission characteristic for the three absorptive transitions model; α, β, and ε. Experimental measurements of peak intensity transmission for CAPC in pyridine up to an intensity of 200 MW/cm^2, with laser pulses of duration 20 nsec (FWHM), are shown in figure IV-16. A theoretical curve from equation (IV-18) with $\beta = 0.22$, $\alpha = 2.5 \times 10^{-3}$, $\varepsilon = 1$ is drawn to give the best fit to all data points. It should be pointed out that the choice of the parameters is not arbitrary; β is taken from the residual loss at saturation of the first transition from the ground state,

α determines the intensity level at which significant population of n_5 is present, and ϵ determines the degree of absorption from the n_5 level. We thus obtain an internal conversion lifetime for n_5 level of $\tau \sim \alpha\tau_3 \sim 2.5 \times 10^{-11}$ sec., and a cross-section of $\sigma_{57} \sim 1.5 \times 10^{-16}$ cm^2 at 6943 Å for the second excited singlet state. H_2PC in 1-chloronaphthalene shows no significant increase in absorption up to an intensity level of 80 MW/cm^2; we can conclude that τ_5 for H_2PC is shorter than $\alpha\tau_3 \sim 10^{-11}$sec to prevent significant absorption by the n_5 level. Recent results obtained by Huff and DeShaze[17], indicated that cryptocyanine exhibits increase of absorption at an intensity level of 400 MW/cm^2, which is not obtainable from our equipment. We cannot specify at present which manifold, singlet or triplet, is responsible for the maximum behavior in transmission for cryptocyanine molecules.

The presence of a maximum in the transmission curve is common to any model involving three absorptive transitions. Higher triplet absorptions give similar maximum behavior in the transmission as shown by Huff and DeShaze[17]. In view of the small triplet-triplet absorption cross-section, and the large residual losses observed for the phthalocyanine molecules, we can conclude that the higher intensity absorption processes are due to interaction with levels in the singlet manifold.

Figure IV-17. Intensity dependence of the blue emission from phthalocyanine. Experimental data showing the peak blue emission versus incident peak intensity for CAPC in pyridine, and H_2PC in 1-chloronaphthalene. Theoretical curves from equation IV-16 for n_5 are also shown for comparison. Vertical scale is relative.

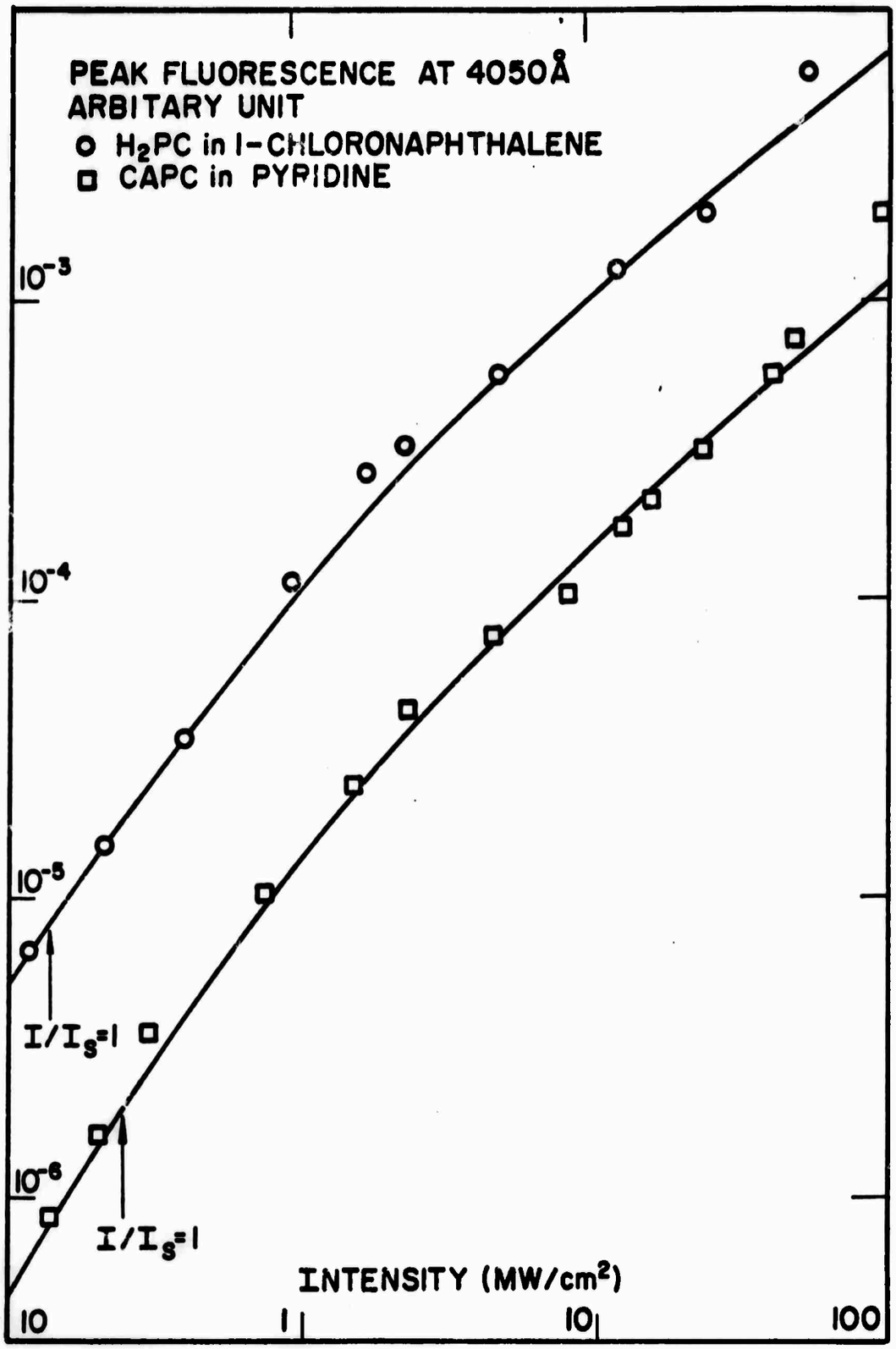
PEAK FLUORESCENCE AT 4050Å
ARBITARY UNIT
o H_2PC in 1-CHLORONAPHTHALENE
□ CAPC in PYRIDINE
10^{-3}
10^{-4}
10^{-5}
10^{-6}
$I/I_S=1$
$I/I_S=1$
INTENSITY (MW/cm^2)
10
1
10
100

Measurements on the peak output of blue fluorescence versus input laser peak intensity were done for CAPC in pyridine and H_2Pc in 1-chloronaphthalene, with laser pulses of duration 20 nsec. monochromator seting at 4050 Å. The results are shown in figure IV-17. Results for CAPC in pyridine are similar to the results obtained by Gibb for CAPC in 1-chloronaphthalene. Theroetical curves for n_5 from equation (Iv-16) are drawn for comparison, where we have assumed that the transfer of excitation from the second excited singlet to the fluorescing level is very fast, and the expression for n_5 actually describes the population of the fluorescing level. We see that for an intensity up to 50 MW/cm^2, good agreement with the model is obtained, indicating that the blue emission is due to absorption from the first excited singlet state. As the intensity level becomes higher than 50 MW/cm^2, the blue fluorescence shows a superlinear increase, with data points fluctuating greatly. Bubble formation was observed for both solutions at 100 MW/cm^2, with H_2PC in 1-chloronaphthalene eventually carbonizing. We attribute this increase in blue fluorescence as due to high field effect produced by the high intensity laser pulse, probably dielectric breakdown[18] due to filement formations in the solutions, and is probably not associated with any non-linear increase in the n_5 level population.

IV-8 Conclusion

It is found that a simple three-level model including excited-state absorption can adequately (if not completely) describe the saturation of absorption for the three molecules; CC, H_2PC and CAPC. Experimental results on the saturation of absorption and fluorescence for the three molecules indicate that CC and H_2PC can be described as steady-state saturable (for typical Q-switched laser pulses), and CAPC can be described as transiently saturable. Absorption cross-sections deduced from results on the saturation of absorption are in good agreement with values obtained from other measurements. Residual losses associated with the saturation of absorption were found to be due to excited singlet-singlet absorption. The excited singlet-singlet absorption cross-section for the phthalocyanine molecules was found to be on the order of 10^{-17} cm^2. The increase in the transmission of CAPC to some maximum value with a subsequent decrease at a still higher intensity level was determined to be caused by the effects of three absorptive transitions in the singlet manifold. Comparing experimental results with the theoretical curve, we deduced a value of $\sim 10^{-11}$ sec for internal conversion from the second excited singlet to the first excited singlet state.

REFERENCES

1. C. L. Tang, J. Appl. Phys. 34, 2935 (1963).
2. N. Broembergen and Y. R. Shen, Phys. Rev. 133, A37 (1964).
3. M. Hercher, Appl. Opt. 6, 947 (1967).
4. C. R. Giuliano and L. D. Hess, IEEE J. Quantum Electronics QE-3, 358 (1967).
5. F. Gires, IEEE J. Quantum Electronics, QE-2, 624 (1966).
6. W. R. Sooy and M. L. Spaeth, J. Chem. Phys. 48, 2315 (1968).
7. W. West, S. Pearce and F. Grum, J. Phys. Chem. 71, 1316 (1967).
8. H. Kuhn, "Progress in the Chemistry of Organic Natural Products", Springer-Verlag OHG, Vienna, 1959.
9. W. K. Kosonocky and S. E. Harrison, J. Appl. Phys. 37, 4789 (1966).
10. S. E. Harrison and J. M. Assour, J. Am. Chem. Soc. 87, 651 (1965).
11. D. Stockman; private communication.
12. J. Villar and L. Lindquist, Compt. Rend. Acad. Sci. (Paris) B264, 1807 (1967).
13. A. C. Selden, Brit. J. Appl. Phys. 18, 743 (1967).
14. W. E. K. Gibbs, Appl. Phys. Letters 11, 113 (1967).

15. I. Chen, J. Mol. Spectry. 23, 131 (1967).

16. V. D. Kotsubanov, et al., Opt. and Spectry. 25, 251 (1968).

17. L. Huff and L. G. DeShaze to be published.

18. M. W. Dowley, et al., Phys. Rev. Letters 18, 531 (1967).

BLANK PAGE

CHAPTER V

TEMPORAL OUTPUT CHARACTERISTICS OF LASERS Q-SWITCHED BY SATURABLE ABSORBERS

V-1 Introduction

The saturation characteristics of organic molecules excited by an intense light pulse have been studied in the last chapter. Here, we continue to investigate the interaction of the dye molecules inside the laser cavity, in relation to the formation of Q-switched pulses. Temporal behavior and power output of the Q-switched laser pulses will be considered analytically.

V-2 Rate Equation Approach

A laser can generally be described a an amplifying medium placed in a regenerative cavity.[1,2] In the case of a Q-switched laser, an initially lossy switching device is included in the cavity, which will withhold the onset of regenerative oscillation until the gain of the amplifying medium is high. Then the device will switch to a low loss level to permit the laser to start oscillation.

This situation creates an enhanced regeneration with the result that the system will discharge its energy very quickly.

A simple set of rate equations describing the evolution of the photon density and the population inversion of the laser medium inside the laser cavity were used by Vuylsteke[3], and by Wagner and Lengyel[4] to determine the output characteristics of a fast switched laser. Szabo[5,6,7] generalized the treatment to the case of a two-level saturable absorber as a switching element inside the laser cavity. Here, we will extend the treatment to include the residual losses of the absorbers.

We assume that the absorber is a two-level absorbing system. In view of the analysis in the last chapter, molecules which fall into either steady-state saturation or energy saturation can equally well be described as a two-level system with an effective life-time τ_s for the excited level. Where τ_s is short in the former case, and approaches infinity in the latter case. For molecules belonging in the transient saturation category, a two-level scheme is approximately true since the triplet states are not significantly populated until the laser flux reaches its peak value. Thus the effective life-time τ_s in this case will correspond to the excited singlet state life-time τ_3.

The system being considered is a laser cavity of

length ℓ containing the laser rod of length d and absorber cell length S. Spatial and spectral distributions of the radiation are neglected; in effect the laser is assumed to be operating at the center of the gain line. The rate of change of the photon density Φ can be written as

$$\frac{d\Phi}{dt} = \left(\frac{\alpha_m d}{t_1} - \frac{\alpha_n S}{t_1} - \frac{\gamma}{t_1}\right)\Phi \qquad \text{(V-1)}$$

Where $t_1 = \ell/c$ is the single pass cavity time, $\alpha_m = \alpha_{om} m$ is the absorption coefficient for the laser medium with m the normalized population inversion, α_n is the absorption coefficient for the absorber, and γ is the fractional photon loss for a single pass in the cavity due to reflection or scattering losses.

The rate of change of the population inversion for the laser and the ground state population of the absorber can be written as

$$\frac{dM}{dt} = -\frac{2\alpha_m d}{t_1}\Phi \qquad \text{(V-2)}$$

$$\frac{dn}{dt} = -\Phi c\sigma n + \frac{(1-n)}{\tau_s} \qquad \text{(V-3)}$$

where $M = M_o m$ is the inversion density for the laser medium, n is the normalized ground state population for the absorber, τ_s is the effective lifetime for the excited state of the absorber, and σ is the absorption cross-section

for the absorber. To take into account the residual absorption by the absorber, we write

$$\alpha_n = \alpha_{on} [n + \beta(1 - n)] \qquad \text{(V-4)}$$

Where $\beta = \sigma'/\sigma$, as σ' is the absorption cross-section from the excited state of the absorber. Letting $m_p = \frac{\gamma + \alpha_{on} S\beta}{\alpha_{om} d}$ and changing the time unit to $\tau = \frac{t}{T}$, where $T = \frac{t_l}{\gamma + \alpha_{no} S\beta}$, we have for $\phi = \Phi/M_o$,

$$\frac{d\phi}{d\tau} = (\frac{m}{m_p} - \frac{\alpha_{on}(1 - \beta)S}{\gamma} n - 1)\phi \qquad \text{(V-5)}$$

$$\frac{dm}{d\tau} = - \frac{2m}{m_p} \phi \qquad \text{(V-6)}$$

$$\frac{dn}{d\tau} = - \frac{\sigma/\sigma_m}{m_p} (\frac{\ell}{d}) n\phi + \frac{(1 - n)}{\tau_s/T} \qquad \text{(V-7)}$$

where we used $\alpha_{mo} = M_o \sigma_m$, σ_m being the absorption cross-section for the laser medium.

In the derivation of equations (V-5), (V-6) and (V-7), we have neglected the effect of pumping on the laser medium; in effect we assume that the laser medium inversion had reached an initial value of m_i as the Q-switched pulse began to evolve. Then, having the initial conditions that $m \sim m_i$, $n \sim n_i \sim 1$, and approximately

$\frac{d\phi}{d\tau} \sim 0$, equation (V-5) becomes

$$\frac{m_i}{m_p} - 1 = \frac{\alpha_{on}(1 - \beta)S}{\gamma} \qquad \text{(V-8)}$$

Thus (V-5) can be written as

$$\frac{d\phi}{d\tau} = [\frac{m}{m_p} - (\frac{m_i}{m_p} - 1)\ n - 1]\phi \qquad \text{(V-5')}$$

It should be noted that (V-5') is identical in form to the expression given by Szabo[5], however, the parameter m_p in this case depends on the residual loss factor β.

V-3 Absorber with Long Excited State Lifetime $\tau_s \to \infty$

Absorbers in this case are energy saturated with τ_s longer than the evolution time for the Q-switched pulse. Equation (V-7) reduces to

$$\frac{dn}{d\tau} = \frac{\sigma/\sigma_m}{m_p} n\phi \qquad \text{(V-7')}$$

Solving (V-6) and (V-7') for $n_i \sim 1$

$$n = (\frac{m}{m_i})^{2\sigma/\sigma_m}$$

then (V-5') can be put into the form

$$\frac{d\phi}{d\tau} = \left[\frac{m}{m_p} - \left(\frac{m_i}{m_p} - 1\right)\left(\frac{m}{m_i}\right)^{2\sigma/\sigma_m} - 1\right]\phi \qquad \text{(V-9)}$$

Solving (V-9) and (V-6), we have

$$\phi - \phi_i = \frac{1}{2}(m_i - m) + \left(\frac{m_i}{m_p} - 1\right)\frac{m_p}{4}\frac{\sigma_m}{\sigma}\left[\left(\frac{m}{m_i}\right)^{2\sigma/\sigma_m} - 1\right] + \frac{m_p}{2}\ln\frac{m}{m_i} \qquad \text{(V-10)}$$

At the peak of the photon density, $m \sim m_p$ from (V-9) for σ/σ_m very large. We have used the fact that for most organic saturable absorbers, $\sigma \sim 10^{-16}\text{cm}^2$, and σ ruby at 6943 Å $\sim 10^{-20}\text{cm}^2$, such that $\sigma/\sigma_m \sim 10^4$. The peak photon density inside the laser cavity is then obtained from (V-10), neglecting ϕ_i,

$$\phi_p \cong \frac{1}{2}(m_i - m_p) + \frac{m_p}{2}\ln\frac{m_p}{m_i} \qquad \text{(V-11)}$$

If γ_o is the portion of the cavity loss that goes into useful output, then the total energy and peak power outputs available from the laser can be written as

$$E = \frac{1}{2}\left[M_o(m_i - m_f) - 2\frac{S}{d}N_o(n_i - n_f)\right] Adh\nu\,\frac{\gamma_o}{\gamma} \qquad \text{(V-12)}$$

$$P_m = \phi_p M_o A d h \nu \frac{\gamma_o}{t_i} \qquad (V\text{-}13)$$

Where A is the cross sectional area of the amplifying medium. The approximate pulse width can be obtained as $\tau \sim \frac{E}{P_M}$. Neglecting the energy loss due to the absorption by the absorber, which is small compared to the total energy emitted by the amplifying medium, we have

$$\tau \sim \frac{m_i - m_f}{m_p \ln m_p/m_i + (m_i - m_p)} T \qquad (V\text{-}14)$$

For a typical Q-switched ruby laser system, $m_p \sim \frac{1}{2}(m_i - m_f)$, $m_i \sim 3m_p$, we obtain an approximate pulse width of $\sim 2T$ Under these conditions, with $\gamma_o \sim \ln 1/R \sim 0.4$, R = 65% as the output mirror reflectivity, and ℓ = 30 cm, d = 10 cm, A = 1 cm^2, peak power will be on the order of hundreds of megawatts per cm^2 in 10 nsec pulses.

For most of the organic molecules used as saturable absorbers for ruby laser, $\sigma/\sigma_m \sim 10^4$ at room temperature. Thus the second term in (V-9) can be neglected, and the equations reduce to the fast switch case as discussed by Lengyel[4]. The condition for the growth of the Q-switched pulse from noise requires that $\frac{d^2\phi}{d\tau} \geq 0$ with $n_i \sim 1$. From (V-5') we arrive at $\sigma/\sigma_m \geq \frac{m_i}{m_i - m_p}$. This inequality is always true for large values of σ/σ_m; thus a small amount of the spontaneous emission from the laser medium will

Figure V-1. Analog computer solutions to equations V-5', V-6, and V-7, for the evolution of the Q-switched laser pulse with $\tau_s = T$.

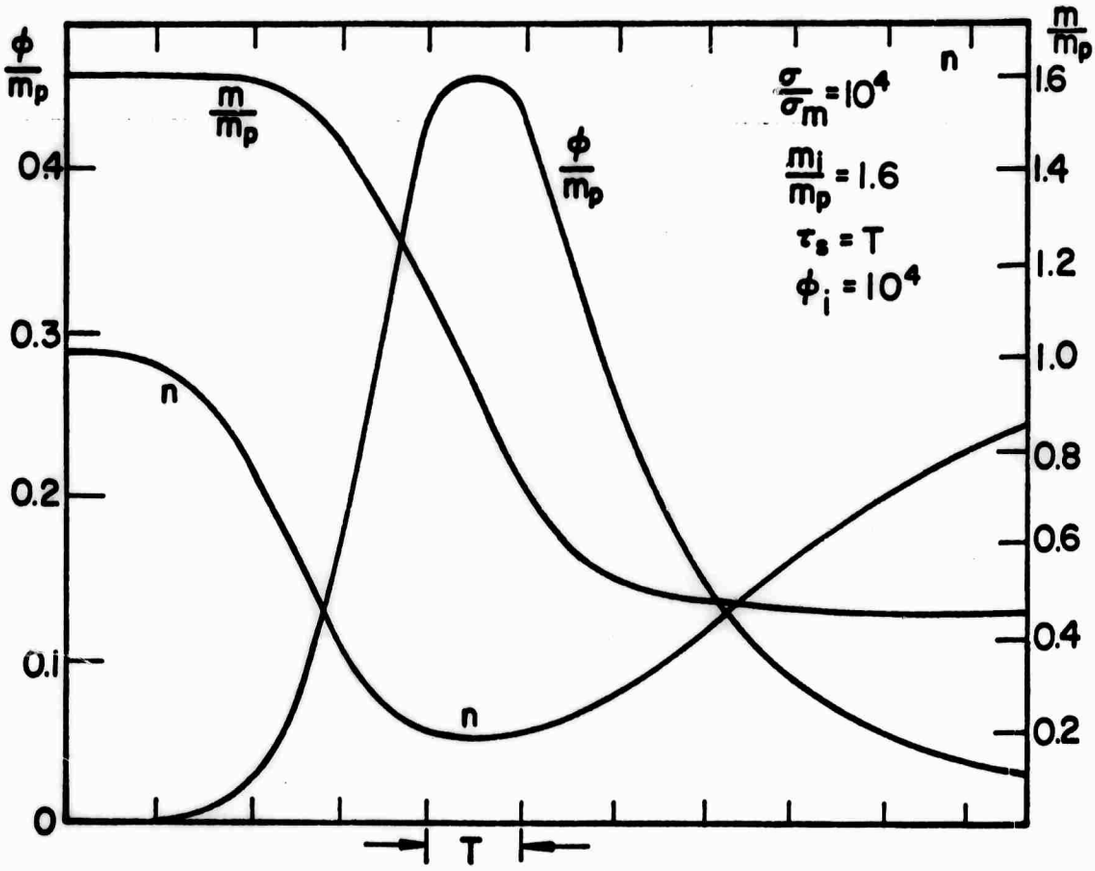
$\frac{\phi}{m_p}$
$\frac{m}{m_p}$
0.4
0.3
0.2
0.1
0
n
$\frac{m}{m_p}$
$\frac{\phi}{m_p}$
n
n
$\frac{\sigma}{\sigma_m} = 10^4$
$\frac{m_i}{m_p} = 1.6$
$\tau_s = T$
$\phi_i = 10^4$
T
$\frac{m}{m_p}$
1.6
1.4
1.2
1.0
0.8
0.6
0.4
0.2

enable the growth of the Q-switch pulse.

V-4 Absorber with Short Excited-State Lifetime

Absorbers in this case are either steady-state saturated or transiently saturated. Solutions for the photon density ϕ cannot be obtained analytically in a simple form. Solutions to equations (V-5'), (V-6), and (V-7) were programed on an analog computer with parameters appropriate for ruby lasers. A typical result with absorber excited-state lifetime of $\tau_s = T$ is shown in figure V-1. ϕ_i is of the order of 10^{-4} as set by the computer noise (which simulated amplified spontaneous emission). In order to compare this to the case of absorbers with long excited-state lifetime, solutions for identical laser parameters with $\tau_s \to \infty$ were obtained from the analog computer. Comparing the two cases, we found that the characteristics of ϕ, in peak power, risetime and falltime, are similar to within a few percents. These results indicate that the lifetimes of the absorbers do not have a significant effect on the Q-switched pulse evolution. Similar conclusions have been reached by Szabo,[7] and Mcleary,[8] in which they showed that for $\sigma/\sigma_m \sim 10^4$, the characteristic of ϕ depends solely on the two parameters; $\frac{m_i}{m_p}$ and $\frac{\sigma\tau_s}{\sigma_m T}$, for large value of $\sigma\tau_s/\sigma_m T$,

the result approaches that of the fast switch case. Since most absorbers saturate at an irradiance on the order of megewatts per cm^2, from $I_s \sim (\sigma T_s)^{-1}$ we have $\frac{\sigma T_s}{\sigma_m T} \geq 10^3$. Thus the lifetime of the absorber will have negligible effect on the characteristic of the output pulses provided $\sigma/\sigma_m \sim 10^4$.

V-5 Discussion

The simple theory presented here does predict several features which are common to most of the Q-switched lasers. The power output and the pulse width depend significantly on the initial inversion achieved for the laser medium. Peak power output predicted by this theory as compared with experimental results is generally smaller by a significant factor. The shortcoming of this theory is that certain nonlinear effects, such as the interaction between different modes, and rod focusing effects[9], cannot be taken into account.

For the three dye molecules H_2PC, CAPC, and CC, used as saturable absorber in the ruby laser, similar temporal behavior of the output pulses has been observed. Since CC dye has a high saturation irradiance of $I_s \sim 2 Mw/cm^2$ so it is commonly used to Q-switch ruby lasers in order to obtain high peak power output pulses.

The exhibition of a maximum in transmission at ~20MW/cm^2 for CAPC molecules will have a bearing on its performance as saturable absorber. Nonlinear devices with intensity dependent losses when placed in the laser cavity will exhibit stabilization of the laser output.[10,11] The bleaching and subsequent increase of absorption for CAPC at high radiation flux may be useful for simultaneous passive Q-switching and power stabilization of the laser outputs. It is found that CAPC when used as a saturable absorber for ruby laser does give more stable output with peak intensity ~10MW/cm^2 compared with other absorbers being used.

REFERENCES

1. G. Birnbaum, "Optical Masers", Academic, New York (1964).
2. B. A. Lengyel, "Introduction to Laser Physics", Wiley, New York (1966).
3. A. A. Vuylsteke, J. Appl. Phys. 34, 1615 (1963).
4. W. G. Wagner and B. A. Lengyel, J. Appl. Phys. 34, 2040 (1963).
5. A. Szabo and R. A. Stein, J. Appl. Phys. 36, 1562 (1965).
6. A. Szabo and L. E. Erickson, J. Appl. Phys. 37, 4953 (1966).
7. A. Szabo and L. E. Erickson, J. Appl. Phys. 38, 2540 (1967).
8. R. Mcleary and P. W. Bowe, Appl. Phys. Letters 8, 116 (1966).
9. G. E. Devlin, et.al., Appl. Opt. 1, 11 (1962).
10. H. Statz, et.al., J. Appl. Phys. 36, 1510 (1965).
11. R. H. Pantell and J. Warszawski, Appl. Phys. Letters 11, 213 (1967).

BLANK PAGE

CHAPTER VI

SPECTRAL OUTPUT OF A Q-SWITCHED LASER WITH SATURABLE ABSORBERS; RELATED PROBLEM OF HOLE-BURNING

VI-1. Introduction

Owing to the effective inhomogeneous broadening[1] of the laser line in a standing wave cavity, Q-switched lasers will not generally operate in a single axial mode. Ruby lasers Q-switched with optical shutter (rotating mirror) show an output spectral width of ~1 cm^{-1},[2,3]. Early attempts to Q-switch ruby lasers with saturable absorbers showed a marked purity in the spectral output; spectral widths of ~0.05 cm^{-1} were obtained without any mode selective device inside the cavity.[4] For a laser cavity of length 30 cm, an output spectral width of 0.05 cm^{-1} corresponds to oscillation in three to four axial modes of the Fabry-Perot cavity. Hercher[5] has shown that by incorporating a special resonant reflector as the output mirror in a passively Q-switched ruby laser, single axial mode operation can be reproducibly obtained.

If the absorption lines of the saturable absorbers

are homogeneously broadened (which is true for H_2PC and CAPC), one expects that no inherently frequency-selective property would be exhibited by these absorbers when used for Q-switching laser. Sooy[6] has shown that for a passively Q-switched laser, natural selection of modes could be enhanced due to the slow switching process of the absorber. Another possibility was pointed out by Soffer and McFarland,[7] who showed in their experiments with the frequency-locking of two lasers that some degree of hole burning does occur in the absorbers.

In this chapter we will briefly discuss first the natural selection of modes by the absorbers, and then a number of experiments that indicate the nature of the hole-burning effect exhibited by the frequency-locking of two lasers.

VI-2. Natural Selection of Modes by the Absorber

As pointed out by Sooy[6], the basic mechanism which leads to selection of modes as they grow out of noise arises from the fact that the buildup time for Q-switched laser with saturable absorber is much longer than for fast switched laser with either an optical or mechanical shutter. Since the initial photon density inside the cavity is of the order 10^7 photons/mode, supplied by the spontaneous emission from the amplifying medium, the dominant mode

in a passively Q-switched laser has to reach a value of $\sim 10^{22}$ photons/mode, which is strong enough to bleach the absorber in order for the laser to oscillate. The process is completely different in the fast-switched case, where each mode can simultaneously compete for the gain in the amplifying medium as soon as the shutter is opened. A further support for this type of mechanism is the fact that, by inserting a resonant reflector inside the cavity of a passively Q-switched laser, off-resonant modes can be suppressed with the output wavelength reproducible to ~ 0.005 Å.[5]

Other mechanisms, such as spatial hole-burning in the absorber cell, and Fabry-Perot cavity formed by the absorber cell windows, can produce mode selection to some degree. The former mechanism will be effective only when the absorber is appreciably saturated, which occurs only during the last few transits of the cavity. The latter mechanism will depend on the geometry of the dye cell involved, and can easily be avoided.

If the absorption line of the absorber is inhomogeneously broadened, a spectral hole will be burnt into the absorption line by the predominant mode in the cavity; such that the output spectrum will invariably consist of modes which fall into the spectral width of the hole being burned. Soffer and McFarland[7] have shown that two lasers

Figure VI-1. Experimental setup for frequency-locking of two lasers.

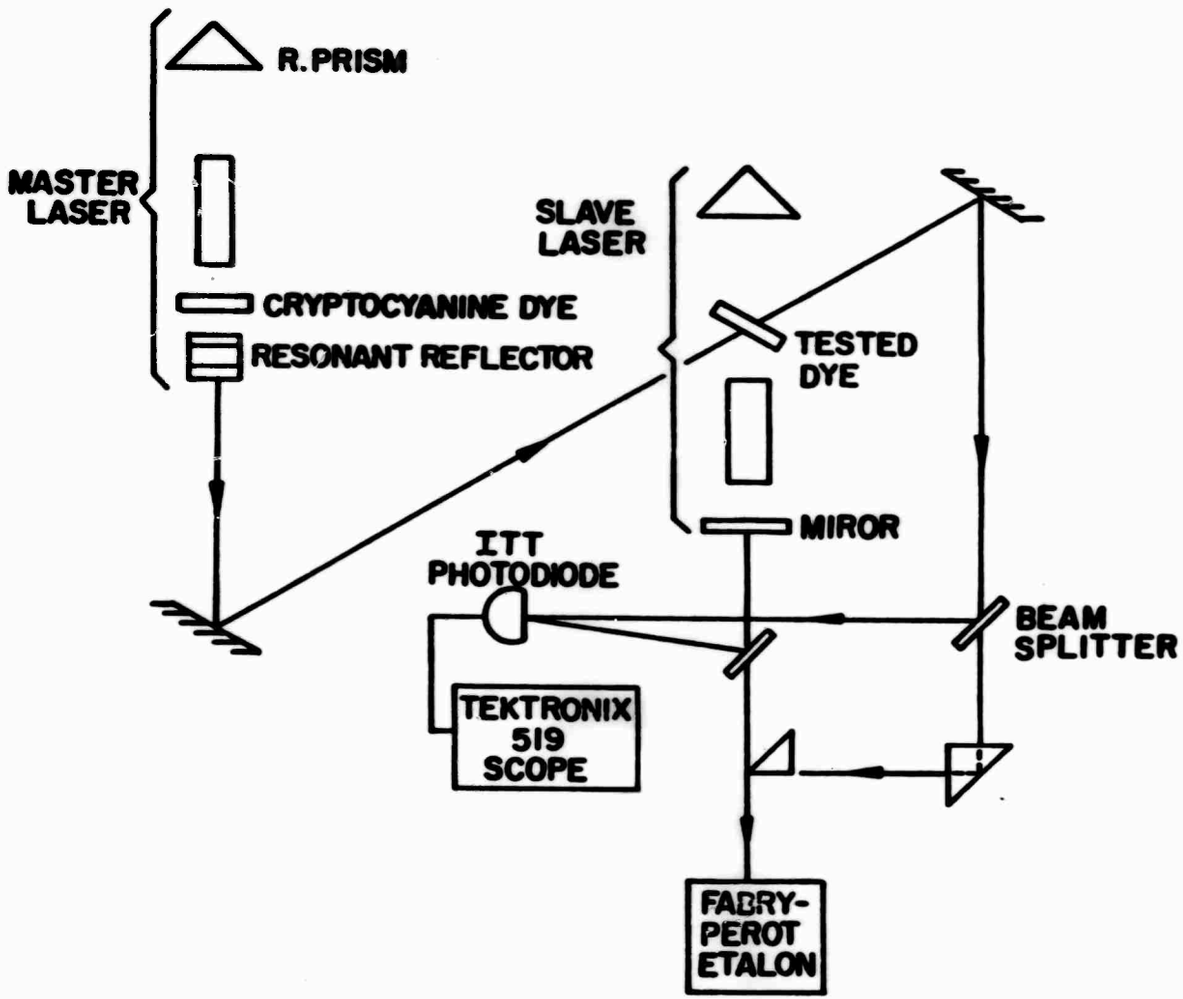
R. PRISM
MASTER LASER
CRYPTOCYANINE DYE
RESONANT REFLECTOR
SLAVE LASER
TESTED DYE
MIROR
ITT PHOTODIODE
BEAM SPLITTER
TEKTRONIX 519 SCOPE
FABRY-PEROT ETALON

can be frequency-locked if the output of the second laser is switched on by saturating its absorber via the output from the first laser. The absorber used in their experiments was metal-free phthalocyanine, which is known to be homogeneously broadened. Their results indicated that spectral hole-burning does exist in an absorber even though its absorption line is homogeneously broadened.

VI-3 Frequency-locking Experiments[8]

Experimental setups similar to those used by Soffer and McFarland[7] were used to investigate the nature of the hole-burning exhibited by saturable absorbers in inducing frequency-locking of two lasers. This is shown in figure VI-1. The first laser, hereafter referred to as the master laser, was a water cooled ruby laser system with an 8-cm ruby rod in a 40-cm cavity consisted of a Brewster angle roof prism and a resonant reflector with peak reflectance of 40%. Cryptocyanine in acetonitrile was used as the Q-switching saturable absorber, giving reproducible output pulses with duration 25 nsec, peak power ~20 MW, and spectral width of ~200 MHZ. The cross-sectional area of the output was approximately 1 cm^2.

The second laser, hereafter referred to as the slave laser, was a similar laser system with cavity length ~75 cm. The output from the master laser was used to

saturate the absorber in the slave laser cavity. The dye solution was contained in commercial Q-switching dye cell with AR-coated windows,and cell thickness 1.6 mm. The concentration of the dye solution was adjusted to give an optical density of 0.35 at 6943 Å. The operation of the two lasers was achieved by synchronizing the two laser power supplys in such a way that the slave laser would only lase due to the saturation of the absorber induced by the output from the master laser. It was found that when the two lasers lased in synchronization, the output from the slave laser was always preceded in time by the master output by 50 to several hundred nsec. For stable synchronization, slave laser was generally operated at a few percent below threshold pumping power required for normal Q-switching operation.

The output from the two lasers were detected by a fast IT & T plano-photodiode and displayed on a Tektronix 519 scope. A Fabry-Perot quartz etalon with a 9 mm mirror separation was used to observe the output spectrum. The fringe pattern of the Fabry-Perot was split along a diameter so that both output spectra could be separately but simultaneously recorded.

(1) Frequency-locking with no mode selection in slave cavity: Using a dielectric output mirror of reflectivity 35% in the slave cavity, consistent frequency-locking of

Figure VI-2. Experimental results on frequency-locking of two lasers. (a) Fabry-Perot interferogram showing master and slave laser spectra to be frequency-locked (free spectral range 16.7 Ghz). (b) Simultaneous scope-photo showing master laser pulse followed by the slave laser pulse. Horizontal scale 50 nsec/div.

SLAVE | MASTER

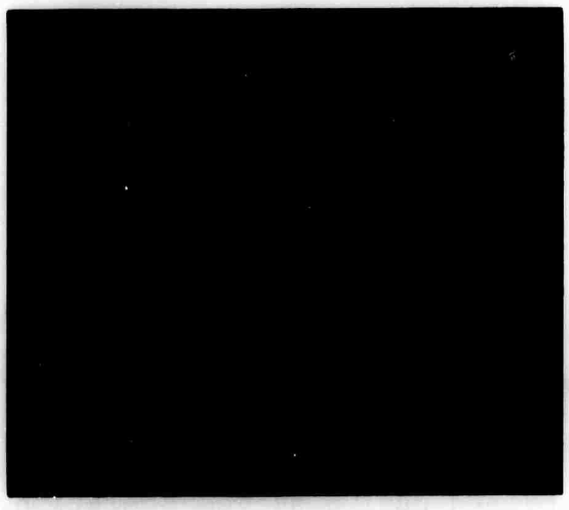

(a)

(b)

Figure VI-3. Experimental results with resonant reflector in the slave cavity. (a) Spectra of master and slave lasers (unslaved mode of operation). (b) Spectra obtained during slaved operation. (c) Scope-photo obtained at the time fig. V-3b was recorded. Note: in this case both the master and slave lasers had frequency selective resonant reflectors, which precluded frequency-locking but did not prevent slaved operation. Horizontal scale: 50 nsec/div.

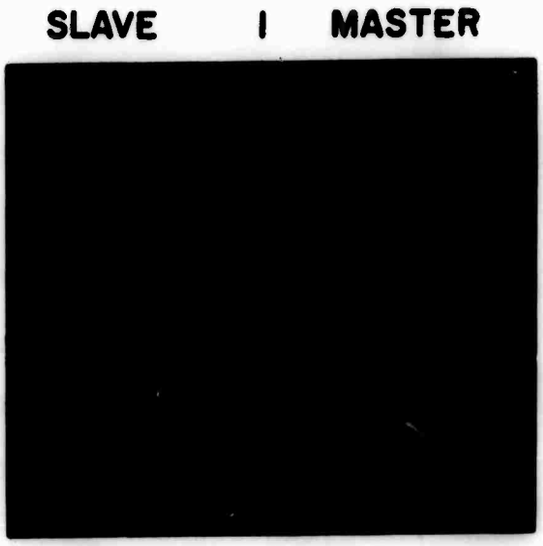

(a)

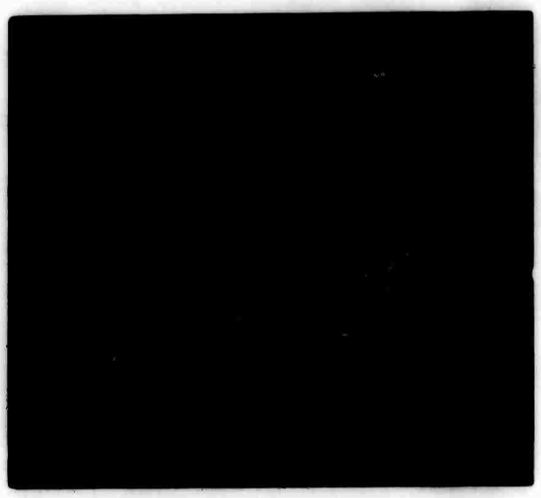

(b)

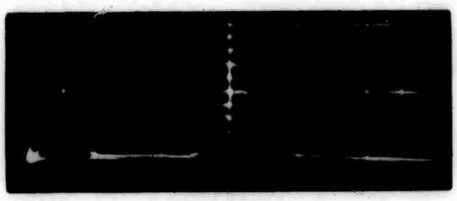

(c)

the slave and the master lasers were observed for both H_2PC in 1-chloronaphthalene and CAPC in pyridine used as the saturable absorber. The spectral output from the slave laser generally consisted of two adjacent axial modes (separation 200 MHZ for cavity length 75 cm) of unequal intensity, bracketing the frequency of the single spectral component of the master laser. A typical interferogram and scope photograph are shown in figure VI-2 for the case in which the two lasers were frequency-locked together. When the slave laser was not synchronized to the master laser, its output invariably consisted of a number of spectral lines which were not reproducible. The above results showed a much more pronounced spectral hole-burning in the absorbers than that observed by Soffer and McFarland, in which additional spectral components from the slave laser were observed[7].

(2) Slave laser with resonant reflector as output mirror: The same experiments were repeated using a resonant reflector for the slave laser with peak reflectivity 35% as the output mirror. The resonant reflector for the slave laser had a resonant frequency which differed from that of the resonant reflector in the master laser by about 6.8 GHZ, which was checked by firing the two laser separately. The results obtained by synchronizing the two lasers are shown in figure VI-3. The slave laser lased at the same

frequency as it did without synchronization to the master laser, however, the slave output exhibited synchronization to the master output with approximately the same time delay as in the case of frequency-locking. One thus sees that the resonant reflector in this case was sufficiently effective to prevent the slave laser from locking on spectrally to the master frequency, but that the saturation produced by the master laser pulse was responsible for triggering the slave laser.

(3) Time delay between master and slave laser pulses: Since the absorbers used in these experiments have been shown to be homogeneously broadened,[8,9] the operation of the slave laser in the synchronized mode is essentially a fast-switched laser as described by Lengyel.[10] The pulse buildup time from the moment of switching is approximately proportional to the cavity length, and depends on the initial population inversion for the amplifying medium. A number of experiments were performed under different conditions to investigate the time delay between the master and the slave laser pulses, and its effect on the frequency-locking of the two lasers. A dielectric output mirror of 35% was used for the slave laser in these experiments. At first, the slave laser cavity length was increased to 150 cm, the time delay for the two pulses increased to ~600 nsec with the same effectiveness

Master Peak Output MW/cm^2	20	5.0	2.0
Master Peak to Slave Peak (nsec.)	100	145	165

(a) Slave delay as a function of master laser intensity

Master Peak Output MW/cm^2	20	5.0	2.0
From the point the absorber is 5% bleached to Master Peak (nsec.)	100	70	55
From the point the absorber is 5% bleached to Slave Peak (nsec.)	200	215	220

(b) Slave delay from the point of switching (the absorber is 5% bleached)

Table II

* See reference 11

of frequency-locking as before. In the second series of experiments, the pumping power from the slave laser power supply was varied. A decrease of the time delay between the two pulses resulting from an increase of the pump power was observed. However, as soon as the pumping level was greater than 10% above the minimum level for slave action, the slave laser fired before the master laser. The same type of frequency-locking was observed when the two lasers were in synchronization. The above results qualitatively confirmed the fast-switching nature of the slave laser operation. In the third series of experiments, the master laser output was attenuated with calibrated filters made of solutions of $CuSO_4$, thereby varying the intensity level incident on the absorber in the slave cavity. The results are shown in Table II-a. The time delay between the two pulses increased (measured from peak to peak) as the master output level was decreased, and no slave action could be observed when the master output was below 1 MW/cm^2. Frequency-locking to the same degree was observed down to an intensity of 2MW/cm^2 from the master laser. The cutoff intensity level of ~1 MW/cm^2, at which no slave mode could be operated, does correspond to the intensity level at which the dye molecules begin to saturate completely. In order to find the buildup time for the slave pulse in this case, the starting time should be taken as the time at which the switching process of the

absorber has just begun. Since the initial photon flux in the slave cavity will experience increased gain as soon as the absorber shows a few percent bleaching, we can safely assume that this level of bleaching will correspond to the starting time for the slave pulse to evolve. As shown by Stockman,[11] the time interval from the moment the absorber exhibits 5% bleaching to the time the slave pulse reaches its peak, is approximately the same for the three master intensity levels. The results are shown in Table II-b.

Similar experiments were attempted with cryptocyanine as the absorber in the slave cavity, but without success in that the synchronization of the two lasers was not possible. This result is not surprising in view of the nature of the slave operation which is essentially a fast-switched laser. After the passage of the master pulse, phthalocyanine molecules with their long triplet state lifetime will be transparent for ~1 μsec, whereas most of the ground state population for the crypyocyanine molecules will be returned. Kaiser and Power[12] were able to frequency-lock two lasers with cryptocyanine as absorber in the slave cavity. Since the output intensity from their master laser was of the order of a few hundred MW, the frequency-locking results may well have been due to the injection-locking of two lasers observed by Bondarenko.[13]

In all the measurements above, the two lasers were set with their output polarization in the same plane. By setting the two polarizations orthogonal to each other, identical results were obtained, confirming the results obtained by Soffer and McFarland.[7]

Recent experiments on frequency-locking by Stockman[11] give a further indication as to the nature of the spectral hole burned into the absorber. Using two identical resonant reflectors whose adjacent resonant frequencies were separated by about 0.2 cm^{-1}~6 GHZ for both the slave and the master lasers, measurements were performed by pressure scanning the second resonant reflector in the slave cavity. Stockman observed consistent frequency-locking of the two lasers by detuning the resonant frequency of the slave resonant reflector up to 0.1 cm^{-1} ~3 GHZ from the master frequency for CAPC in pyridine as absorber. On the other hand, frequency-locking could be maintained only up to 0.4 cm^{-1} ~1.2 GHZ separation of the resonant frequencies if CAPC in cyclohexenol was used as absorber. Since by tuning the resonant frequency of the second resonant reflector away from the master frequency, one gradually introduces higher losses at the master frequency, this measurement indicates that the depth and/or width of the hole depends on the solvent used.

VI-4. Interpretation and Discussion

The consistent frequency-locking between the slave and the master laser which we observed indicates positively that a spectral hole can be burnt into the absorption line of the absorber. Since the slave mode operation results in essentially a fast-switched laser, the natural selection of modes by the absorber, as pointed out by Sooy,[6] is not very effective in this case. The fact that the output spectrum from the slave laser is always within the spectral output bandwidth of the master laser, indicates that the spectral hole is sufficiently narrow to effectively discriminate against oscillation at further removed frequencies.

The degree of mode discrimination by the spectral hole could be inferred by considering the experimental results in VI-3-(2), in which frequency-locking was prevented by the use of a second resonant reflector. In this case, the slave laser was still triggered by the master laser, with a time delay of approximately 100 nsec between the two pulses. For the slave cavity length of 75 cm, this will correspond to about 20 loop transits for the buildup of the slave pulse in the dominant mode. For the special resonant reflector being used (made of two identical 2 mm quartz plates separated by 2.5 cm), the reflective loss for the adjacent mode separation of

200 MHZ will correspond to about 0.1 dB* per pass. Thus in the 20 loop transits, a net gain of ~2 dB relative to the adjacent axial mode will be provided by the resonant reflector in favor of emission in the axial mode coincident with the resonant frequency. In the case of frequency-locking where a broad-band dielectric mirror was used, the slave laser output consisted of just one or two adjacent axial modes. The output spectrum for the slave laser in this case was determined solely by the spectral hole burned into the absorber. One can then conclude that a minimum net gain of 2 dB will be provided for the mode at the center of the spectral hole. If we assume further that the spectral hole exists only during the passage of the master pulse, of order 30 nsec corresponding to 6 loop transits in the slave cavity, the spectral hole would have to have a maximum hole width (FWHM) of approximately a few hundred MHZ (based on a minimum 2 dB attenuation in 200 MHZ for a hole with Gaussian profile).

The several possible mechanisms which have been proposed to explain the observed frequency-locking experiments will be discussed in the following:

*The definition of dB is;

$$dB = -(10)\ \log_{10}(\text{transmission})$$
$$= -(10)\ \log_{10}(e^{-\alpha x})$$
$$= 4.34\ (\alpha\, x)$$

(1) Scattering: If sufficient amount of radiation from the master laser could be injected into the slave cavity at the time the slave laser reaches threshold, frequency-locking of the two lasers could be obtained.[13] As shown by Stockman,[11] based on a fast-switched model with parameters as listed in Table II-b, and assuming the initial photon density of 10^7 photons/mode[6] at the point the absorber exhibits 5% bleaching, the photon density would be $\sim 10^{12}$ photons/mode when the master laser output of 20 MW/cm^2 reached its peak value. Experimental measurements on the amount of scattering by the dye cell irradiated by 20 MW/cm^2 Q-switched laser pulses were performed. The scattering at 6943 Å was detected with a calibrated EG & G "Lite-Mike" detector. The maximum amount of light that we were able to scatter into the slave cavity was found to be 10^6 to 10^7 photons/mode, a value smaller by a factor of 10^{-5} from the estimate above. We thus conclude that scattering is not responsible for the frequency-locking results. A similar conclusion has been reached by Soffer and McFarland.[7]

(2) Transient hole-burning by selectively populating the upper vibronic sublevel:[8] Even though the absorbers that we used in the frequency-locking experiments are homogeneously broadened (in the sense that uniform depletion of absorption across the absorption profile occurs

during the passage of a Q-switched laser pulse), spectral hole-burning can still occur due to the finite relaxation time of the subvibronic level in the first excited singlet state that was being reached by the intense light pulse. If we consider the energy-level scheme for the molecules as shown in figure II-2, where absorptive transitions originate from the lowest vibronic level in the ground state and excite into the j^{th} vibronic sublevel of the first excited singlet state. There the molecules relax non-radiatively down to the zeroth vibronic level with a relaxation time τ_v. From this zeroth vibronic level, the molecules then decay back to the ground state via different channels with a net relaxation time τ. The rate equations for the populations of these levels are

$$dn_{10}/dt = -I\sigma(n_{10} - n_{30}) + n_{30}/\tau \qquad \text{(VI-1)}$$

$$dn_{30}/dt = n_{3j}/\tau_v - n_{30}/\tau \qquad \text{(VI-2)}$$

$$dn_{3j}/dt = I\sigma(n_{10} - n_{3j}) - n_{3j}/\tau_v \qquad \text{(VI-3)}$$

where σ is the absorption cross-section, and n_i's are the normalized population for the i^{th} level (the second subscript denotes the vibronic sublevels). The absorption coefficient for the 10 → 3j transition is given by

Figure VI-4. Transient spectral hole-burning. Hypothetical time development of a transient spectral hole. The curves labelled $n_{30}(t)$ and $n_{10}(t)$ show the buildup and decline of the lowest vibronic sublevels of the first excited and ground electronic states respectively. The lowest curve is proportional to the spectral hole depth, and shows the population of the excited vibronic sublevel which decays with a lifetime τ_v. It is assumed that the exciting radiation field is a step-function in time. The figure is intended to be illustrative only.

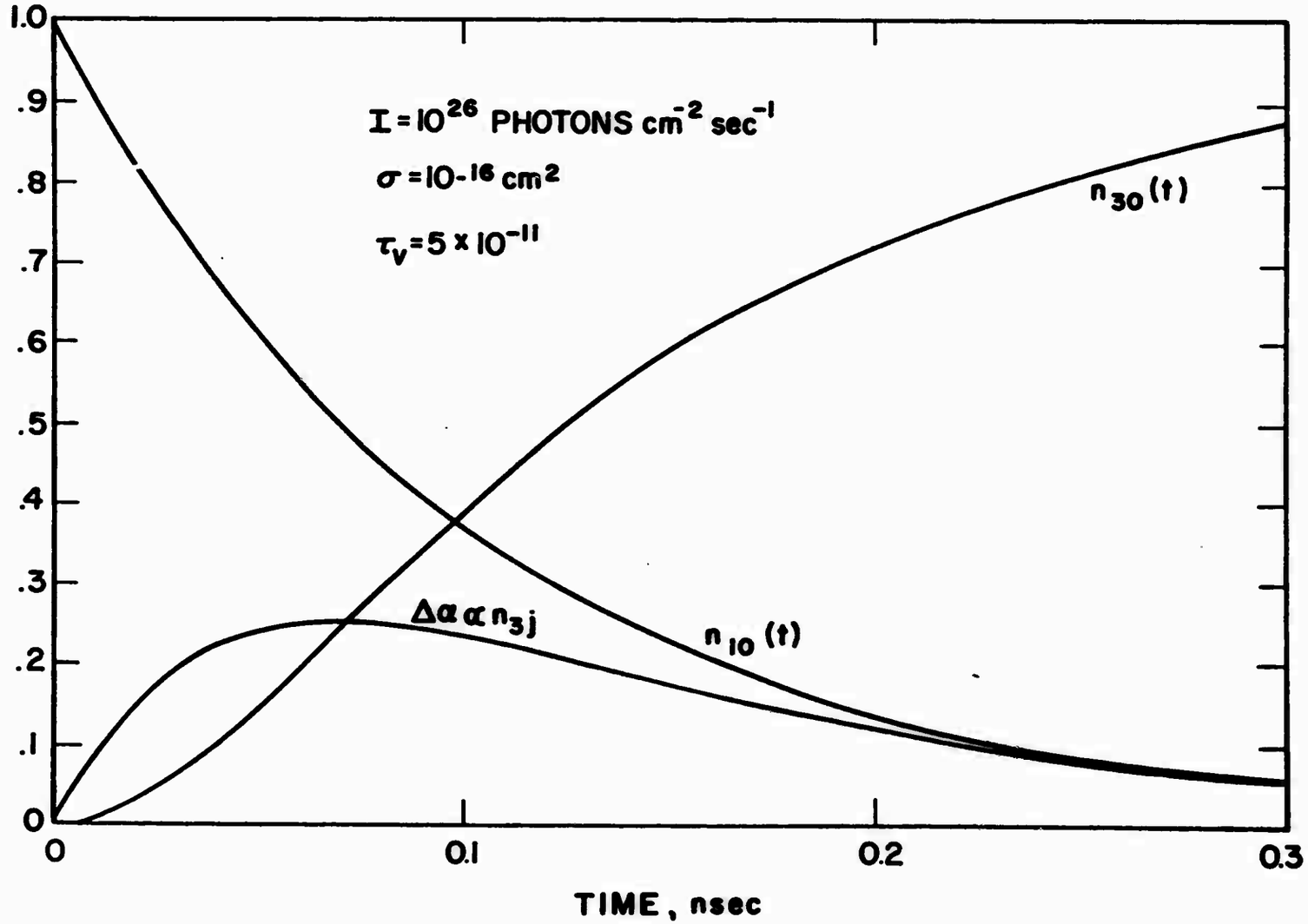
1.0
.9
.8
.7
.6
.5
.4
.3
.2
.1
0
0
0.1
0.2
0.3
TIME, nsec
I = 10^26 PHOTONS cm^-2 sec^-1
σ = 10-16 cm^2
τv = 5 x 10^-11
n30 (t)
n10 (t)
Δα ∝ n3j

$$\alpha_{10 \to 3j} = N_o \sigma (n_{10} - n_{3j}) \qquad \text{(VI-4)}$$

where N_o is the total concentration of the dye molecules. The absorption coefficients for the $10 \to 3i$ ($i \neq j,0$) transitions are given by

$$\alpha_{10 \to 3j} \sim N_o \sigma n_{10} \qquad \text{(VI-5)}$$

The spectral hole produced in this case will be given by $\Delta\alpha$, where

$$\begin{aligned} \Delta\alpha &= \alpha_{10 \to 3i} - \alpha_{10 \to 3j} \\ &= N_o \sigma n_{3j} \end{aligned} \qquad \text{(VI-6)}$$

The maximum depth of the hole can be found from (VI-3) directly

$$\Delta\alpha_{max} = N_o \sigma (n_{10} I\sigma)/(I\sigma + 1/\tau_v) \qquad \text{(VI-7)}$$

Figure VI-4 illustrates the solution for (VI-1, 2,3), assuming that there are no other significantly populated levels, and $\tau >> \tau_v$. Inspection of (VI-7) shows that the maximum spectral hole depth has an upper limit of

$$\Delta\alpha_{max} \leq N_o \sigma(I\sigma)/(I\sigma + 1/\tau_v) \qquad \text{(VI-8)}$$

For absorber of thickness x, the net gain G_{dB} after m loop transits inside the slvae cavity will be

$$G_{dB} = 4.34\ m\ (\Delta\alpha)\ x \qquad \text{(VI-9)}$$

Substituting the expression for $\Delta\alpha_{max}$ from (VI-8), we have

$$\tau_v \cong G_{dB}/[(4.34\ m\ N_o x - G_{dB})\ I\sigma] \qquad \text{(VI-10)}$$

An estimate value of τ_v can be obtained by substituting the parameters appropriate to the experimental condition, $N_o \sim 10^{16}$ molecules/cm^3, $I \sim 10^{26}$ photons/cm^2-sec, $x = 0.16$ cm, $\sigma \sim 5 \times 10^{-16} cm^2$, and a 2-dB net gain figure in two loop transits of the slave cavity from the above discussion, we have $\tau_v \sim 5 \times 10^{-12}$ sec.

This simple account of the spectral hole-burning gives a reasonable value for the vibronic relaxation time. However, experimental results indicated that for a master pulse of peak power 2 MW/cm^2, identical frequency-locking was observed. In this case the net gain provided by the transient hole would be a factor of 10 smaller, which would be insufficient to discriminate against oscillation in off-resonant frequencies.

(3) Hole-burning due to two-wave interaction in the absorber: Tan and Schwartz[14] have shown from their calculation that, for absorptive molecules interacting with a strong wave at frequency ω_1 and a weak wave at ω_2, both near resonance of the molecular transition, the weak wave will experience reduced absorption due to the nonlinear coupling of the two waves by the molecules. The spectral hole width deduced from their calculation (based on density matrix approach to a two-level system[15]) was $2/T_1$, where T_1 is the decay time for the upper level. Furthermore, the depth of the hole was found to be linearly dependent on the strong wave intensity. The interpretation of experimental results by this theory is difficult as the absorber used were not simple two-level systems. Furthermore, this theory does not take into account the solvent interaction which evidently plays a role in the hole-burning processes.

At present, no theory* has adequately explained the type of spectral hole-burning in organic absorbers associated with the frequency-locking of two lasers that we and others have observed. This type of hole-burning will not be effective in determining the output spectrum of a dye Q-switched laser, as the hole will be induced only

* I feel that the recent explanation proposed by Stockman,[11] in which the fluctuation of the indices of refraction of the solvent was responsible for the spectral hole, is incorrect, and was based on an unrealistically large value for Δn.

when a dominant mode reaches sufficiently high intensity. A useful application of the above experimental techniques is in the production of two high intensity light pulses with identical narrow spectra having a time delay which can be varied from 50 to 500 nsec.

REFERENCES

1. C. L. Tang et al., J. Appl. Phys. 34, 2289 (1963).
2. T. V. Gvaladze et al., Soviet Phys. JETP 21, 72 (1965).
3. C. R. Guiliano and L. D. Hess, Appl. Phys. Letters 9, 196 (1966).
4. B. H. Soffer, J. Appl. Phys. 35, 2551 (1964).
5. M. Hercher, Appl. Phys. Letters 7, 39 (1965).
6. W. R. Sooy, Appl. Phys. Letters 7, 36 (1965).
7. B. H. Soffer and B. B. McFarland, Appl. Phys. Letters 8, 166 (1966).
8. Much of this work has been reported in M. Hercher, D. Stockman and W. Chu, IEEE J. Quantum Electronics QE-4, 954 (1968).
9. W. K. Kosonocky and S. E. Harrison, J. Appl. Phys. 37, 4789 (1966).
10. B. A. Lengyel and W. G. Wagner, J. Appl. Phys. 34, 2040 (1963).
11. D. Stockman, to be published.
12. H. Opower and W. Kaiser, Phys. Letters 21, 638 (1966).
13. A. N. Bondarenko et al., Soviet Phys. JETP Letters 6, 692 (1967).
14. S. E. Schwarz and T. Y. Tan, Appl. Phys. Letters 10, 4 (1967).
15. N. Bloembergen and Y. R. Shen, Phys. Rev. 133, A37 (1964).

CHAPTER VII

CONCLUSIONS

VII-1. Summary

In Chapter II and III, we discussed briefly the primary photophysical processes of polyatomic molecules which are applicable to a dilute system using a model based on the modified Jablonski energy-level model. Several different lifetimes for the three molecules: Cryptocyanine, metal-free phthalocyanine, and chloroaluminum phthalocyanine, were determined experimentally. In particular, we found that the intersystem crossing time for H_2PC was 25×10^{-9} sec, indicating that the internal conversion time from the first excited singlet to the ground state was 7×10^{-9} sec.

In Chapter IV, we analyzed the saturation of the molecular absorption for the three molecules under excitation by intense Q-switched ruby laser pulses using the various lifetimes determined from Chapter III. Experimental results were comparable with analytical results based on a simplified four-level model with excited-state absorption. From the range of the Q-switched pulse

durations being used, we concluded that the saturation of cryptocyanine and H_2PC can be described as steady-state saturation, whereas CAPC can be described as transiently saturable. Excited-singlet-state absorptions were found to be the cause for residual losses exhibited by the phthalocyanine molecules. The excited singlet-singlet absorption cross-sections were deduced from the transmission data to be of an order $\sim 10^{-17} cm^2$. The fact that an increase in the transmission of CAPC to a maximum with a subsequent decrease at still higher intensity level was found to be due to the effect of three absorptive transitions in the singlet manifold. A value of 10^{-11} sec for internal conversion from the second to the first excited singlet states was deduced from the transmission curve.

In Chapter V, we discussed the general characteristics of dye Q-switched laser output. A simple two-level model was used for the absorbers in describing the temporal behavior of the Q-switched output. Output pulse parameters such as peak power and pulse half-width were found to have insignificant dependence on the absorber lifetime due to the large absorption cross-section exhibited by the dye molecules. We concluded that phthalocyanine molecules when used as saturable absorbers are best suited for low power level (10 MW/cm^2) applications due to the relatively low intensity required for saturation.

Several mechanisms which lead to mode selection by the absorber for Q-switching ruby lasers were discussed in Chapter VI. In particular, the nature of spectral hole-burning which is responsible for frequency-locking of two lasers was investigated experimentally in some detail. Several possible mechanisms, scattering, transient hole burning, and coupling of waves in the absorber, were found to be inadequate to explain our experimental observations.

VII-2. Suggestions for Further Work

Since the saturation of molecular absorption processes in our investigations are mainly concerned with incident pulses of durations 10 to 30 nsec, it would be interesting to extend the investigation to pulses of shorter duration, say 10^{-11} sec. At present, these type of pulses can be obtained from mode-locked lasers using a single pulse selection technique.[1] There are several advantages of using pulses of shorter duration. One could, for example, use this method to detect molecular relaxation times in the range of 10^{-9} to 10^{-11} sec, and to measure excited singlet-state absorption spectra. Conventional photo-detectors using the ultra-fast light gate technique[2] can be used for detection in this case. The saturation of molecular absorption processes in this case cannot be

described by the rate equation approach, due to the fact that coherent interaction, such as self-induced transparency,[3] will become important.

The problem of spectral hole-burning of the type that induces frequency-locking of two lasers, is still unresolved by our investigation. The difficulty involved is that the exact nature of the spectral hole cannot be measured accurately. Furthermore, molecular processes in the time scale less than 10^{-9} sec are still not well understood. If one can design a sufficiently powerful tunable cw laser, with an output spectrum as narrow as the Q-switched ruby laser output, then the width and the depth of the spectral hole could be measured accurately.

REFERENCES

1. A. W. Penney, and H. A. Heynau, Appl. Phys. Letters **9**, 257 (1966).
2. M. A. Duguay, and J. W. Hansen, Appl. Phys. Letters **15**, 192 (1969).
3. S. L. McCall, and E. L. Hahn, Phys. Rev. Letters **18**, 908 (1967).

Unclassified

Security Classification

DOCUMENT CONTROL DATA - R & D

(Security classification of title, body of abstract and indexing annotation must be entered when the overall report is classified)

(Corporate author) University of Rochester, Rochester, New York, 14627	2a. REPORT SECURITY CLASSIFICATION: unclassified 2b. GROUP

3. REPORT TITLE: INTERACTION BETWEEN INTENSE OPTICAL RADIATION AND MATTER

4. DESCRIPTIVE NOTES (Type of report and inclusive dates): Final Report

5. AUTHOR(S) (First name, middle initial, last name): Michael HERCHER, William P. CHU

6. REPORT DATE: December, 1970	7a. TOTAL NO. OF PAGES: 170	7b. NO. OF REFS: 97
8a. CONTRACT OR GRANT NO: DA-31-124-ARO-D-401 b. PROJECT NO: ARPA Order No. 675 Project DEFENDER Program Code No. 6.25.03.01R	9a. ORIGINATOR'S REPORT NUMBER(S): none assigned 9b. OTHER REPORT NO(S) (Any other numbers that may be assigned this report)	

10. DISTRIBUTION STATEMENT: Distribution of this report is unlimited.

11. SUPPLEMENTARY NOTES	12. SPONSORING MILITARY ACTIVITY: Advanced Research Project Agency, U.S. Army Research Office Durham, Durham, North Carolina

The intent of the research was to study the interaction of intense laser radiation with various optical media, in order to understand the physical processes involved. Gases, transparent solids, and organic dyes were studied.

The radiation-induced breakdown observed in inert gases subjected to a focused laser beam was interpreted as due to inverse Bremsstrahlung. Free electrons, provided by multiphoton ionization of impurities, were accelerated by the intense optical field, producing a chain reaction leading to a copious supply of free electrons and breakdown of the gas. The same inverse Bremsstrahlung chain reaction was found to induce gross permanent damage from thermal stresses in solid transparent media, beginning at a radiation density threshold in the vicinity of 1000 to 10,000 megawatts/cm^2.

An intensive study was made of three organic dyes of basically differing characteristics, all exhibiting saturable absorption at the wavelength of a ruby laser. The dye molecules studied were cryptocyanine, metal-free phalocyanine, and chloroaluminum phalocyanine. Each exhibits nonlinear absorption properties, principally a reduction in the optical transmission when irradiated with intense ruby laser light. Results of the study are reported in detail in an appendix to the report. The saturation characteristics of a dye can provide considerable insight into the energy-level structure of the dye, particularly with regard to excited states and intersystem crossing times.

DD FORM 1473

Unclassified

Security Classification

KEY WORDS	LINK A		LINK B		LINK C	
	ROLE	WT	ROLE	WT	ROLE	WT
Project DEFENDER						
University of Rochester						
Hercher, M., author						
Chu, William P., co-author						
lasers						
optical radiation, effects on matter of intense radiation						
laser-induced breakdown a) in solids b) of gases						
absorption, saturable						
absorption, nonlinear						
dyes, organic						